METEOR-Berichte

EUREC^{4}A Campaign

M161

17 Jan 2020 – 03 Mar 2020

Bridgetown (Barbados) – Ponta Delgada (Portugal)

EUREC^{4}A^{++}

W. Mohr, S. Kinne, K. Baier, D. Baranowski, M. Chilinski, J. Gollop, G. de Groot, R. Grosz, K. Helfer, A Ibáñez-Landeta, H. Kalesse, A. Kidane, S. Los, P. Makuch, M. Meyer, Y. Morfa-Avalos, A. Neuberger, J. Nowak, A. Raeke, C. Rollo, J. Röttenbacher, I. S. Sandiford, Schirmacher, O. Schlenczek, M. Schröder, E. Siddle, W. Szkolka, A. A. Ubele, J. von Arx, L. Worbes

Dr. Wiebke Mohr and Dr. Stefan Kinne

Max Planck Institute for Marine Microbiology (Bremen) and Max Planck Institute for Meteorology (Hamburg)

2020

Table of Contents

1 Cruise Summary

1.1 Summary in English

The R/V METEOR cruise M161 was part of the international EUREC^{4}A campaign in the western tropical North Atlantic off Barbados (12°N to 15°N / 54°W to 60°W). The overarching aim of the campaign was to obtain a better understanding of clouds and convection in the trade wind region which are not yet well represented in climate models. The campaign lasted from mid-January 2020 to mid-February 2020 and work on R/V METEOR focused on lower altitude cloud properties and convection in the context of their atmospheric and oceanic association. Four aircrafts (including the German research aircraft HALO) and three other research vessels (including the R/V MARIA S. MERIAN) participated in the campaign to resolve smaller temporal and spatial scale processes and patterns. Prior to the 17 Jan 2020 departure from Bridgetown, Barbados, a three-day installation cruise offered the time needed to appropriately install and calibrate dedicated atmospheric sensors and test their operation. During our main campaign from 17 Jan 2020 to 19 Feb 2020, the atmosphere and ocean were sampled continuously using underway systems and discretely at regular intervals. To obtain statistically relevant data, a small core working area was repeatedly surveyed with a few exceptions. The area was selected based on the position of the other research vessels and the flight patterns of the research aircrafts. During the cruise, atmospheric conditions were variable with trade winds from subtly changing directions and with variable wind speeds Oceanographic conditions were variable and mostly according to atmospheric forcing. The northern and southern parts of our core working area seemed substantially different in terms of oceanographic state and water masses with deeper chlorophyll maxima in the northern part than in the southern part persisted. After the main campaign, most measurements continued on the transit of R/V METEOR to the Azores which provided a substantially different atmospheric and oceanographic comparison.

1.2 Zusammenfassung

Die FS METEOR Ausfahrt M161 war Teil der internationalen EUREC4A-Kampagne im westlichen tropischen Nordatlantik vor Barbados (12°N to 15°N / 54°W to 60°W). Das allumfassende Ziel der Kampagne war, ein besseres Verständnis von Wolken und Konvektion in der Passatwindregion zu erhalten, da diese bisher in Klimamodellen nicht gut repräsentiert ist. Die Kampagne fand zwischen Mitte Januar 2020 und Mitte Februar 2020 statt und die Arbeiten auf FS METEOR konzentrierten sich auf die Eigenschaften von Wolken in niedriger Höhe und Konvektion im Zusammenhang mit deren atmosphärischen und ozeanographischen Verbindungen. Vier Flugzeuge (unter anderem das Deutsche Forschungsflugzeug HALO) und drei weitere Forschungsschiffe (unter anderem das FS MARIA S. MERIAN) nahmen an der Kampagne teil, um zeitlich und räumlich kleinskalige Prozesse und Muster auflösen zu können. Vor der Abreise aus Bridgetown, Barbados am 17. Jan. 2020 gab eine dreitägige Installationsfahrt die notwendige Zeit, bestimmte atmosphärische Messgeräte zu installieren und kalibrieren sowie deren Funktion zu testen. Während der primären Reise vom 17. Jan. 2020 bis zum 19. Feb. 2020 wurden die Atmosphäre und der Ozean kontinuierlich mittels sogenannter ‚underway'-Systeme und diskret in regulären Intervallen beprobt. Um statistisch relevante Daten zu gewinnen, wurde ein kleines Kernarbeitsgebiet mit einigen Ausnahmen wiederholt untersucht. Das Gebiet wurde aufgrund der Positionen der anderen Forschungsschiffe und der Flugschemata der

Forschungsflugzeige ausgewählt. Während der Reise waren die atmosphärischen Bedingungen variable mit sich leicht ändernden Passatwinden von unterschiedlichen Windgeschwindigkeiten. Ozeanographische Bedingungen waren ebenfalls variable und zumeist entsprechend den atmosphärischen Kräften. Die nördlichen und südlichen Teile unseres Kernarbeitsgebietes unterschieden sich ozeanographisch und Wassermassen mit tiefer liegendem Chlorophyll-Gehalt bestanden im im nördlichen Teil im Gegensatz zum südlichen Teil. Nach der primären Kampagne wurden die meisten Messungen auf dem Transit des FS METEOR zu den Azoren weitergeführt und boten einen in der Atmosphäre und Ozean wesentlich unterschiedlichen Vergleich.

2 Participants

2.1 Principal Investigators

Name	Institution
Stevens, Bjorn, Prof.	MPI-M
Stephan, Claudia, Dr.	MPI-M
Kinne, Stefan, Dr.	MPI-M
Serikov, Ilya, Dr.	MPI-M
Smirnov, Alexander, Dr.	GSFC/NASA
Kalesse, Heike, Jun.-Prof.	LIM
Wagner, Thomas, Prof.	MPI-C
Pöhlker, Mira, Dr.	MPI-C
Bodenschatz, Eberhard, Prof.	MPI-DS
Ament, Felix, Prof.	UHH
Galewsky, Joseph, Prof.	UNM
Malinowski, Szymon, Prof.	U Warsaw
Baranowski, Darek, Dr.	IG-PAS
Makuch, Przemyslaw, Dr.	IOPAN
Mohr, Wiebke, Dr.	MPI-MM
Heywood, Karen, Prof.	UEA
Nuijens, Louise, Prof.	TU Delft
Schneehorst, Anja	BSH

2.2 Scientific Party

Name	Discipline	Institution
Mohr, Wiebke, Dr.	Microb. Ocean. / Co-Chief Scientist	MPI-MM
Kinne, Stefan, Dr.	Atmosphere / Co-Chief Scientist	MPI-M
Kalesse, Heike, Jun.-Prof.	Atmosphere / Scientist	LIM
Röttenbacher, Johannes	Atmosphere / Student	LIM
Worbes, Ludwig	Atmosphere / Engineer	MPI-M
Morfa-Avalos, Yanmichel	Atmosphere / Scientist	MPI-M
Baier, Katharina	Atmosphere / Student	MPI-M
Neuberger, Almuth	Atmosphere / Student	MPI-M

Schirmacher, Imke	Atmosphere / Student	UHH
Schlenczek, Oliver, Dr.	Atmosphere / Scientist	MPI-DS
Ibáñez-Landeta, Antonio	Atmosphere / Scientist	MPI-DS
Meyer, Marcel	Atmosphere / Engineer	MPI-DS
Schröder, Marcel	Atmosphere / Scientist	MPI-DS
Ubele, Alma Anna	Atmosphere / Student	MPI-C
Los, Sebastian	Atmosphere / Scientist	UNM
Chilinski, Michal	Atmosphere / Student	U Warsaw
Nowak, Jakub	Atmosphere / Student	U Warsaw
Grosz, Robert	Atmosphere / Student	U Warsaw
Szkolka, Wojciech	Atmosphere / Student	IG-PAS
de Groot, Geiske	Atmosphere / Scientist	TU Delft
Helfer, Kevin	Atmosphere / Scientist	TU Delft
Kidane, Abiel	Microb. Ocean. / Scientist	MPI-MM
von Arx, Jan	Microb. Ocean. / Scientist	MPI-MM
Rollo, Callum	Oceanography / Scientist	UEA
Siddle, Elizabeth	Oceanography / Scientist	UEA
Baranowski, Darek, Dr.	Oceanography / Scientist	IGF-PAS
Makuch, Przemyslaw, Dr.	Oceanography / Scientist	IOPAN
Sandiford, Sanola	Observer (Scientist)	CMIH
Gollop, John	Observer (Scientist)	BBCG
Raeke, Andreas	Meteorological Technician	DWD
Installation cruise only		
Lund, Søren W.	Engineer	DTU
Lange, Ingo	Scientist	UHH
Könemann, Tobias, Dr.	Scientist	MPI-C
Schäfer, Michael, Dr.	Scientist	LIM
Lenschow, Donald H., Dr.	Senior Scientist	UCAR
Serikov, Ilya, Dr.	Scientist	MPI-M
Brügmann, Björn,	Engineer	MPI-M
Galewsky, Joseph, Prof.	Scientist	UNM
Wagner, Luise	Film Team	FPK
Sichert, Jonas	Film Team	FPK
Asmath, Hamish	Observer (scientist)	IMA

2.3 Participating Institutions

MPI-M	Max Planck Institute for Meteorology
GSFC	NASA Goddard Space Flight Center
MPI-C	Max Planck Institute for Chemistry
LIM	Leipzig Institute for Meteorology, University of Leipzig

UHH	University Hamburg
MPI-DS	Max Planck Institute for Dynamics and Self-Organization
UNM	University of New Mexico
U Warsaw	University of Warsaw
IG-PAS	Institute of Geophysics - Polish Academy of Sciences
IOPAN	Institute of Oceanology of the Polish Academy of Sciences
MPI-MM	Max Planck Institute for Marine Microbiology
UEA	University of East Anglia
TU Delft	Delft University of Technology
BSH	Bundesamt für Seeschifffahrt und Hydrographie
CIMH	Caribbean Institute for Meteorology and Hydrology
BBCG	Barbados Coastguard
DWD	Deutscher Wetterdienst, Geschäftsfeld Seeschifffahrt, Seewetteramt
UCAR	University Corporation for Atmospheric Research
DTU	Technical University of Denmark
FPK	Filmproduktion GmbH, Köln
IMA	Institute of Marine Affairs (Trinidad and Tobago)

3 Research Program

3.1 Description of the Work Area

The EUREC^{4}A campaign area was in a typical trade-wind region and offered the vicinity to a land-based atmospheric station. This allowed the intercomparison of the different measurements on board with those on land, which have been carried out for almost 10 years since the installation of the Barbados Cloud Observatory (BCO). The core working area of cruise M161 during the campaign was centered around 57°14.7'W and between ~ 12°N and ~ 14°30' N east of Barbados (Fig. 3.1.1). Two discrete stations represented intersections with the standard flight pattern of the German research aircraft HALO (points L1 and L2; see Fig. 3.1.1) which served as coordinated reference points.

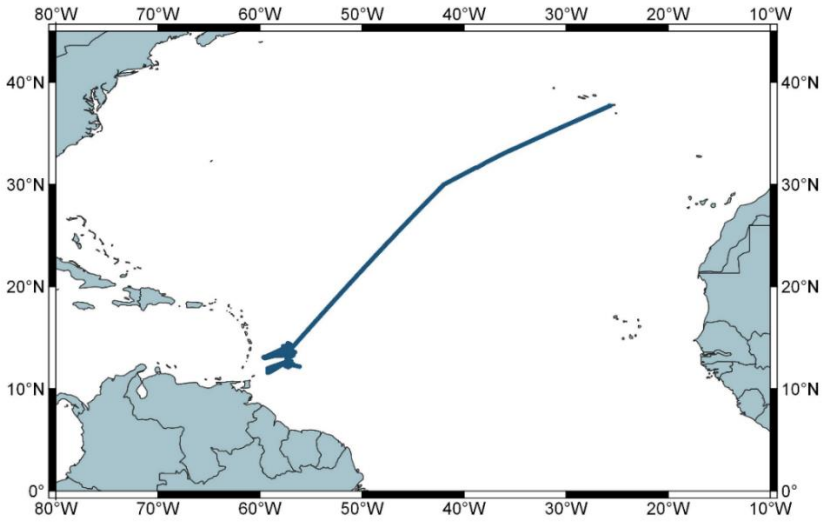

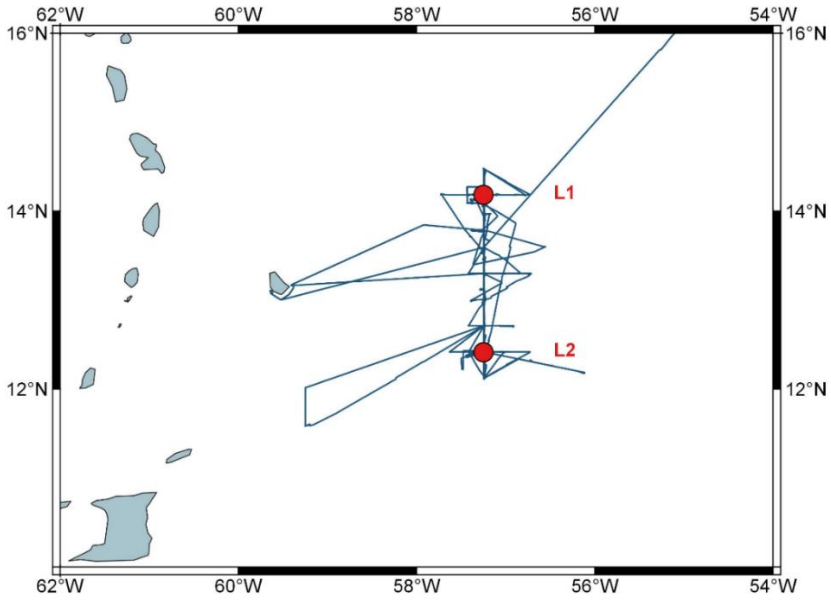

Fig. 3.1.1 Track chart of R/V METEOR Cruise M161 showing the full cruise track (upper panel) and the core working area (lower panel). The two intersections of our core working area with the standard HALO flight pattern are indicated as points L1 and L2 in the lower panel.

3.2 Aims of the Cruise

The aim of the cruise was the collection of properties of lower altitude clouds and convection as well as their corresponding oceanic and atmospheric environment and the observation of the respective atmosphere-ocean interactions in the trade-wind-region upwind of the BCO site.

3.3 Agenda of the Cruise

To characterize oceanic and atmospheric properties the sampling methods involved continuous probes (local state, active and passive remote sensing), regular interval profiling (CTD casts every 2-3 hours, radiosondes every 4 hours) and in-situ samples (glider in the ocean and UAVs and a tethered cloud-kite in the atmosphere). Most of the time during the EUREC^{4}A campaign, the R/V METEOR operated near 57°14.7'W longitude moving north and south between ~ 14°30'N and ~ 12°N in latitude. Extra time (daily cycle analysis) was spent at L1 (14°10.9'N, 57°14.7'W) and L2 (12°25.2'N, 57°14.7'W), the two track-crossing point to the standard flight circle of the HALO aircraft (Fig. 3.1.1). Details of instrument performances are given in the sections of chapter 5.

4 Narrative of the Cruise

The M161 cruise had a resourceful focus on probing the atmosphere and ocean-atmosphere fluxes as part of the EUREC^{4}A campaign. Many of the instruments required specialized personnel and additional time beyond the regular port time for installation and testing. We therefore carried out an 'installation cruise' from 13 January 2020 until 17 January 2020. Before leaving port on 13 January 2020, a group of scientists from the Caribbean Institute for Meteorology and Hydrology (CIMH) visited the R/V METEOR. Once departed, most time of the installation cruise was spent setting up and testing equipment just outside Bridgetown, Barbados and in waters east of the Barbados Cloud Observatory (BCO), a cloud monitoring station managed by the Max Planck

Institute for Meteorology in Hamburg, Germany. While the majority of M161 scientists were already on board during the installation cruise, we also enjoyed the company of an observer from Trinidad and Tobago as well as a German film team. Upon return of R/V METEOR into the port of Bridgetown, Barbados on 17 January 2020, some remaining equipment was brought onto the ship while the technical support staff disembarked and the remaining M161 participants boarded the vessel. R/V METEOR set sail again in the evening of 17 January 2020 with 30 scientists on board, including one person from the German Meteorological Service (DWD) and two observers from Barbados. Only a few hours after leaving port, we stopped east of the BCO site to allow the calibration of the many instruments on board as well as comparative measurements between the BCO site and R/V METEOR. Our activities off the BCO site were joined by the German R/V MARIA S. MERIAN, and we later jointly departed in wind-direction to our core working area about 130 NM east of Barbados along a North-South transect at 57°14.7'W and between 12°N and 14°30'N. This joint transition to the core working area of R/V METEOR allowed both research vessels to carry out comparisons of their instruments and parallel measurements while steaming into the winds and clouds. In the following weeks, the scientific party primarily surveyed its core working area by steaming north-south on the transect line with intermittent excursions in east or west directions to allow, e.g., the launch of the Cloud Kite due to wind restrictions and carry out specific oceanographic observations. Most of our atmospheric and some oceanographic measurements, however, were run continuously during the entire cruise. Towards the end of our first week, participants from the University of East Anglia released two gliders in the northern section of our core working area. The two gliders were later joined by a third glider which was delivered by an Autonaut that started its journey on Barbados. On 24 January 2020, the Cloud Kite from the Max Planck Institute for Dynamics and Self-Organization was launched for the first time but was unfortunately lost in the morning of 08 February 2020 during intense rainfall with heavy wind gusts. The cloud kite was replaced with a smaller cloud kite, and in the course of the cruise a total of about 90 flight hours were recorded. An aircraft-coordinated curtain sampling experiment on 26 January 2020 provided an opportunity for the atmospheric scientists on board R/V METEOR to match their ship-borne measurements with air-borne measurements on the research aircraft HALO. This excursion on a south-eastern leg led us out of our core working area and outside of the exclusive economic zone (EEZ) of Barbados at which point we deployed one of five ARGO floats. Almost mid-cruise, R/V METEOR set out for a 'rescue mission': one of the gliders in the wider research area experienced leakage and needed to be taken on board. As the R/V MARIA S. MERIAN, who originally was planned to pick up the glider at the end of the EUREC^{4}A campaign, was too far away from the glider location, R/V METEOR headed south-west and recovered the glider on 03 February 2020. By now, the scientific work on board had settled in from all the excitement in the first two to three weeks and continuous as well as discrete atmospheric and oceanographic observations became routine. Until the 18 February 2020, our work program allowed us to accomplish about 230 CTD casts of which 26 were also used for microbiological and biogeochemical water sampling. Besides the active and passive remote sensing of the atmosphere, about 200 radiosondes were launched and almost 100 quadcopter flights were completed during this period. To ensure safe operation, the three gliders were also recovered at times of calmer weather. On 19 February 2020, just before the R/V MARIA S. MERIAN headed back to Bridgetown to finish her cruise, a second simultaneous measurement campaign with both ships was carried out east of the BCO site. The rescued glider was then transferred from R/V

METEOR to R/V MARIA S. MERIAN while lying in island-protected waters off Bridgetown due to increasing weather and sea conditions in the region. At this time, we received frozen seawater samples from the R/V MARIA S. MERIAN to be shipped together with our frozen seawater samples later from Ponta Delgada, Azores. As we set sail to reach the Azores in early March, we visited our core working area once more for a last sampling effort in this region. On the subsequent transit of the R/V METEOR to Ponta Delgada, the remaining four of five ARGO floats were deployed, (only) two radiosondes per day were launched, about 25 CTD casts were realized (some were also used for water sampling) and several quadcopter flights were added on days with lower wind speeds. We reached the port of Ponta Delgada, Azores in the evening of 02 March 2020, where containers and equipment were offloaded the next day for shipments back home. On 04 March 2020, the entire scientific party disembarked R/V METEOR to head back to their home laboratories.

5 Preliminary Results

5.1 Atmospheric Measurements

5.1.1 Raman Lidar System LICHT

(L. Worbes, B. Brügmann, I. Serikov)

The Raman lidar system LICHT (LIdar for Cloud, Humidity and Temperature profiling) has been designed and built in 2013 to expand the observation capability of MPI-M.

Three generations of MPI-M Raman lidars were sequentially deployed at BCO since April 2010. Different in capabilities, each lidar in the row (EARLI, LICHT, and CORAL) has been built with very similar conceptual design dedicated for upward profiling of air temperature and humidity as well as for mapping vertical stratification of clouds and aerosol properties at three wavelength of frequency tripled Nd:YAG laser emission (1064, 532, and 355 nm). LICHT lidar having similar measurement characteristics to EARLI was designed for high isolation from harsh outdoor environment. Besides this the LICHT lidar has got the capability of daytime water vapor measurements. Operation range has been extended from 15 km for EARLI to 29 km for LICHT (implemented on June 14, 2017). In addition, it has been equipped with automated window washing installation (built in and activated on July 7, 2017) that allowed significant improvement of data quality thanks to reduced transmission losses on output and input windows of lidar container. LICHT lidar system was deployed at BCO station since July 2016. For the EUREC^{4}A campaign, LICHT lidar was operated on-board of German R/V METEOR. On BCO it is replaced by the third-generation MPI-M Raman lidar, the high power lidar component of CORAL system (Cloud Observation with Radar And Lidar), dedicated primarily for high-resolution water vapor vertical profiling that has been put in operation at BCO in May 2019. Comparing CORAL and LICHT lidar data should help understanding the air-mass evolution over Atlantic.

The onboard operation of LICHT system started on 13 Jan 2020, data acquisition on 17 Jan 2020, which continued till 01 Mar 2020. Targeted was the continuous operation. Data gaps in length of few hours were appearing and mostly out of the following reasons: i) Technical problems due to a photon-counter in the beginning, could be solved by software on board, ii) Legal problems due to operating close to the airport of Barbados or in the exclusive economic zone of Trinidad-

Tobago during a glider rescue operation, iii) Safety problems on board caused by crane/helikite operations. For technical characteristics and measured parameters of the Raman Lidar LICHT, see Table 5.1.1.1 and 5.1.1.2 in Appendix 12.1.

Ship performance

The system (20ft container) was placed on the back (container space 2703/2704) working deck of R/V METEOR. This turned out to be the optimal position: close to the center of the ship. This results in the lowest acceleration due to ship movements. Other positions like the bow, have larger accelerations as well as more sea spray. Sea spray in general turned out not to be a significant problem at wave heights up to 4 m. The cleanness of the optical windows was better than at the BCO due to low spray and the availability of freshwater with very low water hardness.
Overall, the system was operative without any larger problems and good performance, although ship-use was never planned in the design of the system. Minor problems were caused by the ship movements (movement of spring mounted parts) and the amount of water on deck (electrical problems, container leakage). The sensors for rain detection failed due to sea spray. The operation was limited for short periods due to crane operations for boat-use and the position of the helikite with respect to the laser beam.

Example quicklook 25 Feb 2020: Inflow of Saharan dust from 09:00 UTC

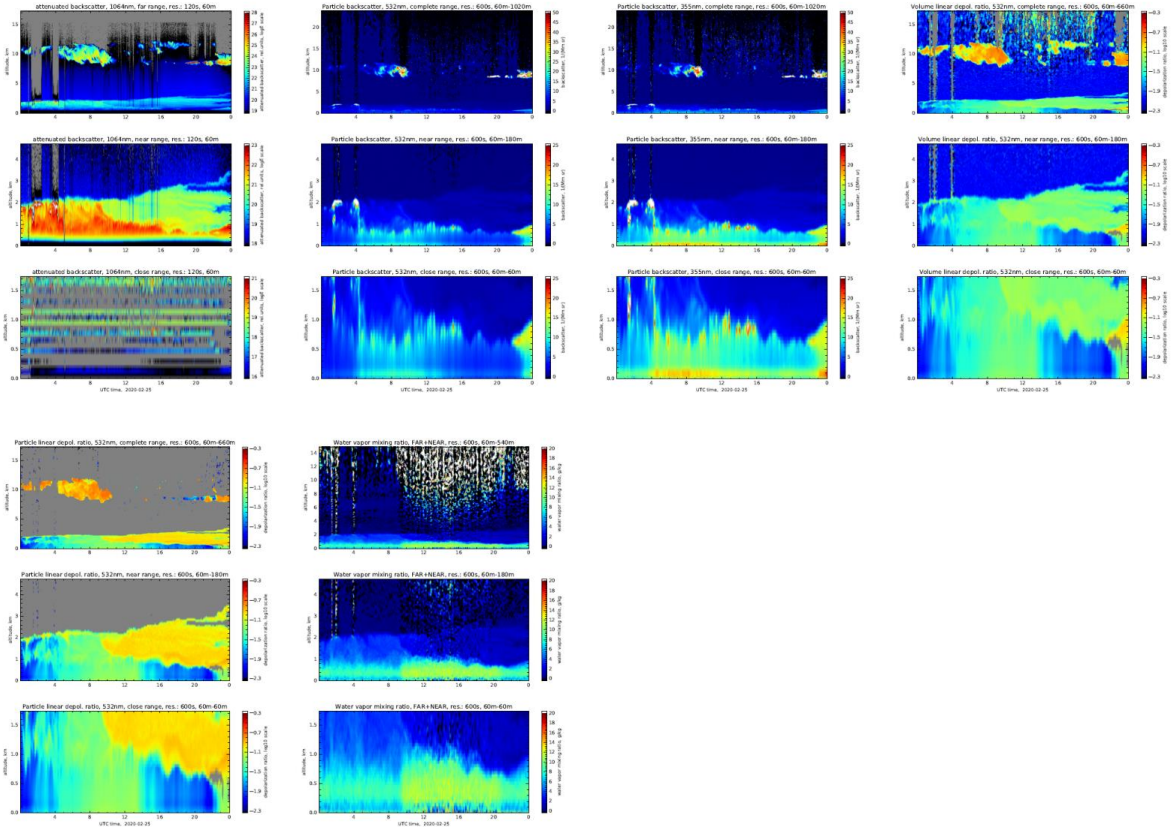

5.1.2 Ceilometer and Cloud camera

(S. Kinne, F. Jansen)

Cloud structures and cloud base altitude were continuously recorded with upward looking imagers of a cloud camera system and with a ceilometer. Both instruments of the Max Planck Institute for Meteorology have been operating on the R/V METEOR since early 2019. The cloud camera system contained a visible whole sky (frog lens) camera and a limited (ca. 30° field-of-view) thermal imager. Images of the sky are sampled every 10 seconds to record instant cloud structures and their changes over time. Particularly valuable are thermal imager data, as they provide information on cloud base altitude (especially with accurate input to temperature profiles), operate also at night and do not suffer from sun glint. A picture of the cloud-camera system during M161 and sample images for a cloud scene are presented in Figure 5.1.2.1 in Appendix 12.2.

The Jenoptik-15K ceilometer repeatedly casts laser beams at a near-infrared wavelength (1µm) vertically upward into the atmosphere and derives vertical distributions of atmospheric particle (e.g. aerosol) concentrations from delay and strength of the backscattered signal. Due to the strong return signal at (optically dense) clouds, cloud base altitudes are accurately captured. Handicaps of the instrument are the restriction to the nadir direction, the limited vertical range for aerosol detection during the day (by scattered sun-light), the inability to sense in and above clouds (laser light is unable to penetrate optically thick media) and the inability to sense near the surface (as sender and receiver are not exactly in the same position). The placement on the upper deck and a screen image of the data-collecting computer are presented in Figure 5.1.2.2 in Appendix 12.2. Thus, in terms of the cloud-base altitude the accuracy of the ceilometer at its nadir only view is complemented by the spatial distribution data of the thermal camera.

Both instruments operated with interruptions during the entire M161 cruise. Hourly averages of cloud fractions - stratified into seven cloud base altitude-ranges [of 0-0.5, 0.5-1 km, 1-1.5 km, 1.5-2 km, 2-3 km, 3- 6 km , >6 km] are presented in Figure 5.1.2.3.

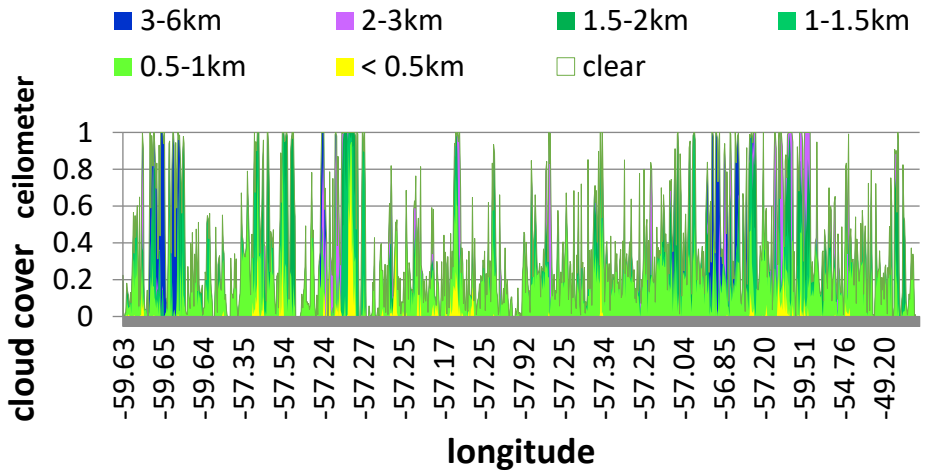

Figure 5.1.2.3 Cloud cover of hourly statistics by the upward probing ceilometer during the M161 cruise (from 13 Jan to 25 Feb). Cover fractions are stratified by cloud-base altitude.

During the campaign, most cloud base altitudes in the sampled oceanic trade wind region were in the 500 to 1000m altitude range (light green color in Figure 5.1.2.3). Sometimes (especially in cases of higher relative humidity at the ground) the cloud-base altitudes dropped to below 500 m. The cloud cover data show relatively few (and then short periods of) overcast conditions and confirm the mostly sunny daytime conditions of the cruise.

5.1.3 Microtops

(S. Kinne, P. Makuch, S. Sandiford, J. Gollop, A. Raeke)

Direct attenuation measurements of the direct sunlight are highly accurate, unlike interpretations of satellite sensor data with assumption to composition and background. Thus, NASA's AERONET group distributes calibrated handheld (MICROTOPS) sun photometer instruments on an opportunity basis for the sampling of atmospheric aerosol column properties and water vapor content. The direct solar intensities are sampled simultaneously at four trace-gas free solar spectral intervals (380, 440, 675 and 870 nm) and at one solar spectral band with water vapor absorption (940 nm). As sampled intensities are always smaller than their top of the atmosphere values (which are simply defined by time and [GPS-] position), each sample represents a solar atmospheric attenuation. These solar attenuation data at cloud-free conditions offer information on aerosol amount, aerosol particle size (thus even aerosol type) and atmospheric water vapor. Measurements are done in handheld mode. Hereby instruments need to be accurately oriented into the sun but only at times during the day, when views of the sun are not obstructed by clouds. Instruments and a sampling event are introduced in Figure 5.1.3.1 in Appendix 12.2.

All sampled aerosol and water vapor data were transferred to NASA's Marine Aerosol Network (MAN) database at the end of each day and the data can serve as reference to satellite remote sensing and modeling almost immediately via web access (https://aeronet.gsfc.nasa.gov/new_web/maritime_aerosol_network.html). The goal was to sample several times during each daytime hours, when clouds did not cover the solar disk. Derived properties are column data for aerosol amount (via AOD at 550 nm), for aerosol size (Angstrom parameter and AOD fraction assigned to smaller sub-micrometer 'fine-mode' sizes) and for atmospheric water vapor. The derived four properties are explained next and then their hourly time-series onboard the R/V METEOR during the EUREC^{4}A campaign are presented in Figure 5.1.3.2.

- The AOD stands for Aerosol Optical Depth, where optical depth is the negative exponential attenuation coefficient normalized with respect to a nadir view. For the interpolation to the AOD value at 550 nm (which is not directly measured) the Angstrom parameter is applied.
- The Angstrom parameter requires AOD data at two different solar wavelengths (here at 380 and 870 nm). The property (with its negative ln[AOD] / ln[wavelength] slope definition) is an inverse measure for particles size. Smaller 'fine-mode' particles (radii <0.5 µm) have a stronger spectral dependence (AP > 1.2), 'coarse-mode' particles (radii > 0.5 µm) have a weaker one (AP <0.5).
- The fine-mode AOD fraction is a generally more useful size information because modeling and retrievals usually distinguish between AOD contributions by super- and by sub-

micrometer sizes. Fine-mode fractions estimate require AOD data at four or more different wavelengths.

– The atmospheric water vapor can be determined, as one of the instrument's spectral sensors records the solar attenuation in a water vapor absorbing band. Knowing the attenuation attribution to aerosol from the other bands and knowing the water vapor absorption strength for the absorbing band, then the total (clear-sky) atmospheric water vapor can be derived.

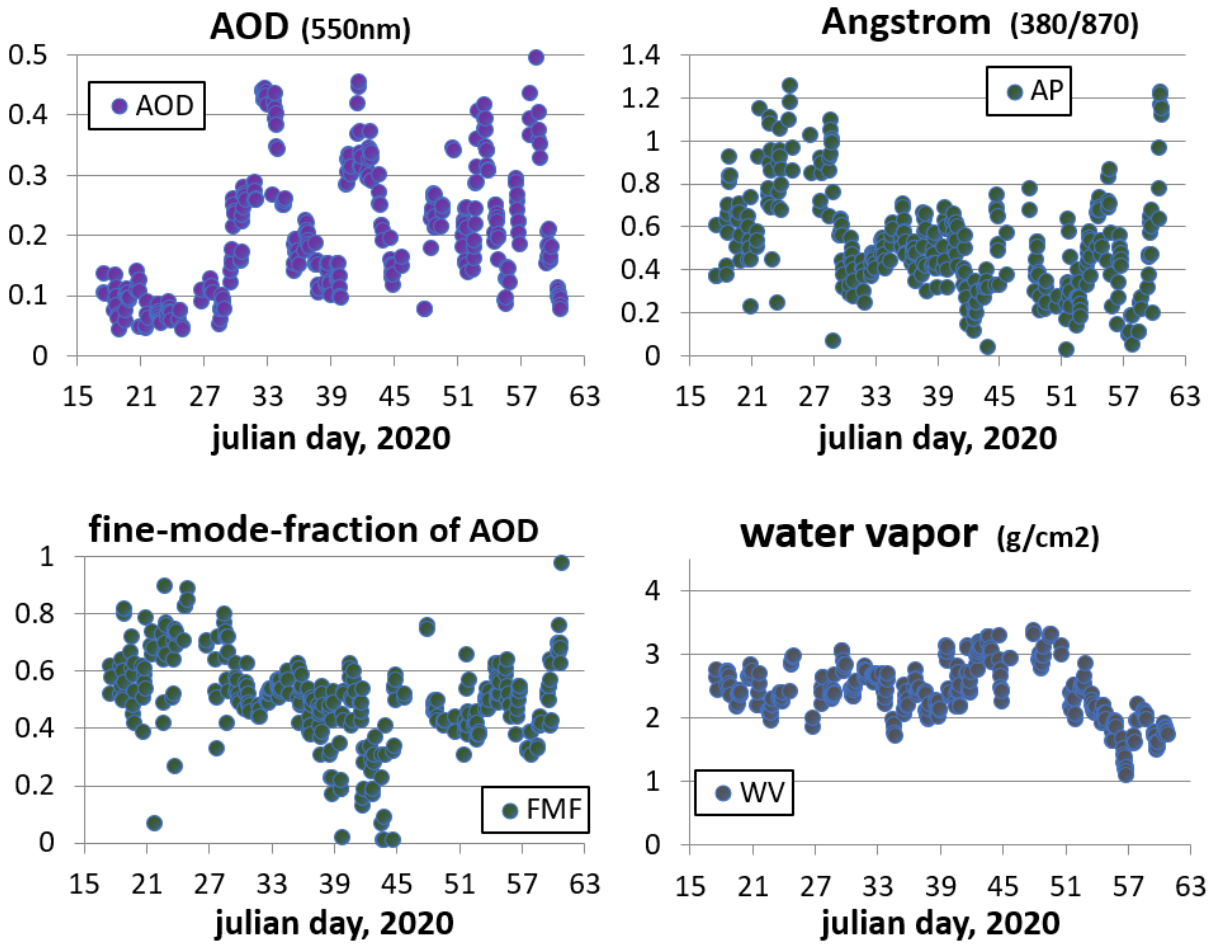

Figure 5.1.3.2 M161 hourly averages for aerosol and water vapor properties (17 Jan – 1 Mar 2020).

The AOD data show relatively weak atmospheric aerosol loads during the first half of the campaign. AOD values varied between 0.04 and 0.16 and contributions from smaller aerosol particles (thus, larger fine-mode AOD fractions) were dominant. During the second half, however, the aerosol loads were usually higher and at times reached AOD values near 0.5. The smaller fine-mode AOD fraction illustrate that the larger AOD values involved the presence of larger aerosol sizes. These larger sizes were the result of both (1) stronger near surface winds (e.g. large seasalt particles from bubble bursting in whitecaps) and (2) transported mineral dust from the Sahara at elevated (1.5 – 2.5 km) altitudes (which prevented colorful sun-rises and sun-sets). Dust events usually lasted for many consecutive days and were also quite regular on the transit to the Azores after the campaign. The (clear-sky) atmospheric water vapor content during the campaign varied between 2.0 and 3.5 g/cm^2. Hereby, the values on the R/V METEOR track (at 57°14.7'W) were on average larger towards the southern end (12°30'N) as compared to the northern end (14°N). On

the transit to the Azores to higher latitudes the atmospheric water vapor content decreased and dropped even to values as low as 1g/cm^2.

5.1.4 Cloud Radar, Microwave Radiometer, Spectrometer

(H. Kalesse, J. Röttenbacher)

The installed instruments of the Leipzig Institute for Meteorology at the University of Leipzig (LIM) are now introduced, their placement on the 5th superstructure of the METEOR during the M161 cruise are illustrated in Fig. 5.1.4.1 in appendix 12.2

"LIMRAD94" – a frequency modulated continuous wave (FMCW) 94 GHz stabilized Doppler cloud radar: The bistatic radar (i.e., two antennas) operates at 94 GHz. Hydrometeors in the atmosphere such as cloud droplets, ice crystals, and rain drops scatter part of the emitted microwave radiation back to the receiver antenna. The return signal is resolved in time (integration time: 1.5 s) and height (range resolution: 20-40 m) and thus the radar provides range profiles of radar moments at high time resolution, which allows for studying microphysical processes in clouds passing over the radar beam. Instead of only return signal strength (reflectivity), the full Doppler spectrum is recorded. From that, other radar moments such as mean Doppler velocity and spectrum width are determined. The mean Doppler velocity consists of the superposition of up- and downdrafts in clouds and reflectivity-weighted particle fall velocity. Spectrum width is a function of particle size distribution width and a dynamical component, the turbulence in the cloud. Cloud base and cloud top can be derived from cloud radar observations in non-rainy conditions. In light rain, the signal is still able to penetrate the entire cloud to give cloud top estimates but the first echo is from falling precipitation (and thus not cloud base). In strong precipitation, the radar signal is attenuated before reaching cloud top. During the EUREC^{4}A-deployment, a new passive radar stabilization platform (cardanic mount constructed by RPG radar company) was deployed for the first time. The cloud radar is "free-swinging" within it to point vertically upwards to exclude the effect of horizontal wind on the Doppler velocities.

"LIMHAT" – a microwave radiometer: The RPG-HATPRO (**R**adiometer **P**hysics **G**mbH **H**umidity **A**nd **T**emperature **PRO**filer) Generation 5 is a microwave detector for measuring humidity and temperature profiles in the earth's troposphere. The radiometer is a passive remote-sensing instrument measuring the sky's brightness temperatures at the center and slopes of absorption lines of atmospheric water vapor (22.23 –31.4 GHz) and oxygen (51.26 – 58.0 GHz) as well as window channels between those spectral lines. Apart from humidity and temperature profiles, the system also retrieves integrated quantities like integrated water vapor (IWV) and liquid water path (LWP) in the troposphere in non-rainy conditions.

"CORAS" – a spectral radiometer: CORAS is a ground-based version of the airborne SMART-albedometer [Wendisch et al., 2001] measuring spectral solar radiation between 300 nm and 2200 nm using grated spectrometers. In principle, it can be operated in different configurations using different optical inlets measuring up- and downward radiances and irradiances. During this cruise, it was used to measure downward radiances transmitted through the clouds to derive information about the cloud optical thickness and the effective radius based on radiative transfer calculations. The above-mentioned instruments in combination with onboard lidar measurements and radiative transfer calculations will be used for cloud droplet number concentration (CDNC) retrievals.

Data acquisition: All instruments were performing well during the cruise after calibrations were completed on 16 Jan 2020, 18:00 UTC. Small gaps in the measurements exist because of
a) trans-calibration of the CORAS spectro-radiometer on approximately a weekly basis
b) optimization of radar chirp tables between 26-31 Jan 2020
c) instrument turn-off in Trinidad and Tobago waters (03 Feb 2020 - 04 Feb 2020)

Post-processing of the radar data (heave-correction, possibly correction of slight radar mispointing (< 1° due to inertia in the movement of the stabilization platform when it tries to level itself out to vertical-pointing) after the cruise will allow for the possibility to use the Doppler signal and thus to apply Cloudnet retrieval algorithms for determination of microphysical properties [Illingworth et al., 2007]. These algorithms require simultaneous operation of three remote-sensing instruments: cloud radar, MWR, and ceilometer (PI S. Kinne).

Instrument	Data availability	Time resolution
Cloud radar	17 Jan – 28 Feb 2020	3 s (until 31 Jan), 1.5 s (from 01 Feb)
Microwave radiometer	17 Jan – 28 Feb 2020	2 s
Spectral radiometer	17 Jan – 28 Feb 2020	5 s

Preliminary results

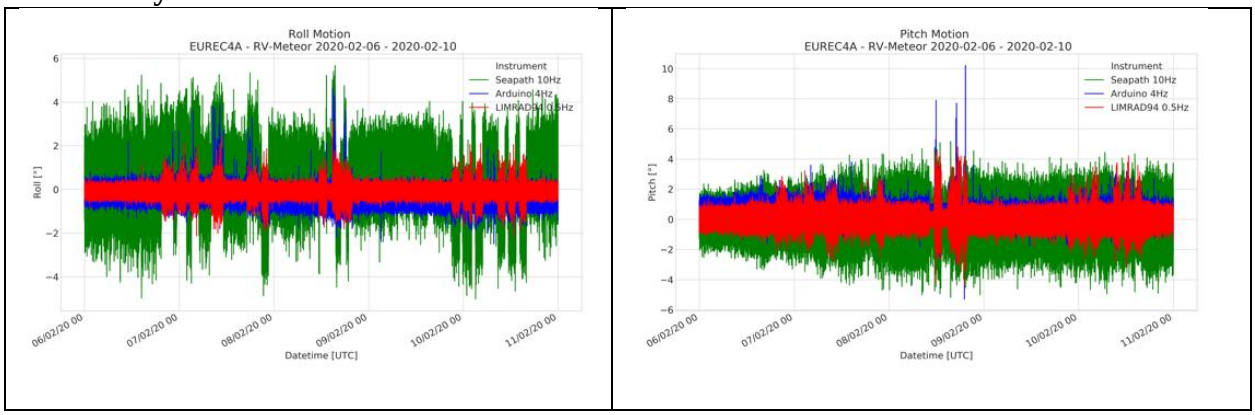

Figure 5.1.4.2 Time series of roll (left) and pitch (right) for 06-10 Feb 2020. Initial analysis suggests that the performance of the cloud radar stabilization platform was satisfactory. As illustrated in Figure 5.1.4.2, the roll and pitch angles measured at the cloud radar (red and blue) are much smaller than attitude angles observed in the center of gravity of the ship (green).

Cloud radar hydrometeor fraction profiles

Profiles of hydrometeor fractions (HF) determined from cloud radar observations for the period 17 Jan – 19 Feb are illustrated in Figure 5.1.4.3a. Hydrometeor fractions are similar to cloud fractions but do however account for the fact that the cloud radar is also sensitive to falling rain drops and precipitating ice virgae. Two features are striking: the expected high HF in the lower troposphere peaking with values of nearly 12 % at 800 m altitude and the HF of 6 % at about 6-8.4 km altitude. Both peaks are separated by near-zero HF values in the dry subsidence altitude region of the Hadley cell at about 3.2-4.5 km height. While the high HF in the atmospheric boundary layer of the trade wind region are expected due to the high occurrence of trade wind cumulus, the high HF at higher altitudes were an exception to the climatological mean caused by a persistent thick layer of cirrus and altostratus between 14-16 Feb 2020 as illustrated in Figure 5.1.4.3b).

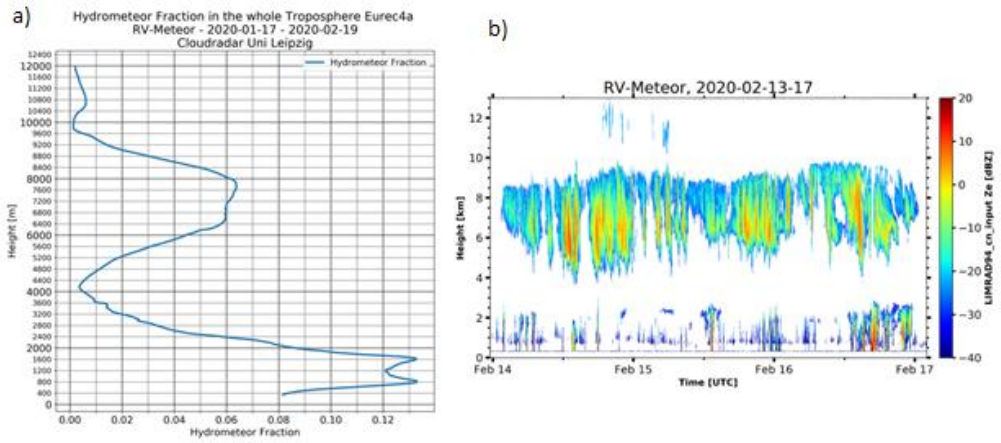

Figure 5.1.4.3 a) Cloud radar derived hydrometeor fraction for 17 Jan – 19 Feb 2020, b) Time-Height image of cloud radar reflectivity for end of 13 Feb to beginning of 17 Feb 2020.

While the radar observations of that event give the impression of *one* thick high cloud layer, Raman lidar observations by MPI-HH show that it is actually two layers: one of a cirrus with cloud top temperature of about -35 °C in roughly 8.5-9 km altitude and an altostratus (As) with cloud top at about 7.5 km. The cloud radar thus also depicts ice precipitating from the upper cirrus into the lower cloud As layer.

Time series LWP and IWV of MWR

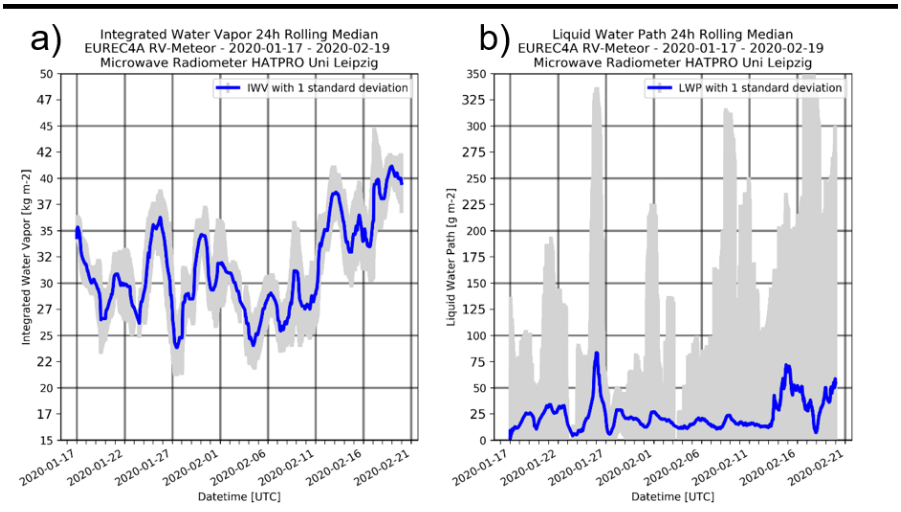

Figure 5.1.4.4 Time series of 24h rolling median a) IWV and b) LWP derived from LIMHAT MWR measurements

Figure 5.1.4.4a and b depict time series of 24h median IWV and LWP derived from the MWR measurements from 17 Jan to 17 Feb 2020, respectively. In a data pre-processing step, values likely caused by own ship plume sampling (IWV > 65 kg/m^2) as well as rain events (DWD rain sensor flag) were excluded. Observed IWV values ranged between 15-45 kg/m^2 with a mean of 31 kg/m^2. Since trade wind cumulus of all developing stages - from developing Cu hum and Cu med to Cu congestus were sampled, observed LWP was very variable with a mean and standard deviation of 47 +- 146 g/m^2 (median of 20 g/m^2).

5.1.5 WIND LIDAR

(G. de Groot, K. Helfer, L. Nuijens, S. Lund)

As part of EUREC^{4}A-Wind, we use LiDAR technology to measure vertical profiles of the wind. A LiDAR sends out a beam of electromagnetic radiation that reflects off water droplets, dust and other aerosols. These particles move with the wind, and this movement causes a Doppler phase shift in the reflected beam. The Doppler shift is then translated to a 3D wind field, typically at heights between 40 m and 2 km. Hence the LiDAR measures the profile of the wind, its temporal evolution at various altitudes, its shear, and momentum fluxes. During M161 we used two instruments from Leosphere: one long-range LiDAR (Windcube WLS70) and one short-range LiDAR (Windcube V2). The devices were provided by the Denmark University of Technology and by the Fraunhofer-Institut für Windenergiesysteme, respectively. In Table 5.1.5.1 in Appedix 12.1, specifications of the two devices are given and pictures of both instruments at their location during the Meteor cruise are shown in Figure 5.1.5.1 in Appendix 12.2.

Both wind-lidars were located on the roof of the R/V METEOR's paint store, thus on the same level as the '3. Aufbaudeck', as shown in Figure 5.1.5.1 (Appendix 12.2). As indicated in Table 5.1.5.1 (Appendix 12.1), the long-range profiler was running smoothly for the entire campaign. The short-range profiler was not operating at the beginning of the cruise presumably because of a problem with the power supply. It however switched itself on for unknown reasons on 26 Jan 2020. It then operated without problems for about 2.5 weeks until 14 Feb 2020 when it ceased operations again. After exchanging the power supply box and cables, the device was again working from 21 Feb 2020 until the end of the cruise. Both devices did not record any data for a few hours on 03-04 Feb 2020 when the vessel entered the EEZ of Trinidad and Tobago (to rescue a sea-glider of the Merian).

Depending on the specific conditions (aerosol concentrations and type as well as other factors), we don't always retrieve a strong enough signal at all altitude levels (as specified in Table 5.1.5.1, Appendix 12.1). For example, high dust concentrations (as we experienced them for instance from 30 Jan until 02 Feb 2020) are advantageous for our measurements, giving us high carrier-to-noise (CNR) ratios. On the other hand, clouds may 'block the view' for our signals. Furthermore, we noticed that the plume of the ship's exhaust occasionally reduced the CNR of our measurements when it blew over the instruments. Too low CNRs are disregarded in further processing, which mostly occurred for the higher levels of the long-range profiler and only rarely for the short-range profiler. After the cruise, the LiDAR data will have to be corrected for the ship's movement (which is recorded as well). This is done on the raw data from which then 10-minute averages are taken. First, the ship's speed will need to be subtracted to retrieve real wind speeds, and the ship's heading/course will need to be taken into account to retrieve real wind directions. The data are also affected by the heave, roll and pitch of the ship. Averaging over time (e.g. 10 minutes) is sufficient to average out such effects on small vessels but on a larger vessel like the R/V METEOR it may be necessary to correct for these additional movements too. Figure 5.1.5.2 shows a typical uncorrected wind profile.

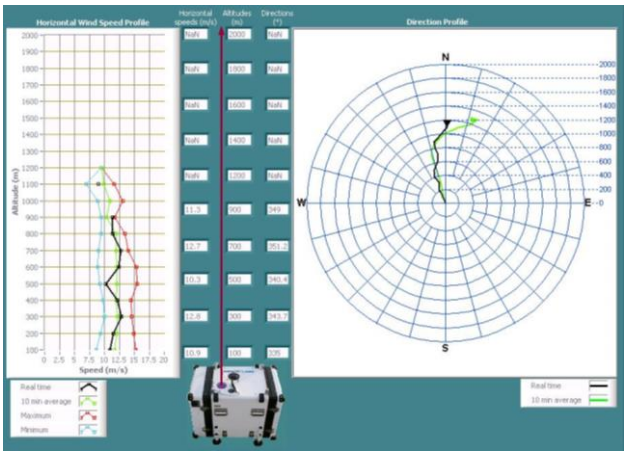

Figure 5.1.5.2 Quick view of a wind profile by the WLS70 long-range Wind LiDAR; The data are not yet corrected for the ship's movements. Left: wind velocity profile; Right: wind direction.

5.1.6 Eddy Covariance Flux Measurements

(K. Baier, I. Schirmacher, I. Lange)

Technical description

For the measurements of gas fluxes, the Eddy Covariance method is one of the most accurate approaches. The installed instruments for the flux measurements during the M161 cruise are summarized in Figure 5.1.6.1 in Appendix 12.2.

In front of the ship and on top of the mast CO_2, momentum, latent and sensible heat fluxes between the ocean and the atmosphere transported by eddies in the atmosphere are investigated. To do so, in situ measurements of the vertical wind speed and the concentrations of the gases of interest have been obtained with a sampling rate of 20 Hz by a sonic anemometer and an open path gas analyzer, accordingly. Furthermore, an HMT investigating the air temperature and humidity, a PTB estimating the air pressure and a GPS-mouse measuring the time and location of the vessel are installed. At the front of the vessel a KT19 thermal camera for water temperature (SST) measurements and two extra GPS receiver were installed.

Data acquisition and processing

The instruments at the top were running throughout the whole campaign (from 17 Jan 2020 to 02 Mar 2020), whereas the instruments at the front of the vessel were operating from 17 Jan 2020 only until 25 Feb 2020. The PTB (pressure sensor) only worked on 15 Jan 2020 during installation tests, however, air pressure was also recorded by the LI-COR instrument. The KT19 (temperature sensor) only worked until 20 Jan 2020 due to sea water damage. For data processing and analyzing, the SST measurements and the heading of the vessel are taken from Dship data server of the ship. For eddy covariance data an undisturbed flow was required. Thus, for data from the front of the ship on events were analyzed when the near surface air-flow hit the ship out of the (general) forward ± 30° direction.

The eddy flux (F) is calculated by the mean covariance between the deviations of the vertical wind speed of eddies (w') and of the gas density (ρ_s'): $F = < w', \rho_s' >$. The data has to be processed and corrected before calculating the fluxes. While the high resolution (20 Hz) native RAW data

will be processed after the campaign, a software (*WM-AUFBEREITUNG* by Ingo Lange) allowed to produce quicklooks of averaging RAW data (though with filtering) over one minute. Therefore, the data has to be despiked and the coordination system had to be rotated, such that the mean vertical velocity is equal to zero. For eddy covariance measurements a correction of the wind speed and direction is required due to the movement of the ship. In addition, the time delay between the USAT and LICOR had to be considered and the data had to be detrended. Another important correction is the Webb-Pearman-Leuning which takes into account that differences in temperature and humidity (followed by air density changes and changes of the concentrations of gases inside the air) will result in a flux of gases, even if no eddies are present.

Preliminary results

In the following, fluxes of momentum, CO_2, latent and sensible heat are shown for 09 Feb 2020 in Figure 5.1.6.2. Hereby, the average period is one hour and all data is still uncorrected.

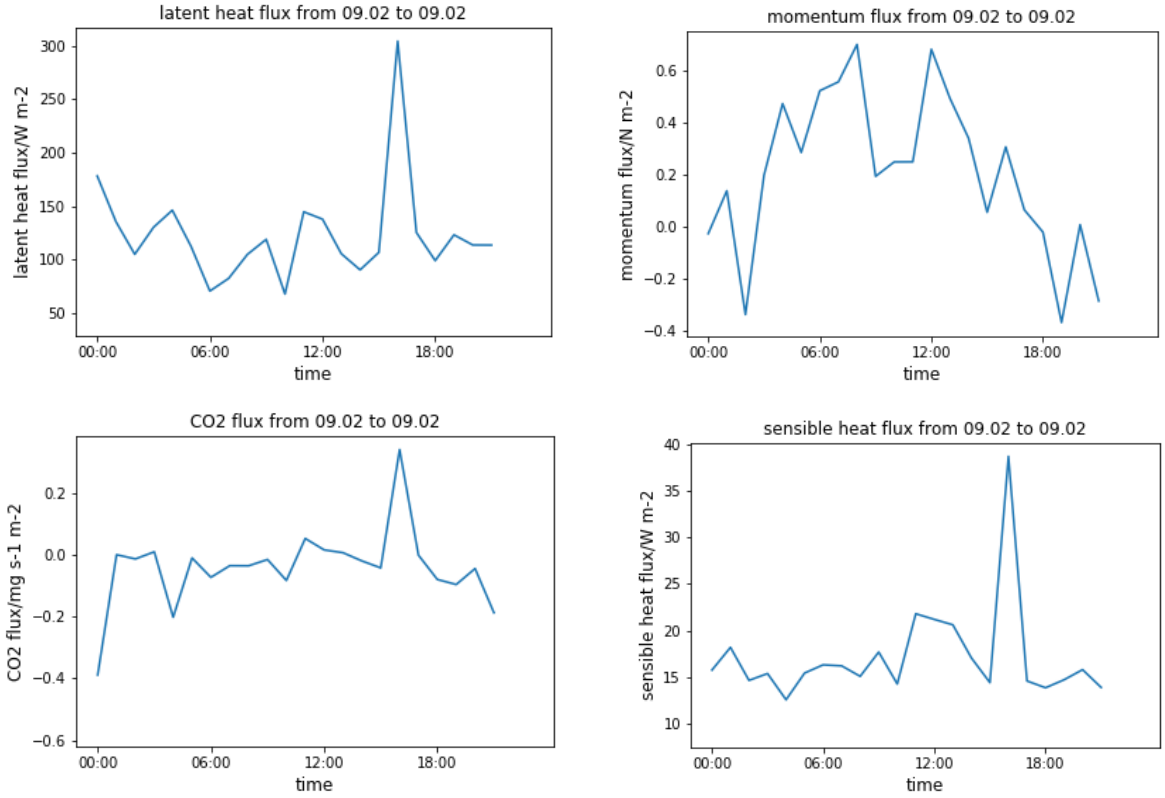

Figure 5.1.6.2 Flux of latent heat, momentum, CO_2 and sensible heat on 09 Feb 2020.

The latent heat flux is mainly directed into the atmosphere, due to evaporation of the ocean water. Thus, the momentum flux is positive most of the time. The CO_2 flux is mostly negative, because the ocean takes up the CO_2 out of the atmosphere. The sensible heat flux is always pointing towards the atmosphere, because at the ocean surface the water temperature (SST) is usually higher than the air temperature. During 16 to 17 time-period in Figure 5.1.6.2 a peak is present in all fluxes which is associated a precipitation event with an air temperature drop for more than one degree, an relative humidity increase by about 3% and a rapid wind direction change. During the event, latent and sensible heat fluxes are increased. The positive CO_2 flux can be explained by the

Webb-Pearman-Leuning effect: The temperature drops, hence the volume of an air parcel gets less and the concentration of CO_2 increases.

5.1.7 Stable Water Isotopologues

(J. Galewsky, S. Los)

During the M161 research cruise, the group from the University of New Mexico collected stable isotope measurements of water vapor, rainwater, and seawater. Most water molecules (>99.5%) in nature consist of stable (non-radioactive) lighter isotopes of oxygen and hydrogen, however, a few water molecules may also have stable heavy oxygen, heavy hydrogen, or a combination thereof. An isotopologue is a variant of a compound that varies only by the isotopic composition of the elements in its molecules. For water, the relative abundances of these light and heavy isotopes are particularly sensitive to phase changes, such as evaporation of water from the ocean, or to mixing of water vapor between differing air masses. Stable water isotopologue measurements can therefore yield useful information for a range of moist atmospheric processes such as large-scale mixing to cloud-scale precipitation microphysics. With water vapor isotopologue measurements collected on three research vessels, two aircrafts, and at the Barbados Cloud Observatory during the EUREC^{4}A campaign, the M161 measurements complement the largest stable water vapor isotopic field effort to date. The EUREC^{4}A isotope group, EUREC^{4}A-iso, seeks to leverage isotopic measurements to better characterize cloud organization patterns, the sub-cloud moisture budget, cold pool events, large-scale subsidence, and coupling between tropical and extratropical air masses.

Water vapor: A Picarro Water Vapor Isotopic Analyzer (L2130-i), utilizing cavity ring-down spectroscopy (CRDS), was used to continuously (~1 Hz) measure the isotopic composition of ambient water vapor during M161. The L2130-i measures the $^{18}O/^{16}O$ and the D/H ($^{2}H/^{1}H$) ratios of water vapor, as well as the total water vapor concentration in ppm. The L2130-i was setup within the Air-Chemistry Laboratory, a climate-controlled environment ideal for operation of the instrument, on the 5th Superstructure Deck (Figure 5.1.7.1a in Appendix 12.2). The instrument draws in ambient air via pumps and an inlet line, the make-up of which is critical to high-quality measurements. This inlet line, a ¼ inch teflon coated tube that minimizes water adsorption, was run from the instrument through a dedicated port in the Air-Chemistry Lab roof and attached to a forward-facing railing above on the 6th Superstructure deck at a height of 25.8 m from the mean sea surface (Figure 5.1.7.1b in Appendix 12.2). This inlet configuration allowed minimally disturbed fetch when the vessel faced into the wind. The end of the inlet line was housed in a downward facing funnel to limit contamination by rainwater and sea spray (Figure 5.1.7.1c in Appendix 12.2). A 0.2 μm inline filter was installed 25 cm from the end of the inlet line to further minimize contamination by sea spray and other aerosols. The entire length of the inlet line (505 cm) was wrapped with a heat trace cable, foam insulation, and foil tape to maintain line temperatures of at least 40 °C so to mitigate condensation within the line that can greatly affect measurement quality.

The L2130-i instrument itself requires little intervention while running; however, to properly calibrate data, standards must be run frequently, preferably daily, to account for various factors such as instrument drift. Standards were run using the Picarro Standard Delivery Module (SDM)

and Picarro A0211 Vaporizer which deliver precise quantities of water vapor of a known isotopic composition to the L2130-i. The SDM can deliver two separate standards for a given standard run, which typically take an hour to complete each day during which time no measurements can be taken. A new standard water was swapped in every 4-5 days allowing a rotation of four total standard waters throughout M161.

Liquid samples: Rainwater samples were collected using a Palmex Ltd RS1 Rain Sampler designed to minimize evaporation and change in isotopic composition (provided by Franziska Aemisegger of ETH Zurich). This sampler was placed on the aft railing of the Navigation Deck. Rain samples were retrieved on an event basis with fifteen rain events collected over nine individual days during the cruise. Samples were collected by filling 2 x 2 ml vials, one for analysis and one for backup, and 1 x 15 ml via syringe with no head space and sealed via parafilm. Seawater samples were collected nearly daily using the Conductivity, Temperature, and Depth (CTD) Profiler at a depth 10 m from the profile closest to 19:00 UTC (15:00 local time) each day. A full diurnal cycle was also collected on 11 Feb 2020, collected every two hours, while the R/V METEOR was on station for 24 hours. In total 38 samples were collected from 23 Jan 2020 – 01 Mar 2020: 22 during the campaign, 11 additional during the 24-hour diurnal station, and 6 during the transit to the Azores. Samples were collected in 2 ml vials that were killed with CuCl to prevent biotic activity that could alter the isotopic composition and then sealed with parafilm.

Data acquisition and processing: The stable water isotopologue data are reported in the standard δ-notation where values are expressed as per mil deviations from a reference standard, here Vienna Standard Mean Ocean Water (VSMOW). Water vapor measurements received corrections for typical known biases including water vapor concentration dependence and δ-value dependence, i.e. the "stretching factor". The raw water vapor measurement of $\delta^{18}O$ and δD are reported with time, latitude, longitude. Corrected water vapor measurements will also include measurement uncertainties. Rainwater and seawater samples will be analyzed against laboratory standards using standard isotopic lab protocols at the University of New Mexico's Center for Stable Isotopes. The 15 ml rainwater sample vials will be stored in an isotopic water archive at ETH Zurich. The rainwater dataset will include information on rainfall duration, intensity, and measurement uncertainties. The seawater dataset will include information on sea surface temperature, temperature at sample depth, and measurement uncertainties. Corresponding meteorological data for water vapor, rainwater, and seawater datasets are available as well.

Preliminary results: The water vapor isotopic dataset shows a number of notable, initial features (Figure 5.1.7.2). Variability was generally much smaller than typical terrestrial datasets, but apparent are low-frequency variations associated with synoptic to mesoscale changes in the marine boundary layer, along with numerous high frequency variations associated with individual cloud or rain events. Most obvious in Figure 5.1.7.2 are positive spikes in δD values associated with rain events.

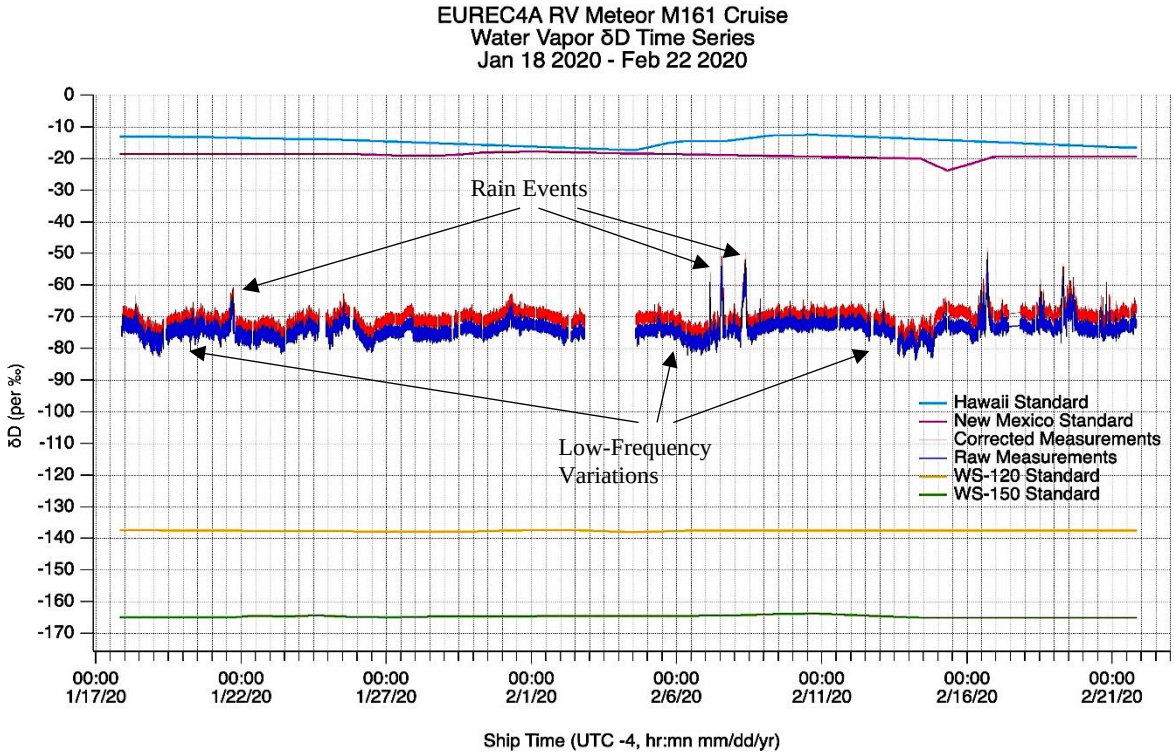

Figure 5.1.7.2 Time series of raw (blue) and corrected (red) water vapor δD for the duration of the EUREC^{4}A campaign from 18 Jan – 22Feb 2020. Also shown are interpolated time series from the four working standard water used for calibration.

Proceeding and following some rain events a smaller but significant negative δD excursion is present, possibly giving information on the vertical origin of downdraft. Smaller but notable excursions are also present when virga was indicated by the vertically-pointing cloud radar, suggesting a signature of rain evaporation. Variations associated with at least a few cold-pool events, an important process for the convective organization that is a focus of the EUREC^{4}A campaign, are noted as well.

5.1.8 MAX-DOAS

(A. A. Ubele, S. Dörner)

The Tube Multi AXes Differential Optical Absorption Spectrometer (Tube MAX-DOAS) measures spectra of scattered sunlight between 303 nm and 465 nm for a series of elevation angles [Platt and Stutz, 2008]. These measurements are used to derive atmospheric profiles of aerosol extinction and trace gas concentrations [Wagner et al., 2011]. In the EUREC^{4}A field study the aim of the Tube MAX-DOAS is to retrieve the following species from the measured spectra: 1) nitrogen dioxide (NO_2) and sulphur dioxide (SO_2) from (mostly) anthropogenic sources like diesel fuel combustion, 2) formaldehyde (HCHO) from anthropogenic and biogenic sources, 3) water vapor (H_2O) and 4) the oxygen dimer (O_4) which holds information on the aerosol extinction [Wagner et al., 2004]. These species help to characterize the chemical composition of the atmosphere, the location and strength of emission sources and provide important input for global modelling and comparisons to satellite data. In addition, measured spectra contain information on

less abundant species like bromine monoxide (BrO), iodine oxide (IO) and glyoxal (CHOCHO) for which tropospheric abundances especially in marine regions are not well known.

First output of DOAS analysis is differential slant column densities (dSCD) of the analyzed trace gases. A preliminary DOAS fit for NO_2 on a selected cloudless and low aerosol content (aerosol optical depth (AOD) below 0.1) day is shown in Figure 5.1.8.1. It can be seen that except for the H_2O all trace gas absorptions are very low but the fit gives confidence in the overall measurement quality. The daily variation of the dSCDs for NO_2, HCHO and O_4 for 22 Jan 2020 (cloudless, AOD below 0.1) is presented in Figure 5.1.8.2 and Figure 5.1.8.3. Data between 12:03 and 12:38 has been removed due to the smoke from the chimney of the ship being blown into the field of view. Also data where solar zenith angle is larger than 75° is excluded.

Since dSCDs depend on the elevation angle of telescope, solar zenith angle and weather conditions it is not useful for data comparison and further analysis steps are required. The MAinz Profile Algorithm (MAPA) [Beirle et al., 2018] will be used to provide aerosol extinction profiles, aerosol optical depths as well as vertical column densities and concentration profiles for different trace gases. MAPA uses radiative transfer simulations to estimate the light paths through the atmosphere and thereby retrieve profile information on aerosol extinction and trace gas concentrations. A more detailed investigation for trace gases will be performed after the ship campaign in order to provide complete profile data for all species. For the derived data set potential links to natural marine sources will be investigated.

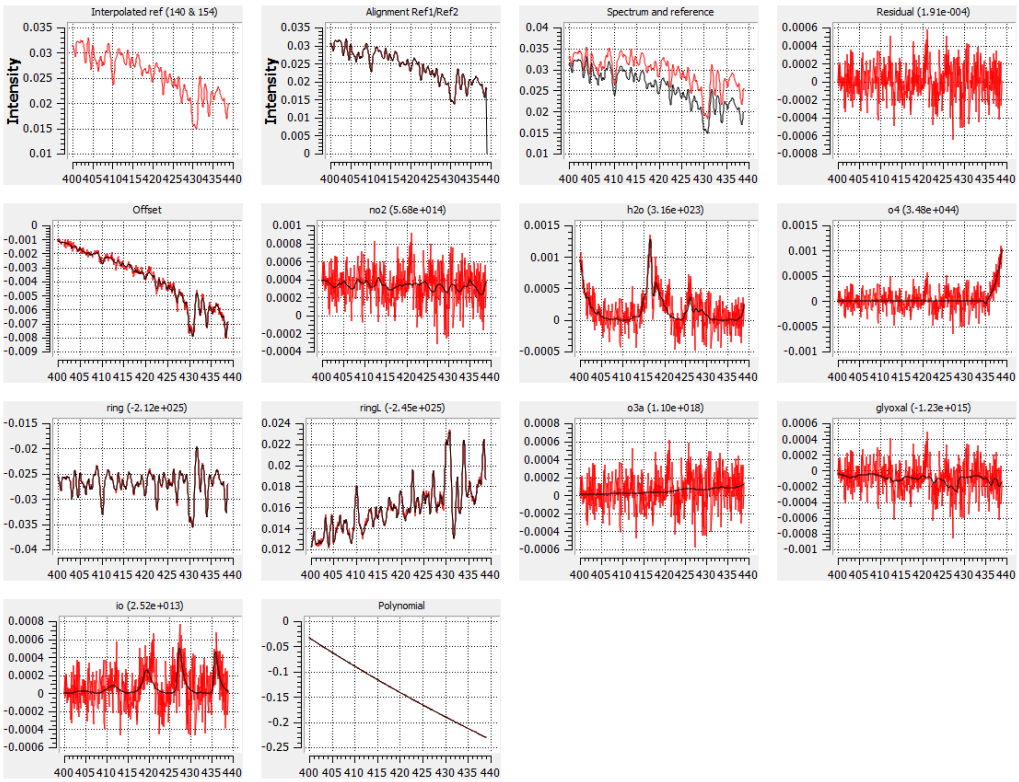

Figure 5.1.8.1 NO_2 DOAS fit results on 26 Jan 2020 from data analysis with QDOAS software. The black lines indicate the fitted spectra, the red lines indicate the corresponding spectral features detected in the MAX-DOAS spectra.

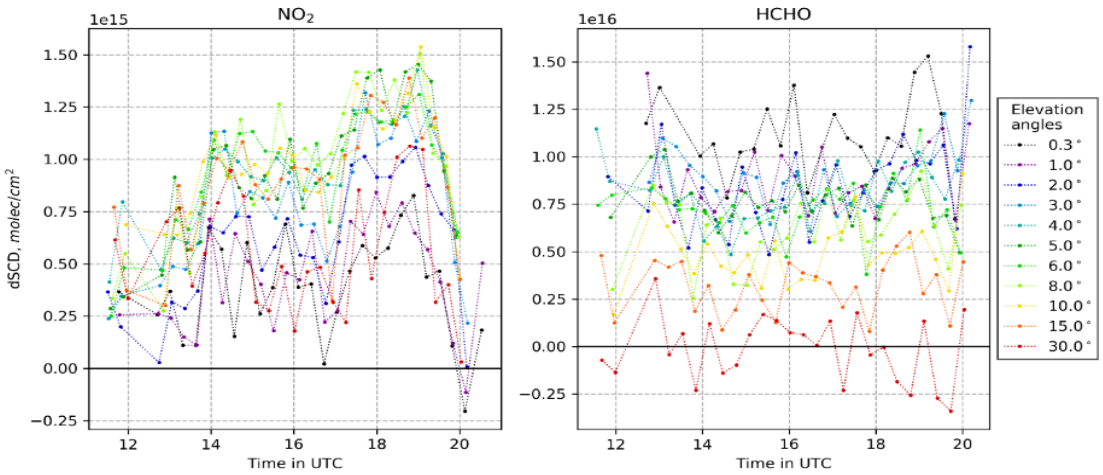

Figure 5.1.8.2 dSCDs of NO_2 and HCHO on 22 Jan 2020 as retrieved from Tube MAX-DOAS spectra of scattered sunlight.

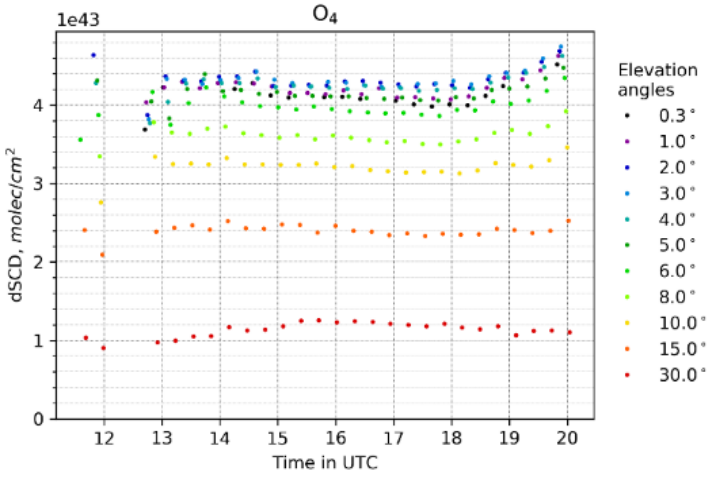

Figure 5.1.8.3 dSCDs of O_4 on 22 Jan 2020 as retrieved from Tube MAX-DOAS spectra of scattered sunlight. The high O_4 dSCDs at low elevation angles indicate very long atmospheric light paths.

5.1.9 In-situ Aerosol Measurements

(A. A. Ubele, M. Pöhlker, O. Krüger, T. Könemann)

A Wide Range Aerosol Spectrometer EDM 665 (WRAS) was operated during EUREC^{4}A in the trade winds of Barbados from 18 Jan 2020 to 03 Mar 2020. The WRAS consists of two instruments to measure aerosol size distributions from 5 nm to 32 µm in 71 particle size channels with a time resolution < 3 minutes. (i) The Scanning Mobility Particle Sizer (SMPS+C) with a butanol condensation particle counter (CPC) for nanoparticles and (ii) the Environmental Dust Monitor (EDM 180) sizing the fraction from 0.25 to 32 µm. In addition, a standalone CPC was measuring the total aerosol number concentration (with 4 nm as lower cut off) in a 1 Hz time resolution. In addition to the aerosol measurements, basic associated meteorological data were captured such as humidity, pressure, wind speed, wind direction, and rain volume. The data acquisition was done by using the SMPS+C, EDM 180 and CPC as well as the WRAS software from GRIMM Aerosol Technik. Pre-processed data from the GRIMM software as well as the raw data is available. The processed data is corrected for double charge as described by Wiedensohler (1988), the DMA

transfer function and for diffusional wall loss of particles as described in e.g. Rose et al. (2010) and Pöhlker et al. (2016). The aerosol number concentrations during the first week of the M161 cruise (from 18 Jan 2020 to 23 Jan 2020) are shown in Figure 5.1.9.1a. The timeline is interrupted by some periods when the data acquisition failed. These gaps can be filled by the integral of the aerosol size distribution shown in Figure 5.1.9.1b.

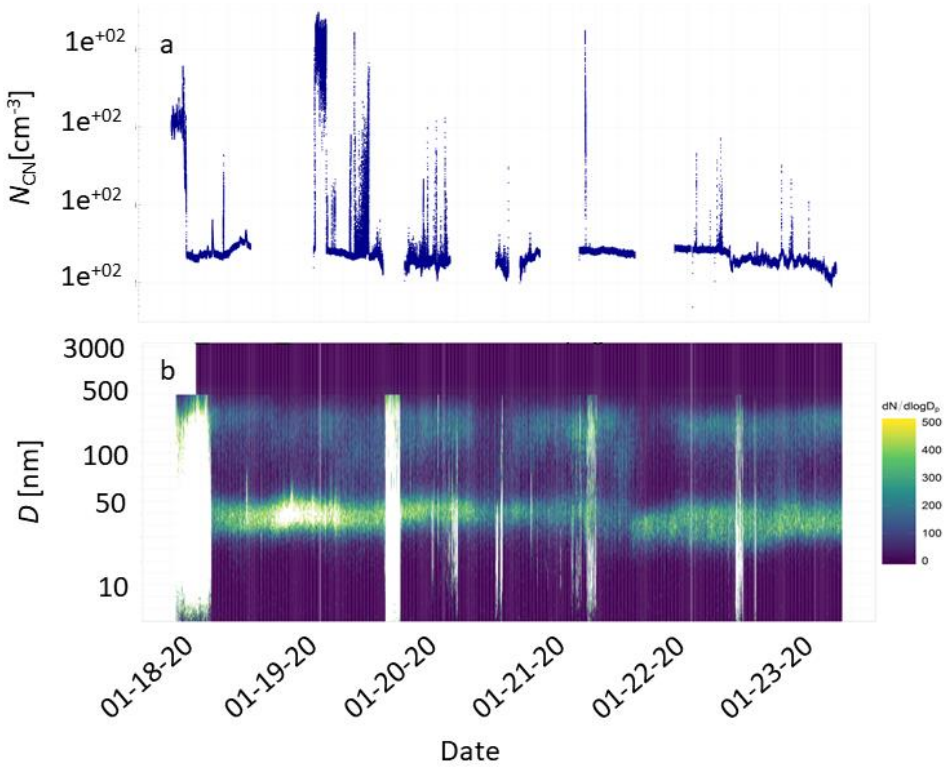

Figure 5.1.9.1 **a)** CPC data and **b)** SMPS and EDM data measured during M161 from 18 Jan 2020 to 23 Jan 2020.

Few hundred particles are measured which is typical for marine background conditions [Wex et al., 2016]. The aerosol size distribution shows a dominant Aitken (radii between 0.005 and 0.05 µm) and accumulation (radii between 0.05 and 0.5 µm) size modes. The total aerosol number shows some periods with very high concentrations. These episodes are likely enhanced by extra aerosol particles from the smoke stack exhaust or other anthropogenic emissions of R/V METEOR and will be carefully checked and marked in the final dataset. The coarse mode particles, larger 500 nm stand for a small number fraction but a significant fraction of the aerosol mass and surface area. These data products will be processed and available in a final data set.

5.1.10 PAX & LOCOMOTIVE aerosol in-situ

(P. Makuch, M. Chilinski)

The Photoacoustic Extinctiometer (**PAX**) is a sensitive, high-resolution, fast-response instrument for measuring aerosol optical properties relevant for climate changes and carbon particle sensing. The instrument directly measures in-situ light absorption and scattering of aerosol particles, from which it derives extinction (attenuation losses), single scattering albedo (the relative absorption strength) and black carbon mass concentration. The PAX uses a modulated diode laser to

simultaneously measure light scattering and absorption. A nominal 1 liter/min aerosol air sample is drawn into the PAX using an integral vacuum pump controlled by two critical orifices. The flow is split into a nephelometer and a photoacoustic resonator for simultaneous measurement of light scattering and absorption. The absorption measurement uses in-situ photoacoustic technology.

The **LOCOMOTIVE** (LOw COst air quality MOnitoring on atlanTIc - Verification and Evaluation) project was dedicated to evaluation of performance of low-cost air quality measurement stations and yielded simple and cost-effective set of sensors. Each instrument is equipped with (1) two Plantower PMS7003 particle counters (retrieving PM_1, PM_2.5, PM_10 and particle counts in 6 size bins), (2) a HTU 21 thermometer and hygrometer combination, (3) a BMP280 barometer and (4) data logger (with 8 GB of internal memory and possibility of live data streaming/syncing through Ethernet or WIFI).

The evaluation during the M161 cruise over the western Atlantic will allow an verification on how those LOCOMOTIVE instrument sets perform in harsh, humid and hot marine environment with dominant role of larger super-micron size (‘coarse-mode’) aerosol particles, such as sea salt (from bubble bursting) of especially mineral dust transported from the Sahara. Results obtained from the LOCOMOTIVE station were compared to results from the WRAS system (GRIMM EDM180) and from the Photoacoustic extinctiometer (PAX). Based on dynamic of signals and measured values by different devices it will be possible to propose correction algorithms.

Preliminary results from Saharan dust event show that low-cost station reports very similar dynamics of the event as scientific grade devices, as illustrated in Figure 5.1.10.1. Pearson correlation between PM_{10} minutely means reported by GRIMM EDM180 and LOCOMOTIVE station during first part of EUREC^{4}A campaign was 0.87+/-0.02.

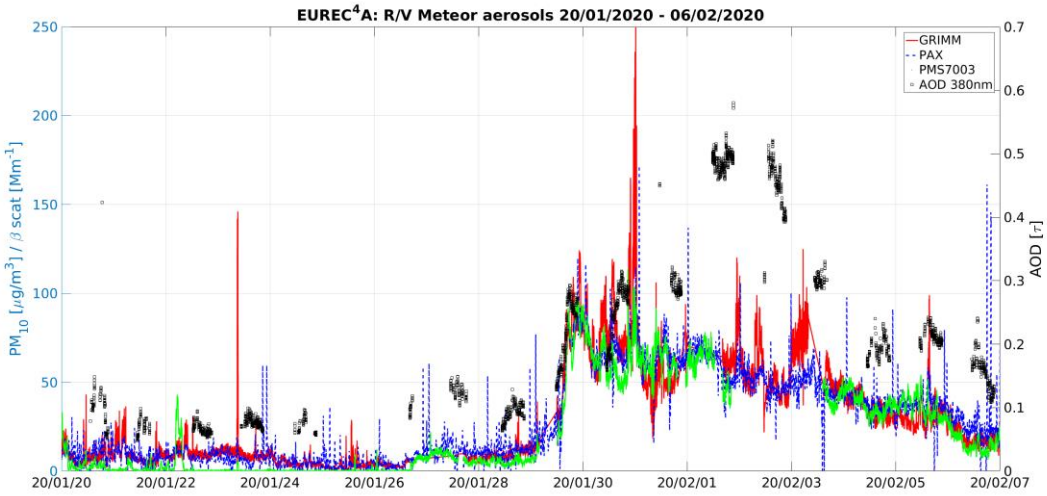

Figure 5.1.10.1 Data comparison from GRIMM, PAX, PMS 7003 and AOD 380 nm (Microtops) in the time of first dust event during EUREC^{4}A campaign.

Data from LOCOMOTIVE during M161 were collected from 17 Jan 2020 to 17 Feb 2020. Total data availability in that period is 81% (604 hours out of 744). Maintenance of the station during the experiment took only 1 hour. Most of the time when data were unavailable are related to lack of power unrelated with operation of the instrument set. All LOCOMOTIVE sensors

remained fully functional in the whole period. The instrument set was removed for cleaning on 17 Feb 2020. On unprotected wires connecting sensors to data logger were visibly rusty, but they did affect the operation of the instrument set. The collected LOCOMOTIVE data during the EUREC^{4}A campaign are summarized in Figure 5.1.10.2.

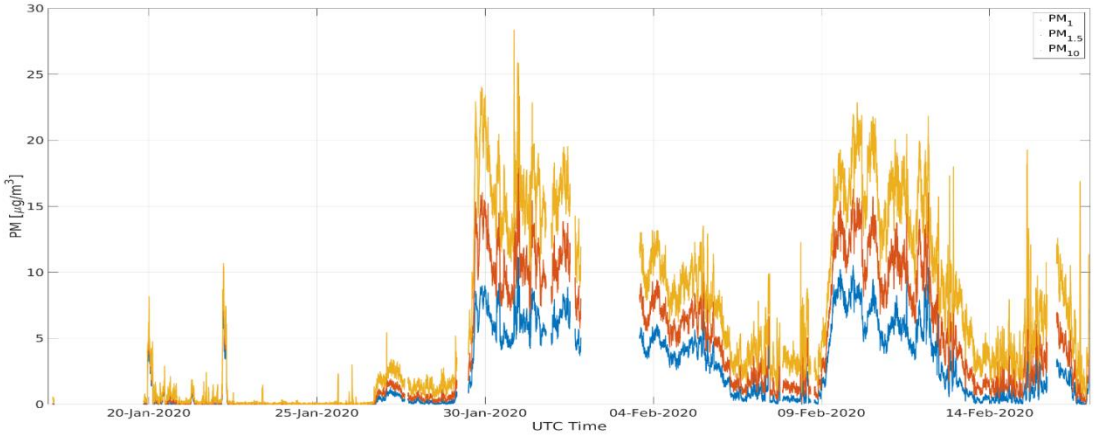

Figure 5.1.10.2. LOCOMOTIVE data during the EUREC^{4}A campaign: PM_1, PM_2.5 and PM_10.

Data from PAX, which in contrast to LOCOMOTIVE was placed inside and fed by an inlet, were collected continuously over the entire cruise. A data summary is shown in Figure 5.1.10.3.

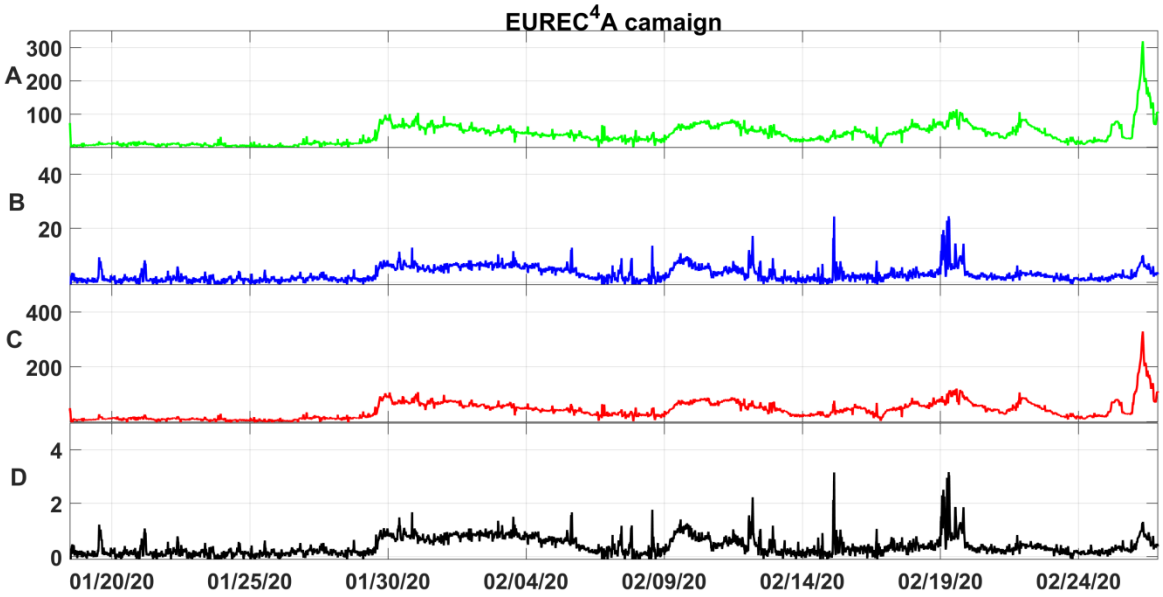

Figure 5.1.10.3 PAX data during the EUREC^{4}A campaign: A – scattering [Mm^{-1}], B – absorption [Mm^{-1}], C – extinction [Mm^{-1}] and D – Black Carbon (BC) mass concentration [μg/m^3].

Simple particle counters used in LOCOMOTIVE project base their PM measurements on fast scattering measurements (over million samples per second). Thus, it is expected to observe high level of correlation between PM values and scattering coefficient reported by PAX. Comparisons of hourly PM means of PAX and LOCOMOTIVE are presented in Figure 5.1.10.4. Pearson correlation coefficient between hourly averaged scattering coefficient from PAX and PM_10 from PMS7003 was r = 0.95 +/- 0.01. Due to high level of noise in PAX data correlation coefficient based on minutely means was much lower (r = 0.68 +/- 0.01).

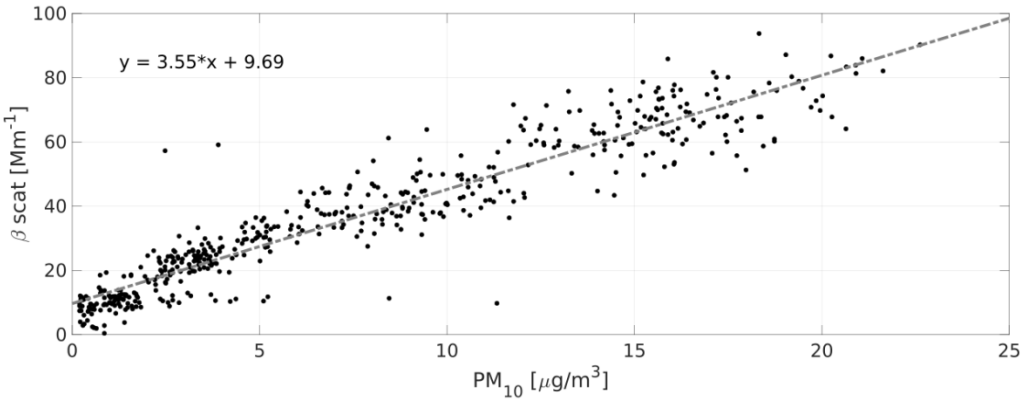

Figure 5.1.10.4 Comparisons of derived scattering coefficients from PAX and LOCOMOTIVE. A given is the linear fit equation yielding the dashed line.

5.1.11 Radiosondes

(K. Baier, I. Schirmacher, Y. Morfa-Avalos, A. Neuberger, G. de Groot, K. Helfer, S. Los, J. Röttenbacher)

The primary aim of the EUREC^{4}A campaign was to gain a better understanding of the processes and mechanisms controlling the interactions between shallow trade-cumuli and tropical circulation. For this purpose, the atmospheric state profiling radiosondes were launches during the entire duration of the campaign from 18 Jan 2020 to 17 Feb 2020. Sounding is a rather traditional observational technique, yet a reliable method for constructing an accurate first guess of the thermodynamic state of the large-scale atmosphere at all levels within the troposphere. The planned schedule for the launches was to deploy four-hourly radiosondes meaning six radiosondes per day (02:45, 06:45, 10:45, 14:45, 18:45 and 22:45 UTC), where the descending profiles were also included, giving an approximated time resolution of 2 hours. In addition, also ascending profiles from 16:30 UTC on were samples with an extra DWD radiosonde launch. These atmospheric profiling observations are complemented by radiosondes launched from the three other research vessels participating in the campaign (R/V MARIA S. MERIAN, R/V RONALD H. BROWN, R/V L'ATALANTE), radiosondes at the BCO site on the east coast of Barbados and dropsondes deployed from the HALO and the NOAA-P3 aircraft in the operation field. The data offers high-frequency sampling and high spatial coverage of the study area in accordance with the desired goals given the spatio-temporal scales of shallow convection and its representativeness of the variability of the tropical large-scale atmospheric environment.

Technical description. In order to launch a radiosonde, first a ground check is required. The ground check was done at the air-chemistry laboratory on the ship, which is located at around 18 m above sea level, as shown in Figure 5.1.11.1 in Appendix 12.2. During the installation process the transmitting frequency was set to 401.5 MHz, assigned to the R/V METEOR. The needed ground data prior to a launch (air pressure, air temperature, relative humidity, wind speed, wind direction and sea surface temperature) were provided by the on board DWD weather station. The antenna for the signal was placed on top of the upper deck air-chemistry lab. The preparation of the balloon and the final launching of the radiosonde took place at the weather container of the

DWD on the ship, 8 m above sea level. For the purpose of homogeneity, a marker in the container defines the optimal amount of helium to fill into the balloons, therefore all the balloons were filled with the same amount. After 09 Feb 2020, the launcher system was changed, since the DWD launching container needed repairs. Therefore, the launching system of the University of Hamburg was installed on the working deck, directly at the stern around 2 m above sea level. Contrary to the DWD container, the balloons were now launched manually. The filling of the balloon with helium was more variable, since only an awning was used for deciding if the balloon had the appropriate amount of helium. This system was used until the end of the campaign. Due to the environment of the ship and the presence of several obstacles, some difficulties occurred while manually launching the radiosondes, for which, special awareness needed to be taken. One of the main problems was the direction of the wind relatively to the ship, especially the occurrence of winds from stern and moderate turbulence. Since the DWD container is located on the port side of the ship, the possibility of the balloon being entangled was encountered sometimes. Therefore, before launching the radiosonde, one had to make sure that the wind came from the front of the ship while at a station or the launcher was upstream while cruising. An effort was made to ensure that the wind direction was from starboard for which the ship needed to turn at our request whenever it was possible. The Cloud Kite (CK) from MPI-DS represented another difficulty, since the balloon could get entangled in the line of the kite. The higher the position of the CK the higher the chances of the radiosonde impacting or getting caught in the line of the balloon, as it was particularly difficult for us to determine the direction of the wind relative to the ship offering the lowest risk.

The measurement data was recorded by the Vaisala software. The data output is an arbitrary formatted buffer file, that does not follow any conventional meteorological data type. Two types of raw data output are taken from the software (BUFR309056 All Levels, BUFR309057 All Levels), one for the ascending and another for the descending profiles. A python package developed in advance was used to convert these data into netCDF files with CF-1.7 convention. Due to some missing software dependencies and the limited internet connectivity on board, minor modifications had to be done on the code without the use of any version-control software. However, special care was taken to ensure that all the data has compatible structure and format and is easily readable. The netCDF files include the following variables: flight-time, ascent rate, altitude, air pressure, air temperature, relative humidity, dew point temperature, water vapor mixing ratio, wind speed, wind direction, latitude and longitude; along with the following metadata: launch starting time and location, name of the launching platform, direction of the sounding, probe name and serial number. In order to visualize the data a Skew-T diagram showing the vertical profiles of temperature and the dew point temperature, was created for each launch (see Figure 5.1.11.2). From that an immediately statement about the current atmospheric situation can be made. Converting the buffer files to netCDF files and generating the Skew-T diagrams was a daily work routine on the ship during the campaign.

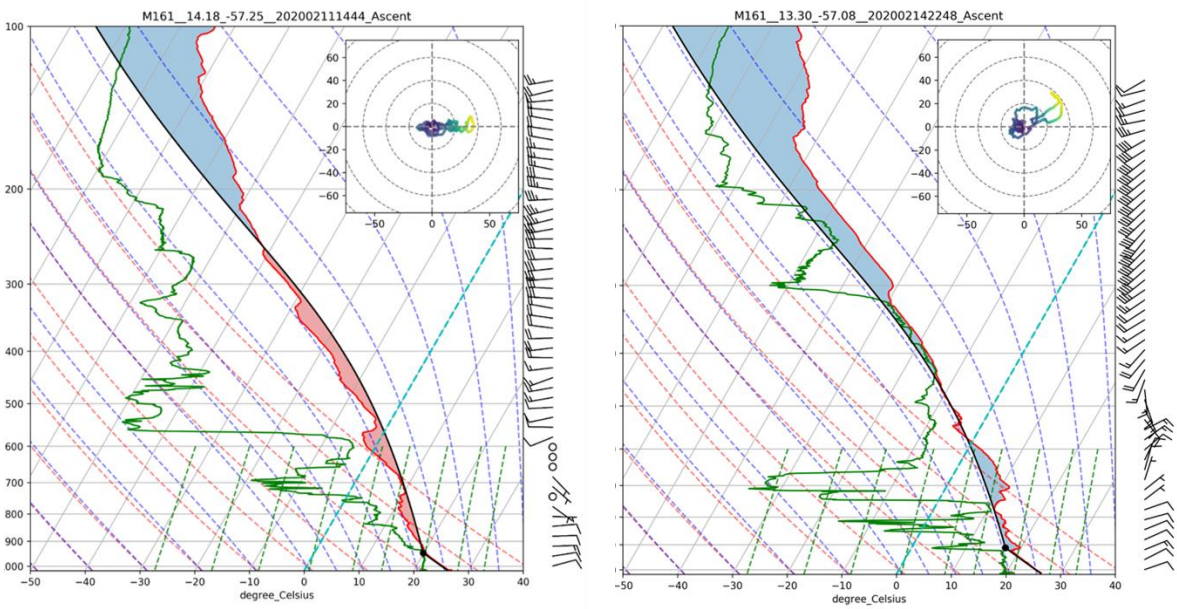

Figure 5.1.11.2 Example of Skew-T diagrams from 11 Feb 2020 at 14:45 UTC (left) and from 14 Feb 2020 at 22:48 UTC (right). Showing the air temperature as a red line and the dew point temperature in green. Lines of constant mixing ratio, dry and moist adiabats are also included. The theoretical parcel profile is shown in black. On the right side the wind direction and wind speed are shown. The box at the upper right on each figure shows the wind hodograph.

During the span of 30 days of measuring, 182 (171 in core working area and 11 during the transit) successful radiosondes were launched. By incorporating the 29 radiosondes launched by the DWD during this period, 200 radiosondes in total were launched on the R/V METEOR during the entire campaign. A total loss of six radiosondes occurred including two defective probes form the manufacturer, and six radiosondes did not measure the descending trajectory. Due to an overpassing HALO flight on the 19 Jan 2020 and the lack of measurement permission in Trinidad and Tobago on the 03-04 Feb 2020, one measurement is missing for each day. Most of the balloons reached an altitude between 23 and 26 km. The highest balloon was launched on the 10 Feb 2020 at 18:45 UTC and reached a height of 28.8 km, while the lowest altitude reached was 14.2 km on the 06 Feb 2020 at 18:45 UTC. Preliminary data comparison among different instruments onboard was also performed during the campaign, especially, the predicted cloud base from the Lifting Condensation Level (LCL) and the observed Cloud base from the Ceilometer. Figure 5.1.11.3 shows vertical cross-sections of relative humidity and observed cloud base data. The ascending and descending profiles overlapping with the CK flight times were also compared showing good overall agreement, as shown in Figure 5.1.11.4. After the end of the official EUREC^{4}A campaign one radiosonde was launched per day. So measurements from 19 Feb 2020 until 01 Mar 2020 were operated. These radiosonde data was also used by the DWD for forecasting (and uploaded on the GTS).

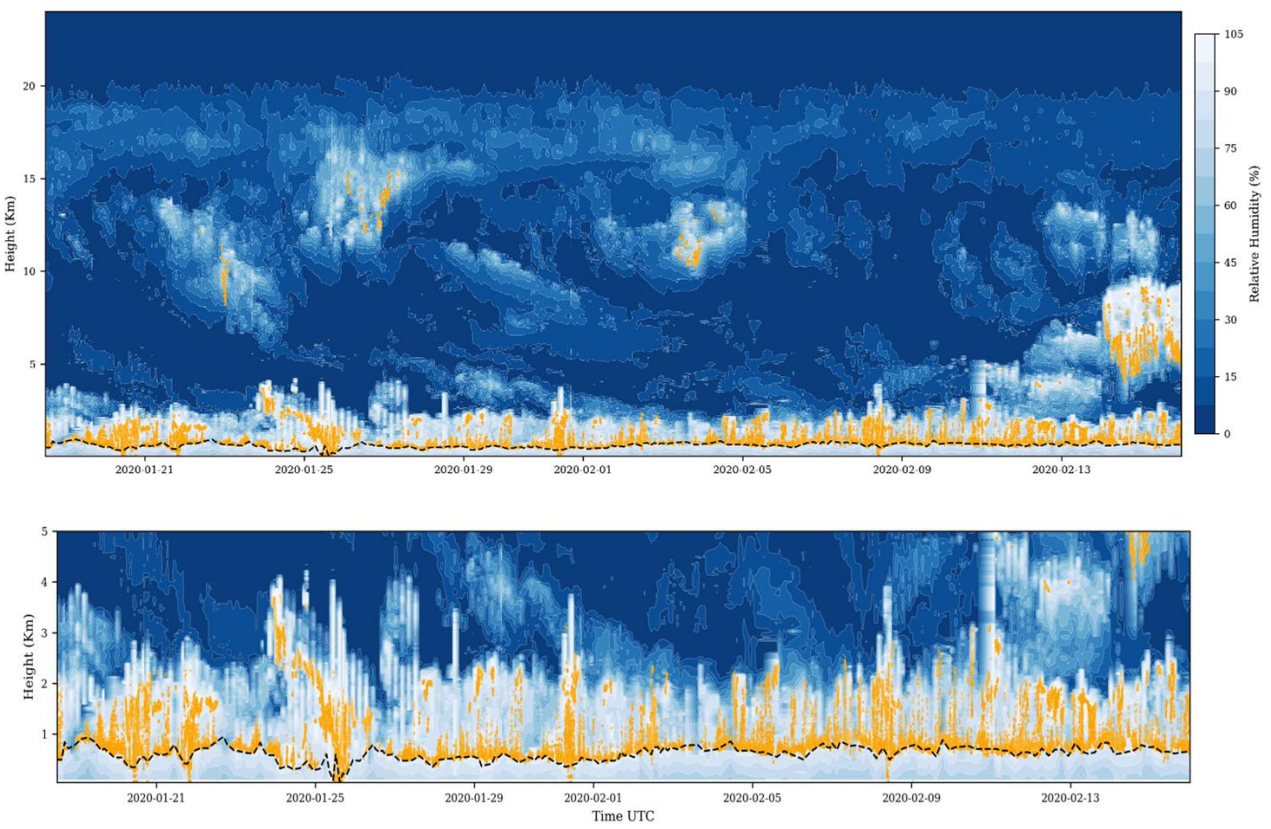

Figure 5.1.11.3 Upper panel shows the time evolution of the vertical profiles of relative humidity including all radiosondes during the campaign on R/V METEOR. The data was vertically interpolated to regular levels with a resolution of 10 m. Showing the relative Humidity (%) in shaded contours. The dashed line represents the Lifting Condensation Level calculated by the radiosonde data using parcel theory. In yellow dots the cloud height base as observed by the ceilometer data is shown. Lower panel represents a zoom into the first 5 km altitude.

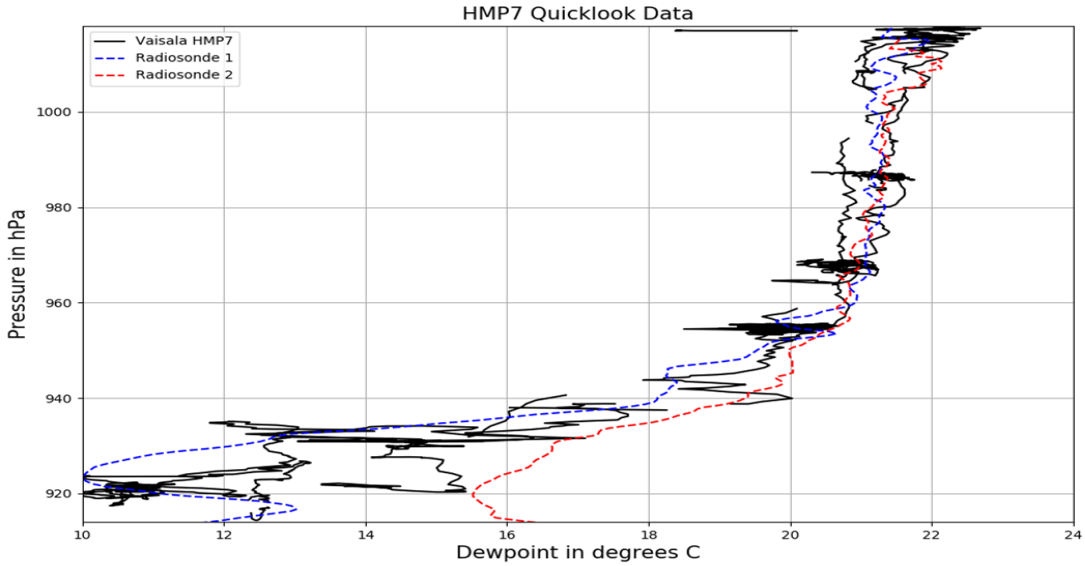

Figure 5.1.11.4 Dewpoint temperature profile measured form the ascending and descending radiosonde launched on 30 Jan 2020 at 06:45 UTC with blue and red lines respectively. The solid black line shows the dewpoint measured by the HMP7 sensor on the Cloud Kite.

5.1.12 UAV

(D. Baranowski, M. Chilinski, W. Szkolka, R. Grosz, J. Nowak; in collaboration with P. Flatau and J. Schmidt)

The UAV system with atmospheric and oceanic payload was used during EUREC^{4}A to assess stratification and its diurnal variability of the low atmospheric boundary layer (from surface to 500 m) and upper ocean (from surface down to 5 m). This was one of the first such quad drone deployments from a research vessel which included near simultaneous oceanic and atmospheric profiling.

UAV: A drone used during the experiment was manufactured by DJI and is classified as an ultra-small multirotor (quadcopter) remotely piloted aerial system with take-off mass below 1 kg. The drone uses 4 plastic quick-release folding propellers 8330 (21.08 cm diameter, 7.87 cm thread). For safety reasons the drone was equipped with propeller guards – plastic rims, protecting propellers in the horizontal axis. The payload was attached to the top of the quadcopter on specially designed 3D printed spacer. The total weight of the whole system was 0.89 kg. The DJI Mavic PRO is powered by 3S (11.4V) lithium-polymer batteries with 3830 mAh capacity, which were sufficient for approximately 12 minutes of flights during meteorological conditions characterized by strong winds during most of the experimental period. The operational range was limited to a radius of 500 meters from a starting point on a ship. The ascent rate was below 4 m/s and the descent rate had a limit set to 3 m/s. The horizontal speed was limited in software to 12 m/s, but because we were performing mostly vertical profiles, this limit on horizontal speed was never reached. The drone was controlled manually during all flights by an operator. A dedicated 2.4 GHz controller was used with a smartphone with the DJI Go software. To improve flight safety, video goggles were used by operators on occasion. Such goggles allowed easy verification of the flight parameters and drone position, especially during strong sunlight hours. The drone had an integrated video camera, which was used to record videos and pictures and to document drone operations.

Atmospheric payload: InterMet (iMet) XQ-2 temperature, humidity, pressure, GPS and time logger was used to measure atmospheric conditions. It is small (16 x 6 x 2 cm), lightweight (60 g) and a self-contained instrument, which logs data with 1Hz frequency and with a response time of less than 1sec. The iMet XQ2 has the following components

- 1200-10hPa for pressure sensor (digital piezoelectric, Measurement Specialties, model MS5607; accuracy +/- 1.5 hPa)
- -40 – +50 °C for temperature sensor (NTC Thermistor, Shibaura, model PB5-41E; accuracy +/- 0.3 °C)
- 0-100% for relative humidity sensor (digital capacitive, Innovative Sensor Tech., model HYT 271; accuracy +/- 5%)

The IMET XQ2 datalogger can operate continuously for up to 5 hours on a single charge; the total storage allows recording of approximately 18 hours of data. During M161 iMet XQ2 data were downloaded and quality controlled after each station during which the measurements were collected. Measurement set up included cross calibration periods between three iMet XQ 2 loggers. For stations 1- 239 a single iMet-XQ2 logger was used for the UAV measurements (s/n 58757).

After deterioration of the humidity sensor of this unit, it was replaced with one of the spare loggers (s/n 58746). This deterioration was noted in near real-time by comparisons of the sUAS vertical profiles with ship rawinsonde releases (Schmidt). The instrument was mounted on top of the UAV, above its front part (close to the camera). It was attached to a small box, which positioned the instrument above rotors with safe clearance from the wings. Figures 5.1.12.4 in Appendix 12.2 and 5.1.12.5 in Appendix 12.2 show iMet-xq2 instrument mounted on a drone.

Oceanic payload: Oceanic payload consisted of two instruments HOBO U24-002 temperature and conductivity logger and RBR duet temperature and depth logger (instrument from NRL Monterey, PI Jerome Schmidt). The instrument was lowered from the UAV on a tethered line of fixed and known length of 9.92m. The HOBO logger records temperature in the range of 5 – 40 °C and conductivity in the range 0 – 5.5 S/m at 1Hz frequency. The time response for temperature is less than 5sec. The upper limit of conductivity range of HOBO sensor was lower than the near surface conductivity measured by the ship-borne CTD. However, with combination with the known length of the tethered line and UAV's altitude, the sampling depth can be determined. Because the upper 5 m oceanic layer does not exhibit significant variability of conductivity, these limitations of the HOBO salinity measurements are not considered an issue. The RBR duet logger records temperature in the range of 5- 40 °C and has a depth sensor chosen for upper ocean measurements (depth limit of 15 m) at 2Hz frequency and its time response is less than 1 second. An important difference between the two instruments is the placement of sensors. HOBO's sensor is mounted in the body of the instrument, whereas RBR's thermistor is located at the top of a narrow needle. Therefore, inertia of HOBO instrument is expected to be larger than that of RBR. However, to a certain degree, a continuous flow of water is expected to mitigate instrument's inertia issue.

UAV operations require sufficiently large and obstacle-free area for take-off and landing. During the M161 cruise, the helipad of the R/V METEOR was selected due to its relatively large, even surface and unobstructed view to the starboard side. To mitigate magnetic interference from the surface, a wooden palette was used to isolate drone from the metal deck (Figure 5.1.12.2 in Appendix 12.2 and 5.1.12.3 in Appendix 12.2). Taking off and landing required that the area was free of unnecessary clutter. The typical procedure involved a fast, vertical ascent and flying the UAV to the starboard side of the ship. A typical horizontal range of operations was 50-100 m upwind from the ship.

There were four types of flights performed during the M161 cruise. Three of them included atmospheric measurements:

- A vertical profile from the near surface (about -5 m relative to the helipad) to predefined altitude (200 m, 300 m or 500 m). Typical vertical ascent velocity was 4 m/s and descent velocity was 3 m/s. However, measurements with slower profile speeds were performed as well.
- A Vertical profile to 300 m with stepwise descent and 1 min stops at multiple levels (typically we stopped at 300 m, 250 m, 200 m, 150 m, 100 m, 75 m, 50 m, 23 m). One purpose of these was to measure l winds.
- 'Tilted' profile from near surface to 50 m or 100 m during which vertical and horizontal velocities were roughly the same – an operator tried to maintain both horizontal and vertical velocities to be equal.

All of these flights were performed with an atmospheric payload positioned to the upwind direction. The fourth type of flight was an oceanic profile with an oceanic payload, either HOBO or RBR instrument tethered to a 10 m long thin line. A special care was given to take off and landing in this configuration. During the take-off, the payload operator holds an instrument, while the UAV operator gently ascended and moved the vehicle to the starboard side. The measurement probe was gently let go to avoid unnecessary swing. During approach and landing these precautions were maintained as well. First, the payload operator caught the probe and decreased the tension on the line to allow the UAV operator to safety land. A special care was given to swell to avoid any uneven strain on the line and the unexpected pull of the vehicle.

Oceanic flights were typically composed of more than one profile, but it depended on the battery drainage level. The landing procedure was initiated at a battery level of 35% and UAVs were landed with no less than 20% the full battery capacity. Landing was the most difficult part of all the operations because the deck moved when the ship pitched and rolled. Following the DJI company safety rules all flights were performed when the sustained wind was below 10 m/s. We performed 141 flights during which drones were operational for 31 hours at 68 different oceanic stations. All measurements were done at the same times as the CTD measurements.

Data processing iMet XQ2 data were downloaded in ASCII format. RBR and HOBO data were downloaded, processed and exported to ASCII format using designated software: Ruskin and HOBOware, respectively. Further processing and plotting was done using Matlab environment. DJI Mavic Pro's log files were downloaded and processed using DJI Log Viewer.

Atmospheric Profiles Total of 129 atmospheric ascending and descending profiles were performed with top altitude ranging from 50 m to 500 m. Figures 5.1.12.6 and 5.1.12.7 present all profiles collected during January 24, 2020. Each of the subfigures shows all profiles performed at a single station within approximately one hour. Rawindsonde data from the nearest upper air sounding performed on R/V METEOR are plotted when the near surface data are available. Comparisons between the UAV profiles and the rawindsonde data show good agreement in temperature. Discrepancies within UAV RH profiles are within the instrumental accuracy of 5%. The results for 24 Jan 2020 show evolution of the thermodynamical structure of the lower troposphere throughout the day. The morning profiles show surface temperatures of about 25.0-25.5 °C and 300 m (990 mb) temperature of 23.5-24.0 °C. Later, the entire profile structure shifts towards the higher values. Later during the day temperature reaches 26.0 °C at the surface and exceeds 24.0 °C at 300 m. RH profiles evolution, is small and stays within the accuracy range of iMet-XQ2 instrument.

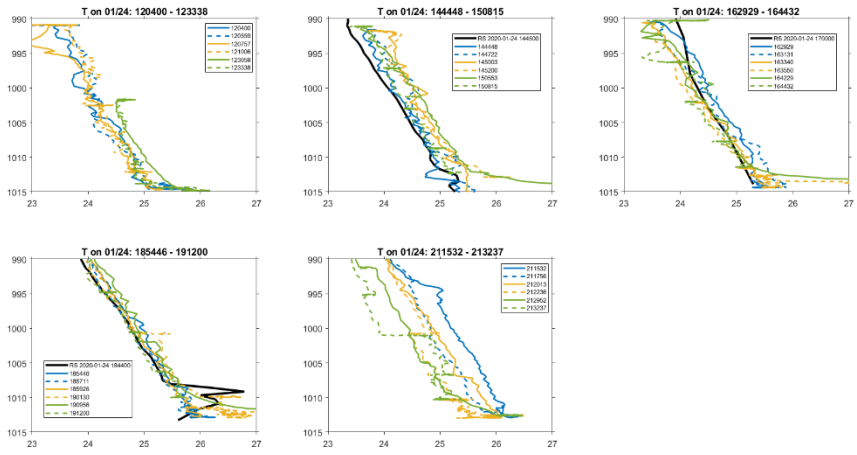

Figure 5.1.12.6 Temperature profiles from all UAV flights on 24 Jan 2020. Ascending profiles are marked with solid lines, while descending are dashed. Each panel presents all profiles at a single station.

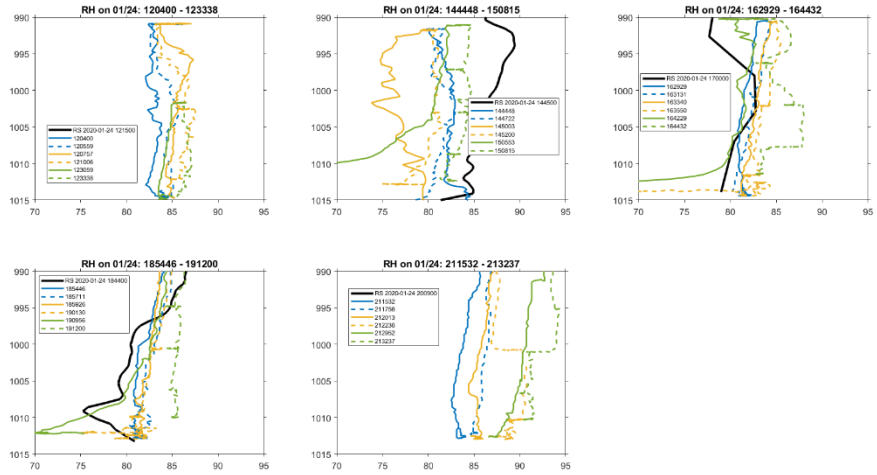

Figure 5.1.12.7 Relative humidity profiles from all UAV flights on 24 Jan 2020. Ascending profiles are marked with solid lines, while descending are dashed. Each panel presents all profiles at a single station

Wind profiles Flights dedicated to wind measurements usually took around 10 minutes and had several stops at different heights for about 60 seconds each. The typical heights were: 23 m which corresponded to the location of R/V METEOR anemometer, 50, 75, 100, 150, 200, 250 and 300 m above take-off point. To estimate wind direction and velocity from the Mavic Pro UAV a simple model based on tilt and motors power consumption was used. Model fitting was performed by comparisons with an on-board meteorological station. Such intercomparisons were performed only when the vessel was stationary and winds were averaged over a 1-minute interval. During the EUREC^{4}A campaign total of 345 data points dedicated to wind estimation algorithm (velocity and direction) were collected.

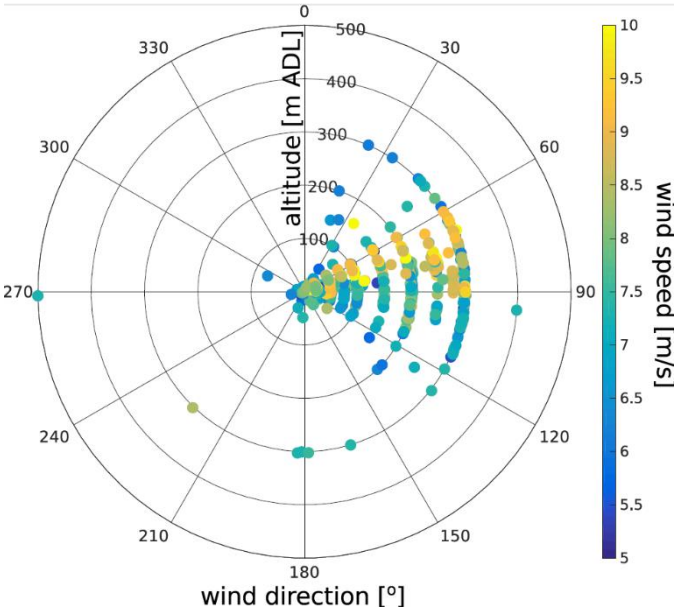

Figure 5.1.12.8 Wind velocity and direction for different levels above home point. Wind direction in degrees is presented as theta angle, radius visualize altitude and color of circles represents wind velocity.

Ocean Profiles

Two ocean profiles were performed. First profiling measurements were performed using the Hobo instrument. During the second set of profiling, both Hobo and RBR instruments were deployed. The data from the Hobo and RBR agree with each other. Profiles were done from the surface down to about 5.5 m. The warm layer was present in the top 3.5 m of oceanic layer and its amplitude is about 0.45 °C. Such a structure was not observed by the CTD cast performed at the same time. Right after the ocean profiling, a 500 m atmospheric profile was performed. To our knowledge, it is one of the first near-simultaneous profiles of the upper ocean (0-5 m) and the lower troposphere (0-500 m) done from a research vessel. These flights help contribute to one of the main objectives of a recent NRL-based research initiative. Figure 5.1.12.9 shows this combined ocean and atmospheric profile. The gap between profiles represents about 5 m distance which was not sampled. The oceanic warm layer surface anomaly of about 0.45 °C is present. The ocean surface temperature is over 1 °C warmer than the atmospheric temperature at 5 m above the surface. The near surface RH was 72% and increased to 82% at 970 mb. A linear decrease of temperature with height is observed.

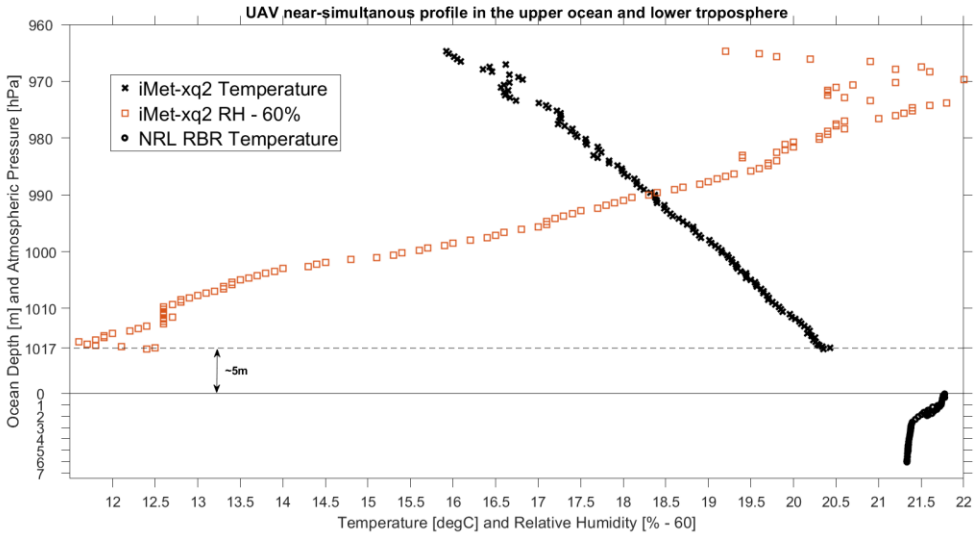

Figure 5.1.12.9 The first near-simultaneous profile of the upper ocean temperature and lower tropospheric temperature and RH. Ocean temperature (black circles) measured by NRL RBR, atmospheric temperature (black 'x' markers) and atmospheric RH (red squares) measured by iMet-xq2 immediately after ocean profile was finished.

5.1.13 Cloudkite

(M. Schröder, A. Ibáñez-Landeta, J. Nowak, M. Meyer, O. Schlenczek)

Objectives

Clouds are crucial for the energy balance of the Earth's atmosphere. Unresolved cloud processes are one of the reasons for the uncertainties in weather forecasting and climate modelling. The dynamics of clouds extend over a wide range of spatial and temporal scales from micrometers to km and milliseconds to hours. Besides Plinian volcanic eruptions, clouds show the highest turbulence level on earth. The multiscale properties of the turbulent flow in combination with moisture and temperature transport, phase transitions, and inertial particle dynamics present a challenge for modelling and parameterization. The main goal of the Max Planck CloudKites (MPCKs) is to overcome the scaling challenge by performing in-situ high spatial/temporal resolution measurements. During EUREC^{4}A, the CloudKite group of the Max Planck Institute for Dynamics and Self-Organization was operating two MPCKs aboard R/V MARIA S. MERIAN (MSM89) and R/V METEOR (M161).

The Mini Max Planck Cloudkite (MINI-MPCK)

The Mini Max Planck CloudKite (mini-MPCK) is a new airborne platform that measures meteorological as well as cloud microphysical properties with high spatial and temporal resolution (Table 5.1.13.1 in Appendix 12.1). The mini-MPCK comprises a 75 m³ helium-filled balloon kite combination (from Allsopp Helikites Ltd.) carrying a tether-mounted instrument for measuring atmospheric state parameters, and the number-density as well as size distributions of cloud particles (Figure 5.1.13.1 in Appendix 12.2 and Table 5.1.13.1 in Appendix 12.1). With the help of the aerostat, we can perform a variety of flight strategies such as soundings, long-term measurements at a desired height over the entire diurnal cycle or even more complex flight patterns build up out of the first two strategies as explained below. In contrast to radiosondes, we can

control the altitude via the winch and tether and, in addition, do long-term measurements. Furthermore, the difference to aircraft borne measurements is that the mini-MPCK can measure with a usually 10 to 20 times higher spatial resolution, acquire cloud droplet sizes and number concentrations of individual clouds and it is able to measure overnight independent of the flight altitude. During EUREC^{4}A, the maximal flight duration of the mini-MPCK exceeded that of the research planes by a factor of 1.5 to 2. In comparison to the operational cost of research airplanes, the mini-MPCK is a low-cost experiment that is able to access remote areas such as the ocean as it can be deployed from nearly any platform including research vessels. Furthermore, we performed long-term measurements in the atmospheric boundary layer and on the navigation deck of the R/V METEOR with the Micro Max Planck CloudKite (MICRO-MPCK). It acquires statistical data of temperature, relative humidity, true air speed as well as velocity fluctuations. The instrumentation of both platforms as well as the related measurement variables is listed in Table 5.1.13.1 in Appendix 12.1.

Flights

Our goal was to measure heat, momentum and moisture fluxes in the subcloud layer, entrainment between the inversion layer and the subcloud layer, temperature and velocity fluctuations as well as the evolution in cloud droplet number concentrations and size distributions. Thus, we performed a flight strategy that includes at least three flight legs at different constant altitudes for at least 30 min where one is at low altitude, another about 100 m below the top of the subcloud layer and the third in between. The height of the subcloud layer was determined from the most recent radiosounding from the vessel, which were typically performed every 4 hours. Depending on the weather conditions, we also performed one flight leg above the boundary layer inversion, which was followed by two soundings between the two highest flight levels. With the mini-MPCK, we performed ten flights in total whereby we acquired data in eight flights. During Flight 11 on 08 Feb 2020, the line fixing the Helikite to the working deck of R/V METEOR snapped at 09:20 UTC. After activating the cutdown/landing mechanism, a search for the balloon and instrument was performed from 10:12 UTC until 20:00 UTC. However, we could retrieve neither the balloon nor the instrument.

Preliminary Results

In total we have flown the mini-MPCK for 68 hours with the planned flight strategy. During our operations, we recorded several cloud events as depicted exemplarily for Flight 10 in Figure 5.1.13.3 while staying at the highest flight altitude of our flight plan. Here we present an example of some preliminary results we collected during Flight 10. It was performed on 06 Feb 2020 with the full setup and started at 13:22 UTC. This flight consists of four legs at approximately constant pressure level (Figure 5.1.13.2, left). From 13:46 until 14:28 UTC, the mini-MPCK was parked at the 993 hPa pressure level (200 m altitude), followed by another flight leg at 957 hPa (550 m altitude) between 14:48 and 15:26 UTC. Between 15:56 and 16:41 UTC, the highest flight leg at 915 hPa pressure level (920 m altitude) was done. A final flight leg between 17:44 and 18:21 UTC at 966 hPa pressure level (450 m altitude) was performed and the mini-MPCK was landed at 19:10 UTC. Figure 5.1.13.2 (right) shows the comparison of the temperatures measured by the AM 2315 and the radiosonde soundings prior to and after the flight operation. The measured temperatures appear to be consistent to each other as they show the same trend with an offset of approximately

1 ˚C modulo the fluctuations measured by the AOSONG AM 2315 during the 40 min legs at constant altitude. During the stay at the highest altitude between 920 and 910 hPa, some cloud events were encountered indicated by large variability of the dewpoint in this region measured by the Aosong AM 2315 sensor (see Figure 5.1.13.2, right). In this part of the flight, the CDP-2 detected cloud droplets proofing that the instrument box was traversing several clouds. The corresponding size distribution of the cloud particles larger than 2 µm in diameter is shown in Figure 5.1.13.3 (left) where the mean droplet diameter of detected particles along the CDP-2 path is 9.3 +/- 3.1 µm. Particle diameters below 2 µm are discarded because of signal noise caused by sea salt particles. The largest detected droplets are about 38 µm in diameter. In Figure 5.1.13.3 (right), the size distributions of the cloud events about 3 hours after takeoff are shown as a function of time. Between 3.02 h and 3.10 h, the mini-MPCK traversed three clouds whose droplet size distribution vary from one cloud to the other. While entering the cloud, both the number of droplets as well as the droplet sizes are smaller than at the center of the cloud. As the clouds were non-precipitating, the size distribution did not indicate an amplified growth of the particle mean diameter. To draw a conclusion, the mini-MPCK performed remarkably well in performing measurements in the lower atmosphere and inside clouds. With its high spatial as well as temporal resolution measurements and the ability to perform long-term measurements at a desired altitude over the entire diurnal cycle, we could acquire one of most promising atmospheric data during the EUREC^{4}A field campaign.

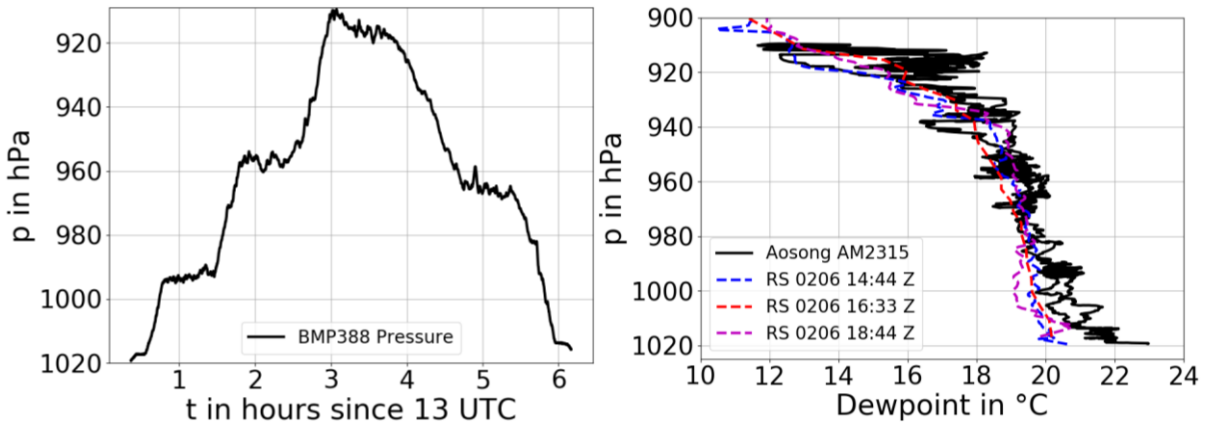

Figure 5.1.13.2 Time series of pressure (left) and profile of dewpoint vs. proximity soundings (right)

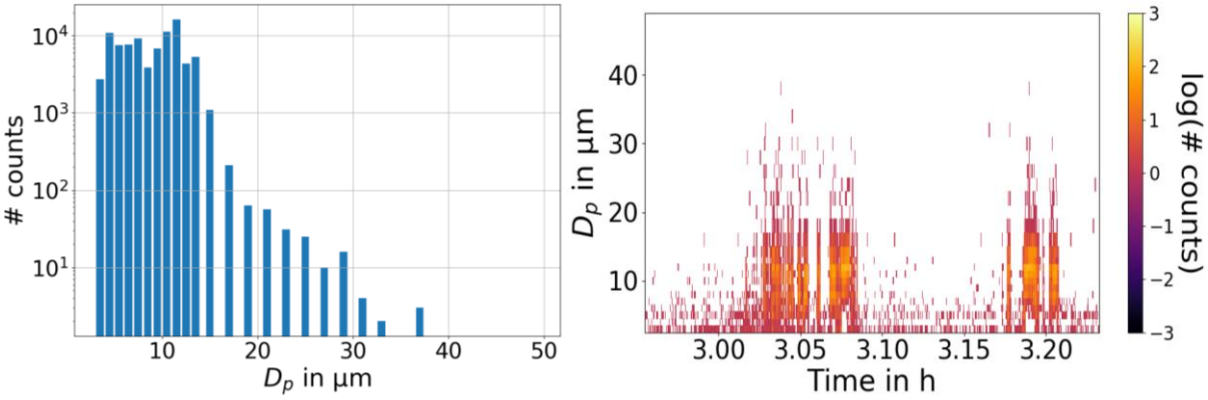

Figure 5.1.13.3 Number of cloud droplet counts as a function of the droplet size (left) and the number of droplet counts as a function of time and cloud particle size D_p of two cloud events for 3 hours after take-off. The histogram is not normalized as it shows the sum over all droplets in each bin.

5.2 Oceanographic Measurements

5.2.1 CTD operations (CTD and RODNEI)

(D. Baranowski, P. Makuch; with the help of J. Gollop, R. Grosz, K. Helfer, A. Neuberger, S. Sandiford, C. Rollo, E. Siddle, A. Ubele and W. Szkolka)

CTD systems configuration, calibration and data processing can be found in Appendix 12.1.

Total number of CTD casts: 255

Casts within EUREC^{4}A core working area: 230

Deepest cast: 4485 m

Preliminary data from M161 CTD operations.

EUREC^{4}A

Measurement strategy for M161

Ocean observations during M161 focused on upper ocean variability and atmosphere – ocean coupling. Therefore, most of CTD stations operations were performed multiple (6-8) times per day with 800 m casts. In addition to those stations, 12 shallower (250 m) night-time stations for biogeochemical sampling were conducted. Those profiles were cast soon after regular 800 m cast. Deeper (1000 m, 2000 m, full depth) casts were performed during UEA glider deployment, Argo float deployment and cross validation CTD with R/V MARIA S. MERIAN. Figure 5.2.1.1 presents map of M161 operations within EUREC^{4}A core working area. Most of CTD stations (175) were done along N-S transect along longitude 57°14.7'W. This section was repeated multiple times during northward and southward transects. Additionally, CTD station along zonal sections at latitudes 14°10.9'N, 13°18.0'N, 12°42.75'N and 12°25.126'N were performed to assess upper ocean conditions across the default M161's section. Time between two stations was roughly 3 hours during transects and 2 h 24-h diurnal cycle stations (total of 4 performed).

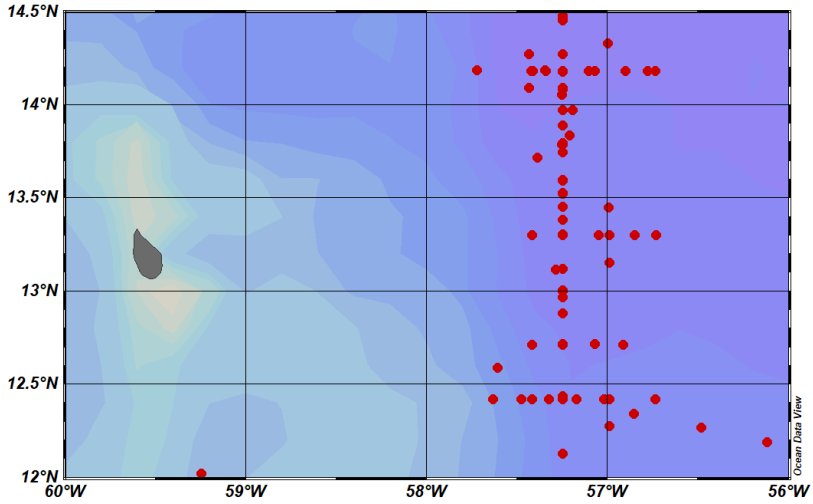

Figure 5.2.1.1 Map of all CTD stations during the EUREC^{4}A part of the M161 cruise.

Mean state of the ocean during EUREC^{4}A field campaign

Figure 5.2.1.2 presents all profiles of temperature, salinity (calculated from temperature and conductivity data), dissolved oxygen and fluorescence. Upper ocean stratification is dominated by surface salinity minimum (median value around 35.5 PSU) and subsurface maximum reaching 37.3 PSU at 120 m. Salinity stratification coincides with persistent temperature inversion. Surface temperature of about 28 °C was 0.5-1.0 °C lower than subsurface maximum below shallow mixed layer (60-80 m). Salinity maximum coincided with maximum in dissolved oxygen and fluorescence.

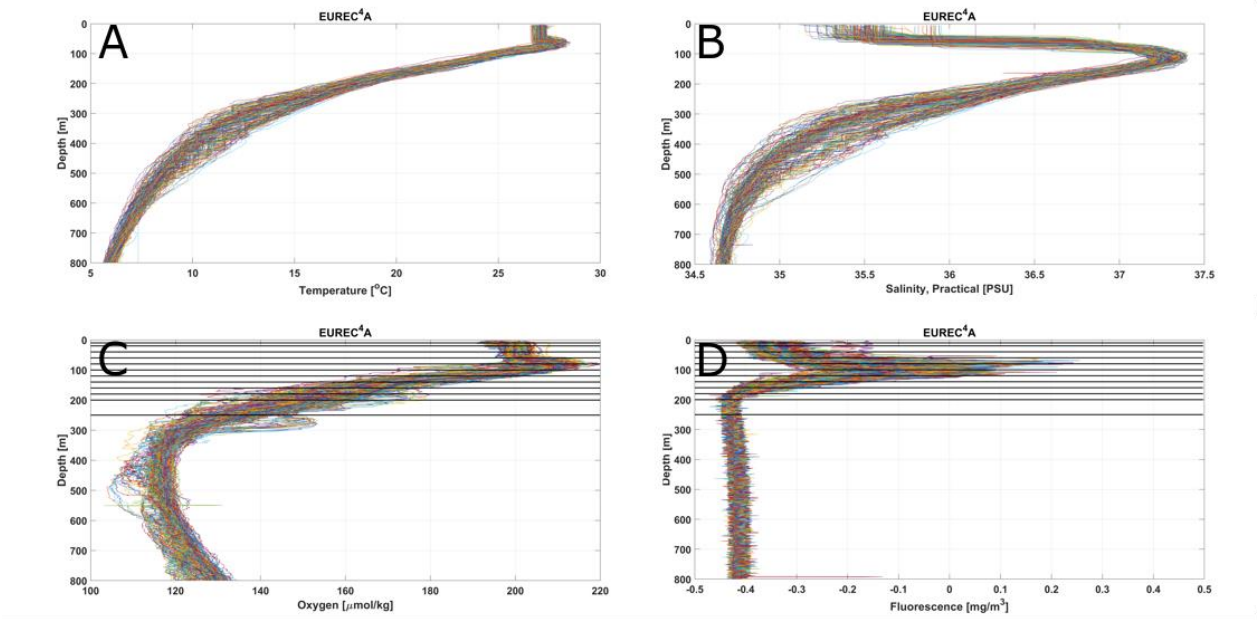

Figure 5.2.1.2 All vertical profiles of temperature (A), salinity (B), dissolved oxygen (C) and fluorescence (D) collected during EUREC^{4}A part of the M161 cruise.

Figure 5.2.1.3 presents evolution (as a function of CTD station) of temperature, salinity, dissolved oxygen and fluorescence during EUREC^{4}A part of the cruise. The features described above persisted throughout the cruise, however station-to-station variability was observed. This variability is related to spatiotemporal variability of the upper ocean, which will be subject of further research.

Temporal variability along the N-S section

Figure 5.2.1.4 and 5.2.1.5 show upper ocean (0-400 m) temperature, salinity, dissolved oxygen and fluorescence at M161 N-S section along 57 14.7W during first (23-25 Jan) and last (17-18 Feb) transect. Persisting subsurface salinity maximum is well visible throughout this period. However, initially the salinity maximum and surface temperatures were characterized by higher values than towards the end of M161 operations in the region. At the end of the cruise, the temperature inversion diminished in the southern part of the transect. Also surface salinity there was substantially lower than in the northern part of the transect.

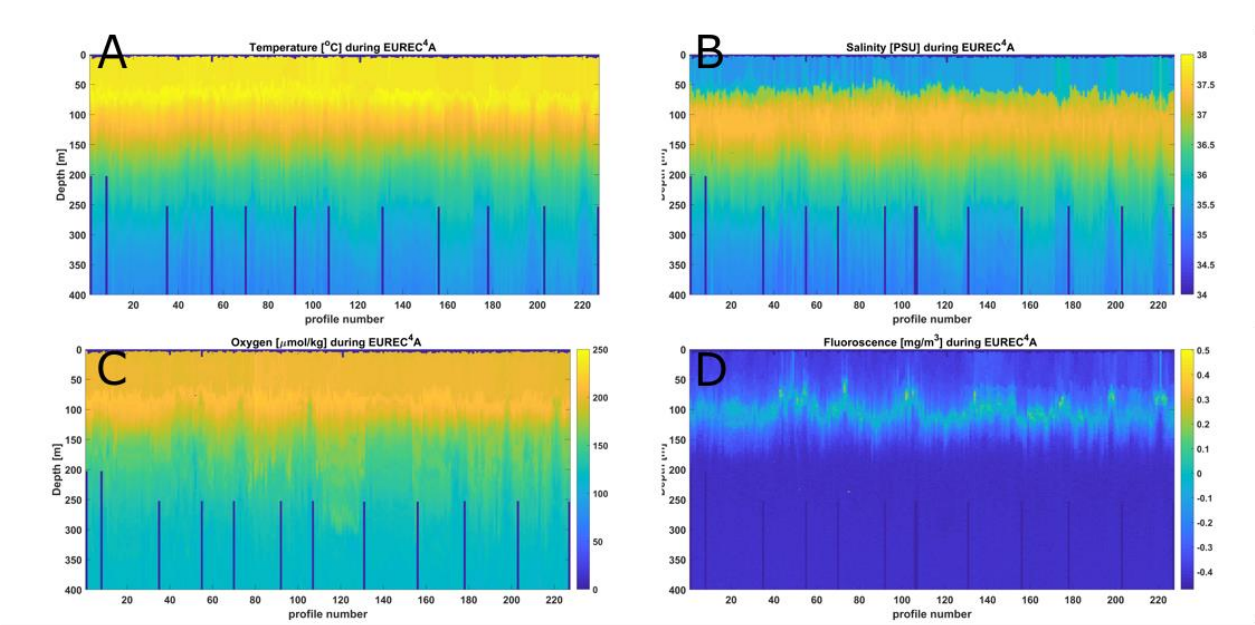

Figure 5.2.1.3 A profile-to-profile (x-axis) evolution of upper ocean (0-400 m, y-axis) temperature (A), salinity (B), dissolved oxygen (C) and fluorescence (D) during EUREC^{4}A part of the M161 cruise.

Transect to Azores

During the transect to the Azores (Figure 5.2.1.6), 22 CTD stations were performed. Three stations were done immediately before deployment of three Argo floats. Most stations were done down to 1000 m to collect a profile across oxygen minimum zone. Additionally, several shallower (500 m) casts were done. CTD profiles (not presented) show a gradual decrease of the upper ocean temperature and decay of subsurface salinity maximum. The dynamical signals coincide with increase in surface dissolved oxygen value and gradual shallowing of the maximum fluorescence.

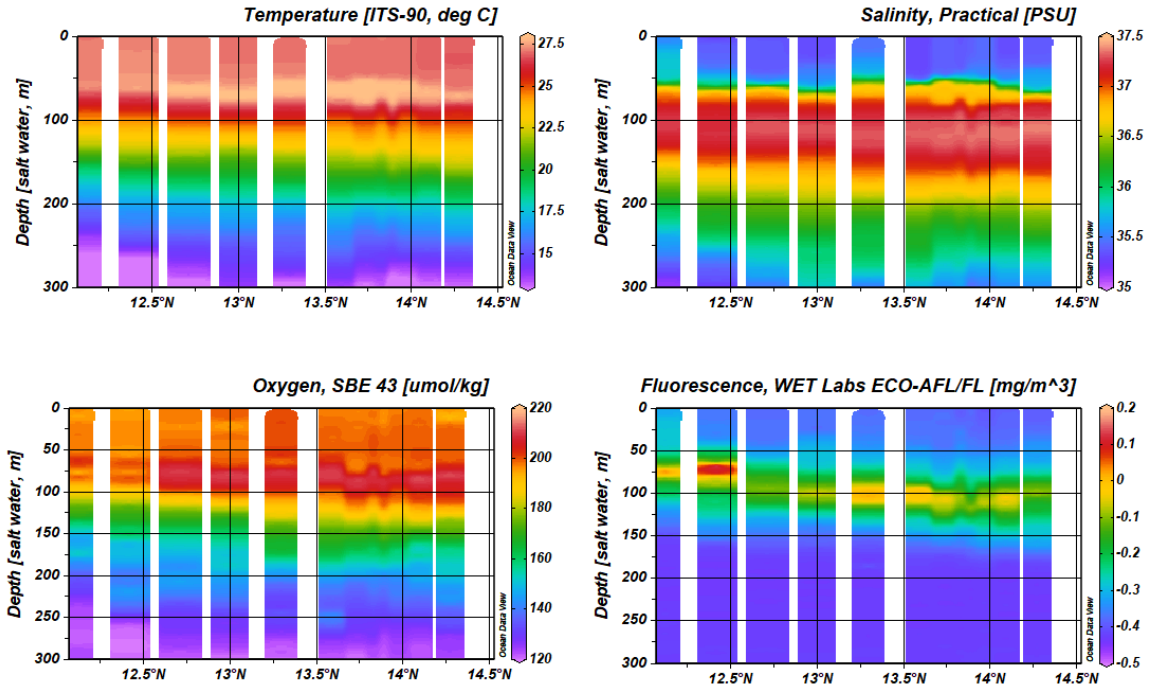

Figure 5.2.1.4 M161 N-S section along 57°14.7'W between 23 and 25 Jan 2020.

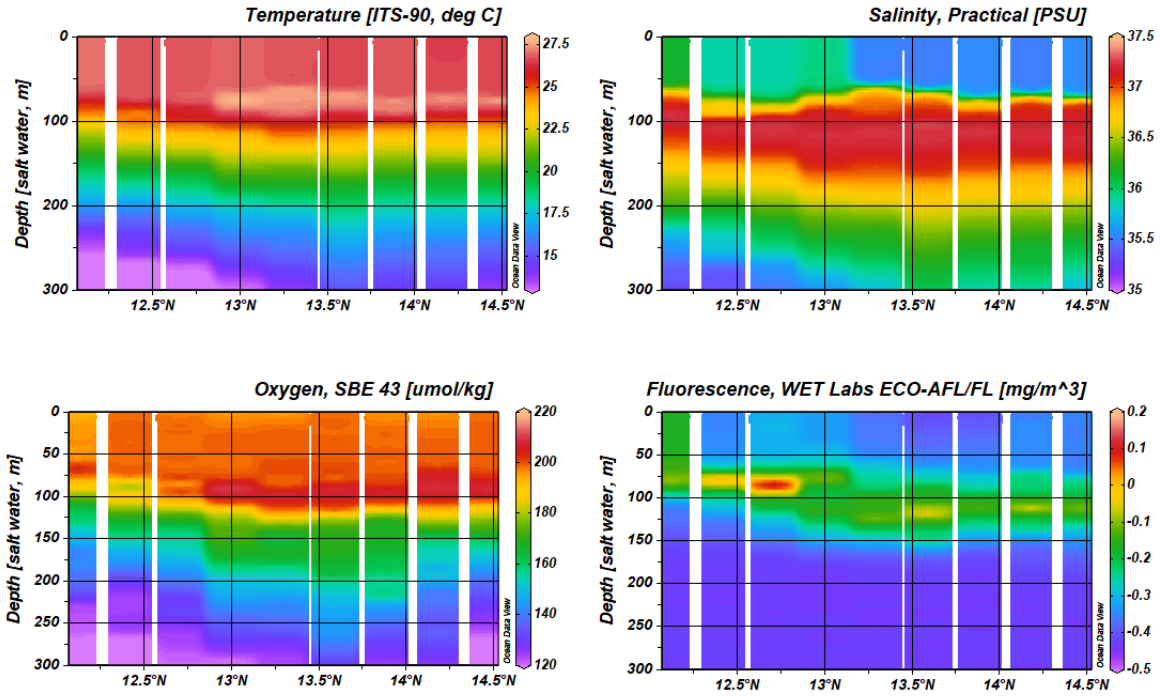

Figure 5.2.1.5 M161 N-S section along 57°14.7'W between 17 and 18 Feb 2020.

Figure 5.2.1.6 Map of CTD stations during the transect from Barbados to the Azores.

Surface water profiling with RODNEI aboard the R/V METEOR on cruise M161

(D. Baranowski, R. Grosz, C. Rollo, E. Siddle)

RODNEI (Research Ordnance Determines Near Equatorial Information) is a 2-instrument system providing seawater temperature, pressure and conductivity information. The aim of the measurements during the EUREC^{4}A field campaign was to assess the functionality of such system in the near surface (down to 10 m depth) waters in the vicinity to the research vessels, compare with ship-borne CTD measurement as well as test and cross validate two instruments and prepare operational procedure for UAV operations with oceanic payload.

System Configuration

Instrumental setup consisted of a HOBO data logger (measures temperature and conductivity at 1 Hz frequency) fixed at the end of a 30 m long line and a RBR data logger (measures temperature

and pressure at 2 Hz frequency) 10 cm above HOBO (Figure 5.2.1.8 in Appendix 12.2). RBR instrument was provided by NRL Monterey (PI J. Schmidt) for sampling of upper ocean temperature. Although, two Hobo instruments were used (serial numbers 20715905 and 20715906), only one was mounted at each cast. More information about instruments can be found in Section 5.1.12 (UAV).

Operational Procedure

During a cast, RODNEI was manually lowered into the water 8 m away from the ship down to 10 m depth and lifted back to the surface. Horizontal distance from the ship was fixed during the cast. Measurements were done in parallel or right after the ship-borne CTD cast providing complimentary data and comparison between measurements. The downcast and upcast speed, time intervals between depths and the location on the ship where measurements were performed were changed during the campaign in order to find the best setup. Initially, RODNEI was mounted at the starboard side, at the back of the ship, about 10 m behind the CTD winch. On 29 Jan 2020, RODNEI was moved to the bow and mounted there. During the M161 cruise, 18 RODNEI casts (including the initial attempt) were conducted. Initial operational set up was to stop for a given time period at 0.5 m intervals between surface and 10 m depth. Accurate stops were ensured by 0.5 m markers on the line. The operator swiftly lowered instruments and stopped them at given depth. The instruments were parked there for a defined period, typically 15 sec or 30 sec. One cast was done with 1 min – long parking at each interval. Casts' parking periods were: 1 min – 30 s (1), 30 s – 30 s (1), 30 s – 15 s (2), 15 s – 15 s (1), 15 s – 30 s (7). The numbers give the parking time on the down-cast and up-cast, while value in brackets indicate number of casts performed using given scheme. Last 6 casts were performed differently: down-cast was performed with constant vertical velocity of approximately 0.25 m/s, whereas up-cast was done with 15 sec stops at each 0.5 m interval.

Preliminary Results

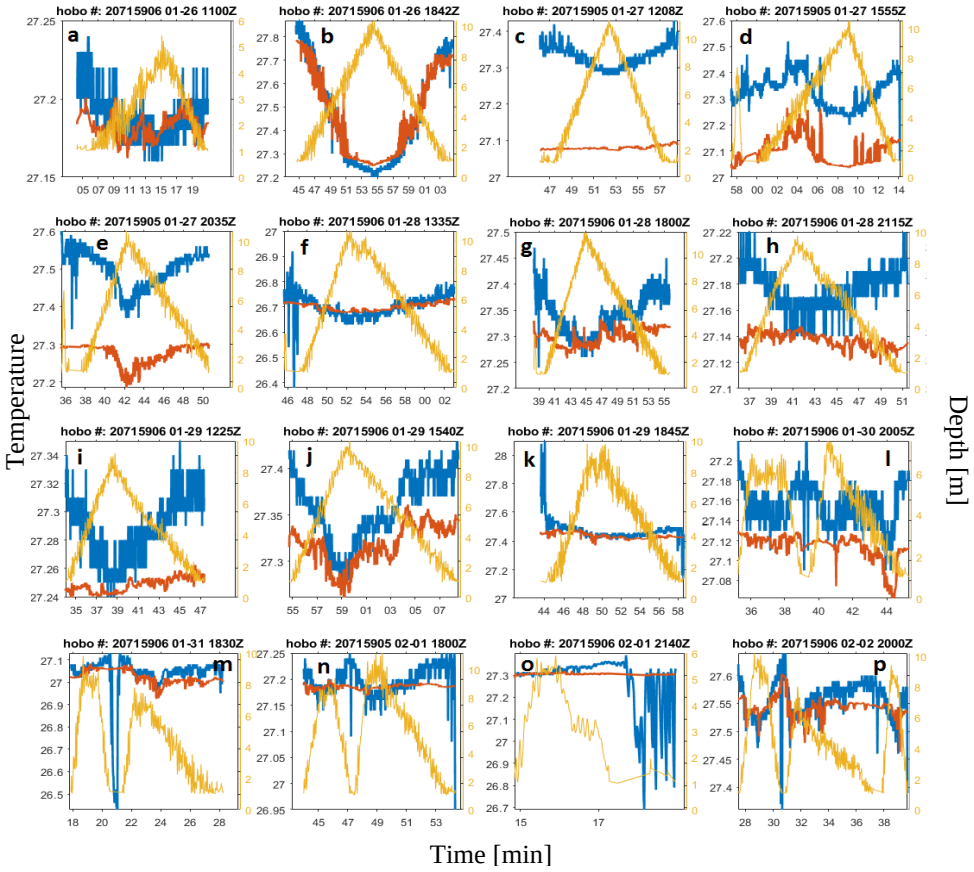

Figure 5.2.1.10 Water depth profiles for period from 26 Jan until 2 Feb 2020 retrieved from RODNEI. Yellow line represents depth, blue is temperature measurements of sensor HOBO, red – temperature measurements of sensor RBR. Time axis are given in minutes, header line gives serial number (hobo #: serial number) of the sensor HOBO, date (month-date) and time (hourminuteZ) of the cast.

Daily measurements were performed from 26 Jan until 02 Feb 2020. Preliminary results are shown in Figure 5.2.1.10. Until 29 Jan 2020 1540Z measurements were performed 10 m to the aft from the CTD measurement site. For profiles a to e in Figure 5.2.1.10 different lowering and lifting speeds were tested. One must note the switch between 2 different HOBO instruments indicated by the serial numbers *20715906* and *20715905* above the graphs. Both were tested and HOBO number *20715906* showed a better agreement with RBR (less bias). Most of the profiles (a, c, f, g, h, i, k) show no or little variation in temperature opposite to what is expected due to weather conditions favorable to the warm layer development, i.e. water temperature near the surface (top 1-2 m) should be higher than below. Such conditions were quantitatively present in the CTD measurements, but data from top 2 m of the water are not recorded by CTD cast and presence of the CTD steel frame distorts the top 10-12 m during initial lowering during beginning of the profile, before any data are being recorded. One measurement shows good agreement between both sensors and a clear temperature profile in the top 6 m with surface anomaly of 0.5 °C (Figure 5.2.1.10b). Although CTD profiles also show warm layer structure, it is much thicker and the anomaly is smaller. When no temperature variability is seen in RBR data, temperature from HOBO often shows a change in temperature of around 0.1 °C which could be explainable by direct heating

of the sensor by solar radiation. In order to mitigate this effect, starting from 30 Jan 2020 the lowering/lifting scheme was changed and the black casing of HOBO sensor was taped over with a yellow electric tape. Profiles l to p show profiles measured with the new scheme. At the same time the positioning of measurement site was changed to the bow and measurements were performed right after a CTD cast while the ship was drifting. This was done to exclude the possibility of water layers being mixed by the thruster used to park the ship at the waypoint which could be the arguable reason why most measurements show little variability in the top 10m of the ocean. However, change of RODNEI's position seems not to have improved the quality of measurements. Retrieved data will be further analyzed while considering the parking of the ship at each station to better understand differences between temperature variability for different casts and improve the setup and measurement scheme for experiments in the future. More possible solutions for limiting the impact of heating of the sensor from direct solar radiation will be considered.

5.2.2 Seagliders

(C. Rollo, E. Siddle)

Three Kongsberg seagliders were deployed during the M161 cruise: The SG579 "Humpback" was a standard physical/biogeochemical glider from UEA, the SG620 "Melonhead" was a microstructure glider from UEA and the SG641 "Omura" was an ADCP equipped glider from the NERC-MARS fleet. All 3 seagliders were prepared, deployed and piloted by UEA personnel. The "Melonhead" and the "Omura" seagliders were tested on the working deck of the R/V METEOR, affixed to the starboard rail 10 m aft of the CTD hangar. This position offered excellent satellite communication but some risk of wave wash so that care had to be taken with field laptops in this position. The "Melonhead" and "Omura" seagliders were deployed via the R/V METEOR's dedicated work boat as shown in Figure 5.2.2.1 in Appendix 12.2.

The primary aim of this mission was to test various platforms and sensors on their first full scientific deployment. This was the first deployment of the ADCP seaglider "Omura" in the open ocean for more than 2 days. This was the first scientific deployment of a glider from an autonomous surface vehicle. The specific scientific goals were:

- To compare ADCP data collected by the glider to that from a similar unit integrated into Caravela and the R/V METEOR's long range, low frequency ADCPs.
- To observe the diurnal cycle of near surface waters, including the formation of warm pools and effects of rain events.
- To measure turbulent kinetic energy dissipation rate in the upper ocean over several tidal and inertial cycles
- To measure, in conjunction with Caravela AutoNaut, oceanic near-surface properties of temperature, salinity, horizontal velocity, and meteorological variables for the determination of surface heat and momentum fluxes.

Once deployed, the "Omura" seaglider occupied a square of side length 10 km centered on 57°20.28′W, 14°10.92′N in an hourglass shape, as illustrated in Figure 5.2.2.2. Details of the glider

deployment, including an interactive map and data quicklooks, are available at this UEA website: http://ueaglider.uea.ac.uk/DIVES/index.php (mission 60).

Glider details and deployment statistics can be found in Table 5.2.2.1 in Appendix 12.1.

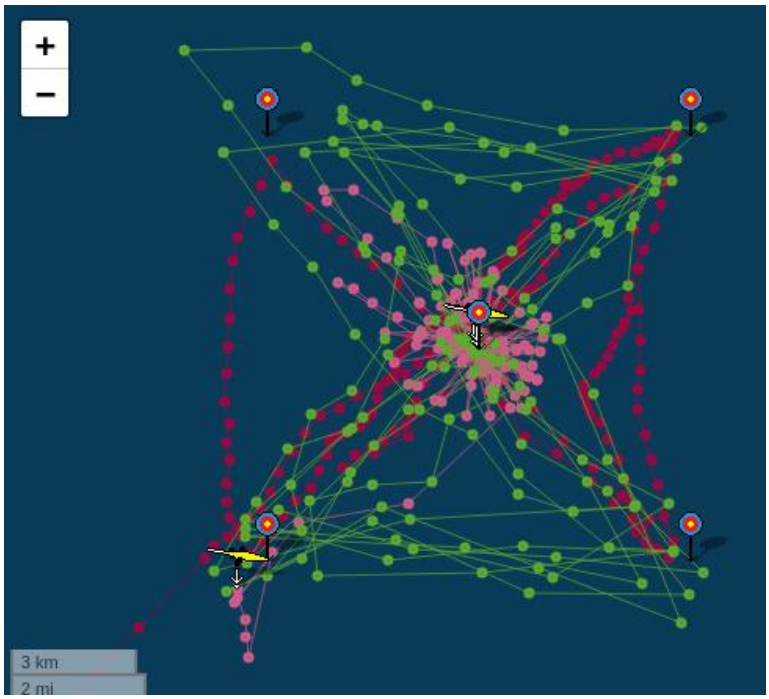

Figure 5.2.2.2 Image of glider hourglass/bow-tie sampling pattern. Each dot is a glider dive cycle by "Omura" (green), "Melonhead" (red) and "Humpback" (pink). The track of "Melonhead" extends out of frame to the WSW for 180 km. Five target symbols mark the vertices of the 10 km square and its centre point. (The image was copied from the UEA seaglider website)

"Melonhead" occupied a virtual mooring at the center of the hourglass. "Humpback" transited 180 km from its deployment location to the glider hourglass over a period of 9 days. Once "Humpback" arrived, it occupied a complementary bowtie shape to "Omura"'s hourglass, using the same box coordinates but completing the eastern and western sides rather than the northern and southern sides. The gliders used different dive profiles during the deployment. "Omura" was restricted to dive at approximately 18 degrees pitch for optimum ADCP data collection. This is a relatively shallow slope for a seaglider. "Omura" conducted 3.75-hour dives to 750 m. "Melonhead" conducted fast (2.25-hour) dives to 750 m to collect high-quality microstructure data and resolve the semidiurnal tidal cycle. "Humpback" conducted 1-hour shallow dives to 250 m to better resolve diurnal and mixed layer processes, as illustrated in Figure 3. "Melonhead" was first recovered on the 05 Feb 2020 with the intention of fitting an electromagnetic current meter and redeploying. Communication issues between glider and logger prevented this and "Melonhead" was not redeployed. "Omura" and "Humpback" were recovered from the working deck on 16 Feb 2020. Melonhead was recovered with the work boat. Omura and Humpback were recovered from the working deck using recovery poles and ropes as the sea was too rough to launch the workboat

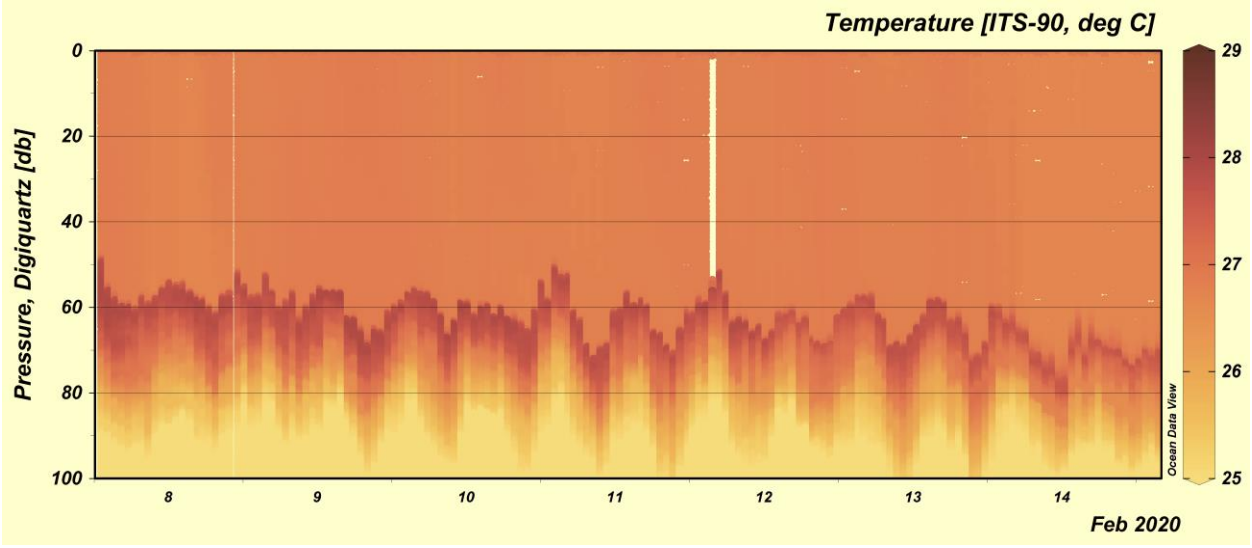

Figure 5.2.2.3 In situ temperature measured during upcasts by Humpback. Vertical displacement of the mixed layer base at semi-diurnal frequency is clearly visible. A deepening trend in the mixed layer depth is also apparent.

The R/V METEOR is a good vessel for glider deployments and recoveries. The crew are experienced with glider operations and willing to launch the work boat in calm to moderate conditions. We were out during a Beaufort 5 with a 2 m swell during one recovery. When a workboat deployment is not possible, the starboard work deck is well suited to recovery with pole and rope, with a long working deck and large crane. The crew can also recover gliders with a seastar net. Special thanks to Darek Baranowski for assistance during glider deployment and recovery and for organizing calibrations with CTD cast data.

5.2.3 Acoustic Doppler Current Profilers

(C. Rollo)

The R/V METEOR operated two ADCPs during the cruise. Both are Teledyne RDI instruments: Ocean Surveyor 38 kHz (OS38) and Ocean Surveyor 75 kHz (OS75). The 75 kHz appliance is installed at a fixed angle of 45° near the bow of the ship, the 38 kHz appliance is used in the hydrographic shaft amidships at an installation angle of 0°. Data were recorded and processed using VmDas software by Teledyne RDI instruments. Lacking any experienced ADCP operators, we used the same configurations as cruise M160. This configuration set both ADCPs to broadband mode. The full configuration is summarized in Table 5.2.3.1 in Appendix 12.1.

The ADCPs were started on 18 Jan 2020 02:10 UTC. The workstation running the 38 kHz was approx. 4 minutes ahead of UTC from starting until 21 Jan 2020 at 15:44 UTC. This does not appear to have affected data collection. Both instruments were turned off on 03 Feb 2020 from 09:33 to 04 Feb 2020 14:26 while the R/V METEOR was in the territorial waters of Trinidad and Tobago.

5.2.4 Thermosalinograph

(E. Siddle, C. Rollo, D. Baranowski)

The R/V METEOR is equipped with two SBE21 Seacat's, one port side and one starboard side. The water inlets are located some meters below the water line, in the bulbous bow. The SBE21 Seacat (thermosalinograph, further abbreviated to TSG) is paired with an SBE38 Digital Oceanographic Thermometer. This is installed upstream of the TSG so an exact water temperature is measured. The SBE38 sensors are situated at the level of the TSG intake, embedded in the supply lines, at the entry point on the outer shell of the R/V Meteor. Data was recorded for the duration of the M161 cruise, including the transect to the Azores. Data acquisition began at 18 Jan 2020 02:20:30 UTC until the end of the cruise in the Azores (data example is shown in Figure 5.2.4.1).

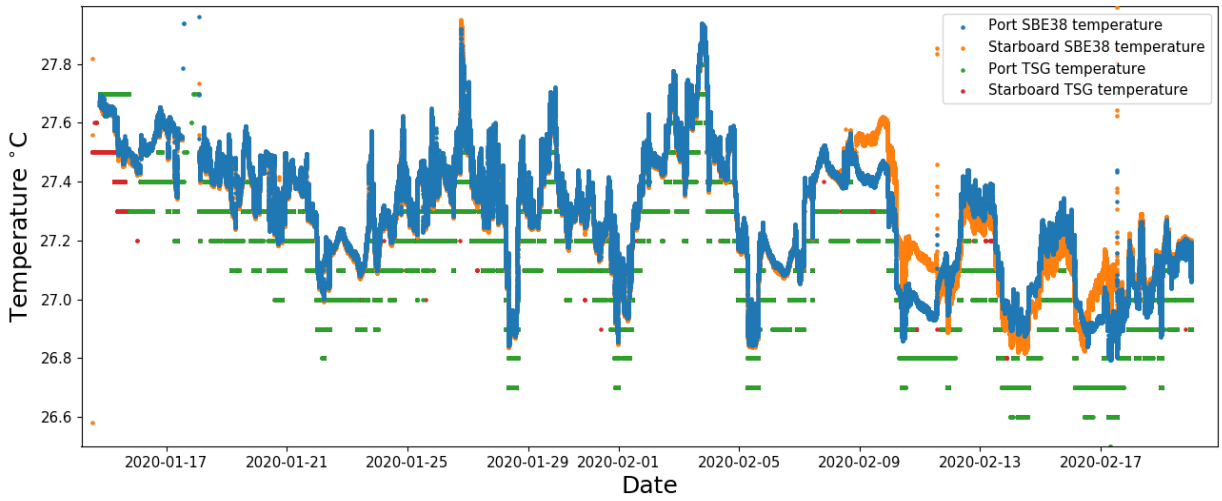

Figure 5.2.4.1 Timeseries of temperature measurements from the Thermosalinographs and Digital Oceanographic Thermometers on both port and starboard sides of the R/V METEOR. These measurements were taken during the EUREC^{4}A campaign between 11.586672N and 14.481257 N, 56.116333 W and 59.65554 W.

5.2.5 ARGO floats

(A. Schneehorst, S. Kinne)

An ARGO float is a diving oceanic robot that regularly takes profiles of temperature, density and pressure of the upper 2000 m of the ocean. A float usually drifts with ocean currents at a depth of 1000 m. A float is activated about every fifth day. During its activation, a float descends to 2000 m before ascending to the surface. On its ascent the ocean state is sampled and the recorded data are sent via a satellite link to the data center after the ocean surface is reached. After the data transmission a float descends back to its resting depth of 1000 m. Currently, there are about 4000 floats operating in all oceans worldwide under the umbrella of the international ARGO initiative. The (battery) lifetime of these floats, however, is limited to only 3 to 5 years. Thus, to maintain ocean monitoring capability new floats need to be added continuously, preferably in regions where the density of the free-drifting ARGO floats is low, as illustrated in Figure 5.2.5.1. However, deep ocean deployments are only permitted outside economic exclusive zones (EEZ).

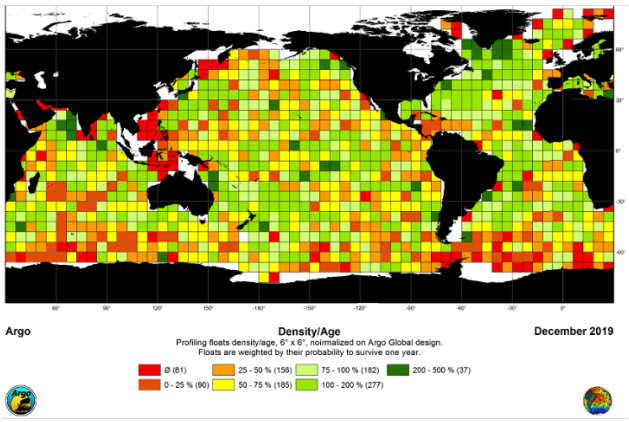

Figure 5.2.5.1. Regional float density on oceans worldwide as of December 2019. Orange and (especially) red colored regions need new deployments. Source: supplied by BSH (Anja Schneehorst) and plot generated by www.jcommops.org 01/01/2020.

Five ARGO floats of the German Bundesamt für Seeschifffahrt und Hydrographie (BSH) in Hamburg, Germany were deployed during the M161 cruise. Two floats were deployed just outside the EEZ of Barbados and the three other floats were deployed during the transit to the Azores in the red region (see Figure 5.2.5.1) west of the Azores Islands. The deployment of all floats was accompanied by CTD casts (to a depth of 2000 m) to validate that the floats were working properly. Details to the five deployments are listed in Table 5.2.5.1 in Appendix 12.1. A relatively light French float type, as illustrated in Figure 5.2.5.2 in Appendix 12.1, was deployed. These floats are easily activated with the removal of a magnet on the outside shell and shortly afterwards regular beeping indicated its readiness for a deployment.

5.2.6 Autonaut Caravela

(E. Siddle and C. Rollo)

Caravela is a wave-powered, unmanned surface vessel produced by AutoNaut Ltd. Designed for unique purpose of transporting and releasing a Seaglider, whilst recording meteorological and oceanographic information. Caravela is equipped with a host of sensors as described in Table 5.2.6.1 in Appendix 12.1, and transported SG579 named Humpback. The focus of Caravela's work during the EUREC^{4}A field campaign was to gather data to determine air-sea fluxes of heat and momentum. By using a surface vehicle (rather than a big ship) measurements close to the ocean surface very possible without perturbation of the ocean boundary layer by a big vessel.

The autonaut deployment was from H.M.B.S Pelican, Barbados on 22 Jan 2020, where Caravela was towed to the south side of the island. From there the unmanned sea-vessel made its way to the location of the UEA Seaglider box. Caravela was travelling slower than anticipated and so Humpback was released early from below Caravela on 28 Jan 2020 14:14 UTC at 13˚20.95'N, 58˚48.61'W. Both Caravela and Humpback then separately and transited around 180 km to the Seaglider box, with Caravela arriving on 5 Feb 2020. The UEA Seaglider box is illustrated in Figure 5.2.6.2 and was defined by the following latitudes and longitudes:

- NE corner: 14˚13.62'N 57˚17.49'W
- SE corner: 14˚08.22'N 57˚17.49'W
- SW corner: 14˚08.22'N 57˚23.06'W

- NW corner: 14˚13.62'N 57˚23.06'W

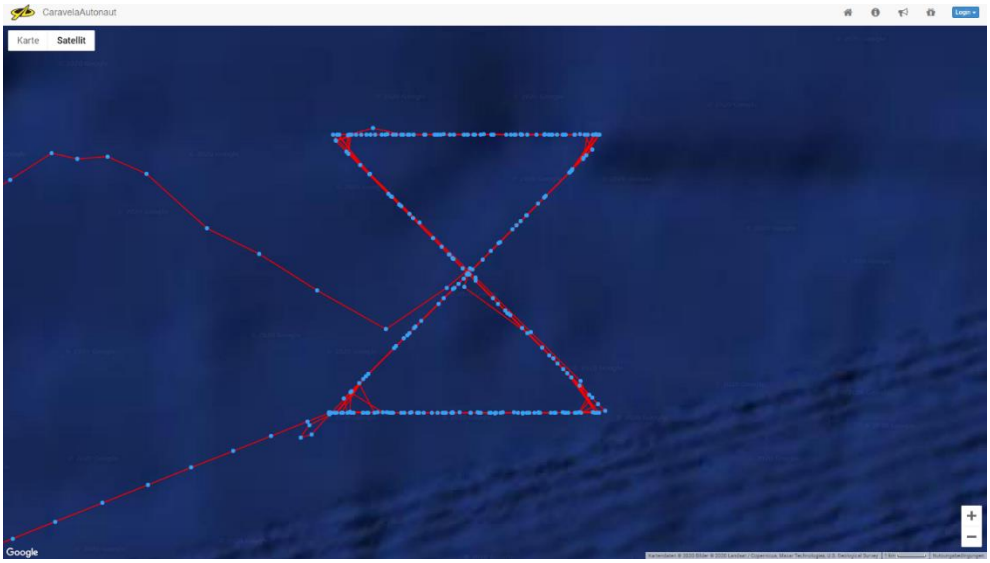

Figure 5.2.6.2 Caravela's track within the UEA Seaglider box, taken from yb.tl/caravelaautonaut. Blue points represent the position of Caravela when a GPS fix was received on the back-up unit (yellow brick).

Caravela spent 11 days repeating an hourglass shape inside the Seaglider box, in the opposite direction to Omura. For most of the mission, the autonaut was piloted over Iridium by a team from UEA and AutoNaut. During the Seaglider recoveries, attempts were made to pilot Caravela over SSSCP and using a joystick. These had varying levels of success, so control was handed back to UEA over iridium. Caravela returned to the coast of Barbados on 21 Feb 2020, where some tests were carried out over 3 days, having her travel 3 km west, south, north and east under different modes of operation.

5.2.7 Microbial Oceanography

(W. Mohr, A. Kidane, J. von Arx)

The biological fixation of atmospheric carbon dioxide (CO_2) by phytoplankton, i.e. primary production, is limited by the availability of nutrient nitrogen (N) in the vast majority of the ocean. The enzymatically catalyzed reduction of dinitrogen (N_2) gas is the largest input of external nitrogen (N) to the ocean and is fertilizing the surface oceans, thereby driving the export of atmospheric carbon dioxide (CO_2) to the deep ocean. The Western tropical North Atlantic is a nutrient-limited yet productive region where some of the highest rates of N_2 fixation in the ocean have been found so far. We have previously identified key players of N_2 fixation in this region (Martínez-Pérez et al. 2016); however, a substantial portion of the N_2 fixation rate cannot be explained by known organisms indicating that other, unknown, diazotrophs are also active and play an important role. One of the known key players in N_2 fixation is the filamentous cyanobacterium *Trichodesmium*. Besides its importance for N_2 fixation, *Trichodesmium* may also play a significant role in the production of the trace greenhouse gas methane (CH_4) which can be produced during the use of methylated, organic phosphorus (P) compounds. These organic P compounds are likely an important source of P for growth of *Trichodesmium* in the Western

tropical North Atlantic due to the extremely low concentrations of inorganic phosphorus, i.e. phosphate.

Our aims of the M161 cruise are: i) to identify unknown N_2-fixing microorganisms, including those that have previously been indicated in other studies, ii) to study the dynamics of iron (Fe) uptake in *Trichodesmium* due to the high influx of Saharan dust in this region, iii) to investigate the importance of N_2-fixing and non-N_2-fixing microorganisms in the production of the trace greenhouse gas CH_4, and iv) to determine the factors driving the spatial and temporal variability of N_2 fixation rates in the Western tropical North Atlantic

In order to achieve these aims, we performed a series of stable isotope tracer incubations at 17 stations during the cruise. At 12 stations in the core working area, incubations were carried out at 4 depths within the upper 200 m of the water column to address i), ii) and iii). At 3 additional stations, surface water experiments dedicated to *Trichodesmium* were completed. Another 2 stations outside the core working area and on the transit to the Azores were used to obtain comparisons to the core working area with respect to trace greenhouse gases. From our incubation experiments as well as ambient seawater, subsamples were taken to determine nutrient and biomass concentrations and bulk rates of biogeochemical processes (e.g. N_2 fixation, primary production, CH_4 production), to determine the importance of individual organisms using single-cell measurements (nanoSIMS) in combination with molecular biological tools such as sequencing and fluorescence in situ hybridization (FISH). To address aim iv) we will be comparing data obtained during the M161 cruise on R/V METEOR to those obtained on the parallel cruise MSM89 on R/V MARIA S. MERIAN, where colleagues from our department participated.

Measurements of nutrients, biomass and bulk rates are expected to be measured within the first 12 months of cruise completion. The molecular biological and single-cell analyses can take up to several years to complete depending on prior knowledge of microbial community and available tools to target these organisms. Data will be released through peer-reviewed publications, ideally in open-access style. Data sets complementary to the publications will be made available either within the publications and/or through publicly available databases such as Pangaea or Genbank (where applicable). The combined studies aim at obtaining a holistic picture of the organisms involved in N_2 fixation and how their activity is driving and is influenced by the prevailing oceanography, its' connection to air-sea gas exchange of trace greenhouse gases, and carbon export in the Western tropical North Atlantic.

5.3 Expected Results

Expected results are included in the individual sections, please see above.

6 Ship's Meteorological Station

(A. Raeke)

After the brief return to Bridgetown for a science staff change and an instrument pick-up the R/V METEOR departed late in the evening on January 17 for the main M161 cruise. On January 18 the R/V METEOR and the R/V MARIA S. MERIAN jointly departed into the wind away from the BCO site into the working area assigned to R/V METEOR during the multi-platform

EUREC^{4}A campaign from mid-January to mid-February, 2020, east of Barbados: A north-south oriented line at 57° W in longitude between 12° and 14°30’ N in latitude - about 240 km east of Barbados. Between an extensive HIGH (1045 hPa) over the Great Lakes which moved to the southeast, and a tropical LOW an increasing northeasterly wind with 6 Bft and a significant wave height of 2 to 3 m were experienced from January 18 onwards. A high swell, originating from a storm depression in the western North Atlantic, reached the R/V METEOR on 20 January 2020. Wave height rose to 4 m with a swell of up to 3 m from different directions. There were frequent showers. On January 22, the swell decreased to 2 m, but still approached the R/V METEOR from different directions. With the shift of the high-pressure wedge to the northeast, the wind decreased to 4 to 5 Bft.

From January 23 to February 4, a decrease of the HIGH influenced mainly the northern region of the working area, where winds decreased to 3 to 4 Bft and wave heights only up to 1.5 m.
After February 04, the Azores HIGH intensified again and so did wind and swell. The wind in the working area came from east to northeast and increased to 5 to 6 Bft with wave heights up to 3m. These conditions remained so until February 19 as the larger scale pressure conditions remained relatively stable. There were only occasional light showers mainly in the morning and afternoon hours. In terms of wind strength, a diurnal variation was observed, with lower winds during the afternoon and the second half of the night. Still during the afternoon, wind and swell were too strong for safe RIB operations (too strong for gilder deployments) and the gliders at the end of the campaign needed to be recovered without RIB. On February 19, the R/V METEOR sailed close to the beaches near Bridgetown into island protected water with wave height only up to 1m to carry out important work on deck and to exchange goods with the R/V MARIA S. MERIAN.
During transit back to the working area in the evening of February 19, the significant wave height rose to 3.5 m with a high swell component and the wind reached again 6 Bft without land protection. After these last activities in the working area on February 20 the R/V Meteor set course for the Azores. On February 21, a LOW (depression) off the east coast moving northeast temporarily reduced the wind in the area of operation to 2 to 3 Bft with a significant wave height of up to 2.5m. With a north-easterly path the pressure gradient between the Azores HIGH and the north-easterly LOW increased. Furthermore, the Azores HIGH was pushed back by a LOW at the Canary Islands which moved in a south-westerly direction. The east-southeast wind blew until February 25 mostly with 5 to 6 Bft for wave height of up to 2.5 m. On February 25, the LOW southwest of the Canary Islands dissolved. A HIGH pressure bridge over the North Atlantic with a weakening cold front led to a longer period of weak winds and a swell of at most 2m. As it moved northeast, the initially weak northerly wind veered west, increasing to 5 to 6 Bft on March 01. Between the Azores high pressure and a storm low complex between Greenland and the North Sea, the significant wave height in the working area also increased to 2 to 3 m. On March 2, shortly before reaching the Azores Island of Sao Miguel was the scientific work concluded. The R/V METEOR entered the port of Ponta Delgada very late on March 2.

7 Station Lists M161

7.1 Oceanographic Station List (CTD, gliders, ARGO floats)

Station	Date / Time UTC	Device	Latitude (°N)	Longitude (°W)	Depth (m)	Rope Length (m)
M161_1-1	18.01.2020 20:40	CTD	13° 40.248'	058° 18.482'	3318	10
M161_2-1	19.01.2020 08:03	CTD	13° 47.103'	057° 15.136'	4842	500
M161_3-1	19.01.2020 11:40	CTD	13° 47.104'	057° 15.136'	4846	200
M161_4-1	20.01.2020 14:53	CTD	14° 03.167'	057° 15.286'	4974	500
M161_5-1	20.01.2020 18:17	CTD	14° 27.034'	057° 14.881'	5472	800
M161_6-1	20.01.2020 20:52	CTD	14° 10.657'	057° 15.193'	5152	800
M161_7-1	21.01.2020 00:05	CTD	13° 47.071'	057° 15.070'	4838	800
M161_8-1	21.01.2020 03:05	CTD	13° 27.178'	057° 14.989'	4929	800
M161_9-1	21.01.2020 06:08	CTD	13° 07.095'	057° 15.032'	4915	800
M161_10-1	21.01.2020 08:43	CTD	13° 06.819'	057° 17.054'	4885	200
M161_11-1	21.01.2020 12:25	CTD	13° 31.510'	057° 15.216'	4940	801
M161_12-1	21.01.2020 14:54	CTD	13° 42.826'	057° 23.551'	4875	800
M161_13-1	21.01.2020 18:51	CTD	14° 10.993'	057° 43.353'	5289	783
M161_14-1	21.01.2020 21:47	CTD	14° 10.924'	057° 25.000'	5170	800
M161_15-1	22.01.2020 00:54	CTD	14° 10.901'	057° 06.343'	5133	800
M161_16-1	22.01.2020 04:01	CTD	14° 10.908'	056° 46.816'	5181	800
M161_17-1	22.01.2020 07:53	CTD	14° 28.478'	057° 14.851'	5504	800
M161_18-1	22.01.2020 10:40	CTD	14° 10.926'	057° 14.703'	5170	1000
M161_19-1	22.01.2020 14:23	CTD	14° 10.922'	057° 14.703'	5207	800
M161_20-1	22.01.2020 16:27	CTD	14° 10.922'	057° 14.703'	5176	801
M161_21-1	22.01.2020 18:22	CTD	14° 10.923'	057° 14.704'	5172	800
M161_22-1	22.01.2020 20:17	CTD	14° 10.923'	057° 14.703'	5174	800
M161_23-1	22.01.2020 22:25	CTD	14° 10.920'	057° 14.704'	5170	1000

M161_24-1	23.01.2020 00:20	CTD	14° 10.919'	057° 14.703'	5178	800
M161_25-1	23.01.2020 02:16	CTD	14° 10.920'	057° 14.704'	5170	800
M161_26-1	23.01.2020 04:20	CTD	14° 10.921'	057° 14.704'	5173	800
M161_27-1	23.01.2020 06:19	CTD	14° 10.921'	057° 14.704'	5178	800
M161_28-1	23.01.2020 08:18	CTD	14° 10.919'	057° 14.704'	5172	800
M161_29-1	23.01.2020 10:22	CTD	14° 10.922'	057° 20.283'	5172	1000
M161_30-1	23.01.2020 14:19	Glider deployment	14° 10.922'	057° 20.285'	5172	0
M161_31-1	23.01.2020 14:56	Glider deployment	14° 10.920'	057° 20.287'	5171	0
M161_32-1	23.01.2020 15:24	CTD	14° 10.921'	057° 20.284'	5170	500
M161_33-1	23.01.2020 17:47	CTD	14° 05.526'	057° 25.849'	5100	500
M161_34-1	23.01.2020 19:51	CTD	14° 16.355'	057° 25.906'	5249	500
M161_35-1	23.01.2020 22:31	CTD	14° 16.341'	057° 14.749'	5322	500
M161_36-1	24.01.2020 00:58	CTD	14° 05.516'	057° 14.719'	5015	500
M161_37-1	24.01.2020 03:33	CTD	13° 53.350'	057° 14.707'	4870	800
M161_38-1	24.01.2020 05:57	CTD	13° 44.772'	057° 14.753'	4825	799
M161_39-1	24.01.2020 08:13	CTD	13° 44.772'	057° 14.753'	4827	250
M161_40-1	24.01.2020 12:20	CTD	13° 58.185'	057° 14.703'	4829	800
M161_42-1	24.01.2020 16:52	CTD	13° 58.201'	057° 11.571'	4816	760
M161_43-1	24.01.2020 19:11	CTD	13° 50.171'	057° 12.436'	4839	800
M161_44-1	25.01.2020 00:03	CTD	13° 35.700'	057° 14.711'	4831	800
M161_45-1	25.01.2020 03:27	CTD	13° 17.978'	057° 14.724'	4952	801
M161_46-1	25.01.2020 06:32	CTD	12° 59.957'	057° 14.705'	4737	800
M161_47-1	25.01.2020 09:29	CTD	12° 42.761'	057° 14.724'	4462	800
M161_48-1	25.01.2020 12:45	CTD	12° 25.063'	057° 14.747'	4494	800
M161_49-1	25.01.2020 15:42	CTD	12° 07.527'	057° 14.696'	4471	800
M161_50-1	25.01.2020 19:18	CTD	12° 25.086'	057° 01.038'	4458	800
M161_51-1	25.01.2020 20:54	CTD	12° 25.117'	057° 10.122'	4486	800

M161_52-1	25.01.2020 22:41	CTD	12° 25.120'	057° 19.342'	4495	800
M161_53-1	26.01.2020 00:28	CTD	12° 25.122'	057° 28.541'	4468	800
M161_54-1	26.01.2020 02:29	CTD	12° 25.109'	057° 37.781'	3566	800
M161_55-1	26.01.2020 07:15	CTD	12° 42.813'	057° 14.684'	4458	800
M161_56-1	26.01.2020 10:04	CTD	12° 25.126'	057° 14.702'	4493	800
M161_57-1	26.01.2020 19:32	CTD	12° 11.220'	056° 07.059'	4495	2000
M161_58-1	26.01.2020 20:17	ARGO float deployment	12° 11.204'	056° 07.009'	4481	0
M161_59-1	26.01.2020 22:40	CTD	12° 15.860'	056° 28.705'	4437	800
M161_60-1	27.01.2020 01:23	CTD	12° 20.471'	056° 51.065'	4446	801
M161_61-1	27.01.2020 05:06	CTD	12° 07.501'	057° 14.735'	4471	800
M161_62-1	27.01.2020 07:13	CTD	12° 07.502'	057° 14.736'	4471	250
M161_63-1	27.01.2020 10:07	CTD	12° 25.123'	057° 14.705'	4495	800
M161_64-1	27.01.2020 13:20	CTD	12° 42.750'	057° 14.737'	4459	801
M161_65-1	27.01.2020 16:26	CTD	13° 00.024'	057° 14.717'	4738	800
M161_66-1	27.01.2020 22:45	CTD	13° 18.024'	057° 14.734'	4954	800
M161_67-1	28.01.2020 01:47	CTD	13° 35.638'	057° 14.716'	4828	801
M161_68-1	28.01.2020 04:49	CTD	13° 53.337'	057° 14.694'	4863	800
M161_69-1	28.01.2020 07:48	CTD	14° 10.917'	057° 14.723'	5170	800
M161_70-1	28.01.2020 10:50	CTD	14° 28.549'	057° 14.728'	5509	800
M161_71-1	28.01.2020 14:04	CTD	14° 10.926'	057° 14.731'	5175	801
M161_72-1	28.01.2020 18:58	CTD	13° 47.638'	057° 14.738'	4844	800
M161_73-1	28.01.2020 21:53	CTD	13° 31.228'	057° 14.744'	4939	800
M161_74-1	29.01.2020 00:49	CTD	13° 18.004'	057° 14.728'	4953	800
M161_75-1	29.01.2020 03:32	CTD	13° 00.066'	057° 14.721'	4741	801
M161_76-1	29.01.2020 05:21	CTD	12° 52.849'	057° 14.697'	4506	800
M161_77-1	29.01.2020 07:17	CTD	12° 52.850'	057° 14.696'	4506	250
M161_78-1	29.01.2020 09:23	CTD	12° 42.784'	057° 14.737'	4459	800

M161_79-1	29.01.2020 12:50	CTD	12° 25.206'	057° 14.742'	4494	800
M161_80-1	29.01.2020 16:13	CTD	12° 07.498'	057° 14.708'	4471	800
M161_81-1	29.01.2020 19:13	CTD	12° 25.141'	057° 14.741'	4494	800
M161_82-1	29.01.2020 22:37	CTD	12° 42.751'	057° 14.740'	4458	800
M161_83-1	30.01.2020 01:37	CTD	13° 00.044'	057° 14.709'	4738	800
M161_84-1	30.01.2020 04:44	CTD	13° 18.111'	057° 14.767'	4951	800
M161_85-1	30.01.2020 07:48	CTD	13° 35.621'	057° 14.727'	4834	800
M161_86-1	30.01.2020 11:01	CTD	13° 17.995'	057° 25.044'	4924	800
M161_87-1	30.01.2020 20:11	CTD	13° 17.990'	056° 50.842'	4941	800
M161_88-1	30.01.2020 22:24	CTD	13° 17.997'	057° 02.942'	4950	800
M161_89-1	31.01.2020 01:13	CTD	13° 17.998'	057° 25.017'	4924	800
M161_90-1	31.01.2020 07:16	CTD	13° 18.003'	056° 50.905'	4943	800
M161_91-1	31.01.2020 09:42	CTD	13° 26.891'	056° 59.538'	4869	800
M161_92-1	31.01.2020 12:44	CTD	13° 35.642'	057° 14.753'	4833	800
M161_93-1	31.01.2020 15:42	CTD	13° 53.347'	057° 14.705'	4869	800
M161_94-1	31.01.2020 18:49	CTD	14° 10.915'	057° 14.696'	5179	800
M161_95-1	31.01.2020 22:04	CTD	14° 28.565'	057° 14.733'	5506	800
M161_96-1	01.02.2020 00:34	CTD	14° 16.333'	057° 14.728'	5322	800
M161_97-1	01.02.2020 02:40	CTD	14° 16.320'	057° 25.891'	5251	800
M161_98-1	01.02.2020 04:53	CTD	14° 05.516'	057° 25.900'	5100	800
M161_99-1	01.02.2020 06:56	CTD	14° 05.515'	057° 25.899'	5101	250
M161_100-1	01.02.2020 09:26	CTD	14° 05.529'	057° 14.775'	5015	800
M161_101-1	01.02.2020 11:53	CTD	13° 53.351'	057° 14.734'	4863	800
M161_102-1	01.02.2020 15:10	CTD	13° 35.643'	057° 14.732'	4827	800
M161_103-1	01.02.2020 18:19	CTD	13° 18.054'	057° 14.780'	4953	800
M161_104-1	01.02.2020 21:52	CTD	13° 00.041'	057° 14.785'	4740	800
M161_105-1	02.02.2020 00:39	CTD	12° 42.752'	057° 25.016'	4511	802

M161_106-1	02.02.2020 06:38	CTD	12° 42.751'	056° 54.855'	4454	800
M161_107-1	02.02.2020 08:40	CTD	12° 42.756'	057° 04.062'	4500	800
M161_108-1	02.02.2020 10:42	CTD	12° 42.748'	057° 14.742'	4460	800
M161_109-1	02.02.2020 13:58	CTD	12° 25.133'	057° 14.706'	4494	800
M161_110-1	02.02.2020 17:08	CTD	12° 07.515'	057° 14.738'	4473	800
M161_111-1	02.02.2020 20:06	CTD	12° 25.136'	057° 14.750'	4494	800
M161_112-1	02.02.2020 23:15	CTD	12° 42.765'	057° 14.712'	4464	800
M161_113-1	03.02.2020 13:03	Glider recovery (MSM)	11° 35.228'	059° 14.875'	1676	0
M161_114-1	03.02.2020 16:22	CTD	12° 01.074'	059° 14.570'	1943	1000
M161_115-1	04.02.2020 05:28	CTD	12° 35.274'	057° 36.416'	3848	800
M161_116-1	04.02.2020 07:31	CTD	12° 35.274'	057° 36.416'	3846	250
M161_117-1	04.02.2020 11:36	CTD	12° 42.756'	057° 14.741'	4459	800
M161_118-1	04.02.2020 18:52	CTD	13° 00.035'	057° 14.752'	4742	800
M161_119-1	04.02.2020 22:07	CTD	13° 18.021'	057° 14.751'	4952	779
M161_120-1	05.02.2020 01:15	CTD	13° 35.644'	057° 14.723'	4829	800
M161_121-1	05.02.2020 04:28	CTD	13° 53.306'	057° 14.698'	4862	800
M161_122-1	05.02.2020 07:40	CTD	14° 10.908'	057° 14.726'	5171	800
M161_123-1	05.02.2020 10:48	CTD	14° 28.553'	057° 14.751'	5509	800
M161_124-1	05.02.2020 14:06	CTD	14° 10.898'	057° 14.731'	5170	800
M161_125-1	05.02.2020 17:08	Glider recovery	14° 07.769'	057° 23.673'	5124	0
M161_126-1	05.02.2020 19:54	CTD	14° 04.928'	057° 14.744'	5005	800
M161_127-1	05.02.2020 22:47	CTD	14° 04.927'	057° 14.745'	5003	809
M161_128-1	06.02.2020 00:50	CTD	14° 04.928'	057° 14.744'	5005	800
M161_129-1	06.02.2020 02:48	CTD	14° 04.929'	057° 14.744'	5002	800
M161_130-1	06.02.2020 04:54	CTD	14° 04.929'	057° 14.744'	5004	801
M161_131-1	06.02.2020 06:53	CTD	14° 04.926'	057° 14.745'	5004	800
M161_132-1	06.02.2020 08:52	CTD	14° 04.927'	057° 14.745'	5005	800

M161_133-1	06.02.2020 10:59	CTD	14° 04.928'	057° 14.745'	5004	800
M161_134-1	06.02.2020 12:51	CTD	14° 04.929'	057° 14.743'	5004	800
M161_135-1	06.02.2020 14:53	CTD	14° 04.927'	057° 14.743'	5004	800
M161_136-1	06.02.2020 16:48	CTD	14° 04.933'	057° 14.745'	5006	800
M161_137-1	06.02.2020 18:34	CTD	14° 04.931'	057° 14.745'	5004	800
M161_138-1	06.02.2020 22:56	CTD	13° 35.666'	057° 14.798'	4827	800
M161_139-1	07.02.2020 02:18	CTD	13° 18.009'	057° 14.725'	4952	800
M161_140-1	07.02.2020 05:24	CTD	12° 58.030'	057° 14.761'	4659	800
M161_141-1	07.02.2020 07:35	CTD	12° 58.033'	057° 14.759'	4660	250
M161_142-1	07.02.2020 12:07	CTD	12° 26.154'	057° 14.789'	4494	1736
M161_142-2	07.02.2020 14:31	CTD	12° 26.152'	057° 14.788'	4493	4485
M161_143-1	07.02.2020 20:24	CTD	12° 07.524'	057° 14.801'	4473	800
M161_144-1	07.02.2020 23:42	CTD	12° 25.122'	057° 14.701'	4493	800
M161_145-1	08.02.2020 02:47	CTD	12° 25.123'	057° 14.701'	4492	800
M161_146-1	08.02.2020 05:14	CTD	12° 25.123'	057° 14.701'	4494	800
M161_147-1	08.02.2020 07:08	CTD	12° 25.123'	057° 14.701'	4493	799
M161_148-1	08.02.2020 09:00	CTD	12° 25.124'	057° 14.699'	4493	799
M161_149-1	08.02.2020 20:46	CTD	12° 25.129'	057° 14.701'	4492	800
M161_150-1	08.02.2020 22:45	CTD	12° 25.127'	057° 14.702'	4494	800
M161_151-1	09.02.2020 00:49	CTD	12° 25.127'	057° 14.703'	4492	800
M161_152-1	09.02.2020 02:49	CTD	12° 25.125'	057° 14.702'	4492	800
M161_153-1	09.02.2020 04:54	CTD	12° 25.129'	057° 14.701'	4493	800
M161_154-1	09.02.2020 06:48	CTD	12° 25.126'	057° 14.702'	4495	800
M161_155-1	09.02.2020 08:46	CTD	12° 25.130'	057° 14.702'	4494	800
M161_156-1	09.02.2020 10:46	CTD	12° 25.128'	057° 14.702'	4494	799
M161_157-1	09.02.2020 12:49	CTD	12° 25.128'	057° 14.702'	4492	800
M161_158-1	09.02.2020 14:47	CTD	12° 25.127'	057° 14.701'	4492	800

M161_159-1	09.02.2020 16:53	CTD	12° 25.128'	057° 14.701'	4493	800
M161_160-1	09.02.2020 18:45	CTD	12° 25.131'	057° 14.701'	4494	799
M161_161-1	09.02.2020 20:46	CTD	12° 25.129'	057° 14.702'	4494	800
M161_162-1	09.02.2020 23:28	CTD	12° 42.733'	057° 14.741'	4459	800
M161_163-1	10.02.2020 02:34	CTD	13° 00.031'	057° 14.702'	4739	800
M161_164-1	10.02.2020 05:20	CTD	13° 17.997'	057° 14.723'	4951	800
M161_165-1	10.02.2020 07:22	CTD	13° 17.997'	057° 14.724'	4950	250
M161_166-1	10.02.2020 10:57	CTD	13° 35.641'	057° 14.708'	4828	800
M161_167-1	10.02.2020 13:44	CTD	13° 53.330'	057° 14.722'	4862	800
M161_168-1	10.02.2020 16:27	CTD	14° 10.920'	057° 14.726'	5171	800
M161_169-1	10.02.2020 18:49	CTD	14° 10.922'	057° 14.725'	5173	800
M161_170-1	10.02.2020 20:51	CTD	14° 10.922'	057° 14.724'	5172	800
M161_171-1	10.02.2020 22:45	CTD	14° 10.924'	057° 14.726'	5177	800
M161_172-1	11.02.2020 00:48	CTD	14° 10.922'	057° 14.725'	5172	800
M161_173-1	11.02.2020 02:49	CTD	14° 10.921'	057° 14.725'	5170	800
M161_174-1	11.02.2020 04:49	CTD	14° 10.919'	057° 14.725'	5181	800
M161_175-1	11.02.2020 06:45	CTD	14° 10.923'	057° 14.725'	5172	800
M161_176-1	11.02.2020 08:50	CTD	14° 10.921'	057° 14.725'	5171	799
M161_177-1	11.02.2020 10:43	CTD	14° 10.923'	057° 14.703'	5173	800
M161_178-1	11.02.2020 13:55	CTD	14° 10.927'	057° 14.702'	5173	800
M161_179-1	11.02.2020 16:44	CTD	14° 10.927'	057° 14.701'	5172	800
M161_180-1	11.02.2020 18:38	CTD	14° 10.928'	057° 14.704'	5172	800
M161_181-1	12.02.2020 12:52	CTD	12° 25.128'	057° 14.702'	4495	800
M161_182-1	12.02.2020 16:15	CTD	12° 25.149'	056° 59.369'	4452	800
M161_183-1	12.02.2020 18:54	CTD	12° 25.126'	056° 44.011'	4437	800
M161_184-1	12.02.2020 21:39	CTD	12° 16.508'	056° 59.414'	4462	800
M161_185-1	13.02.2020 00:53	CTD	12° 07.521'	057° 14.706'	4471	800

M161_186-1	13.02.2020 04:47	CTD	12° 25.132'	057° 24.915'	4492	800
M161_187-1	13.02.2020 06:55	CTD	12° 25.132'	057° 24.915'	4493	250
M161_188-1	13.02.2020 10:06	CTD	12° 42.725'	057° 14.755'	4462	800
M161_189-1	13.02.2020 12:55	CTD	13° 00.040'	057° 14.755'	4742	800
M161_190-1	13.02.2020 15:53	CTD	13° 18.003'	057° 14.701'	4954	800
M161_191-1	13.02.2020 18:38	CTD	13° 35.638'	057° 14.714'	4829	799
M161_192-1	13.02.2020 21:33	CTD	13° 53.294'	057° 14.756'	4863	800
M161_193-1	14.02.2020 00:43	CTD	14° 10.923'	057° 14.711'	5172	801
M161_194-1	14.02.2020 03:47	CTD	14° 28.559'	057° 14.712'	5495	800
M161_195-1	14.02.2020 06:42	CTD	14° 10.917'	057° 14.746'	5172	800
M161_196-1	14.02.2020 09:42	CTD	13° 53.314'	057° 14.775'	4861	800
M161_197-1	14.02.2020 12:50	CTD	13° 35.656'	057° 14.712'	4834	800
M161_198-1	14.02.2020 15:50	CTD	13° 17.989'	057° 14.711'	4951	800
M161_199-1	14.02.2020 18:16	CTD	13° 17.996'	057° 24.938'	4921	800
M161_200-1	14.02.2020 20:31	CTD	13° 18.017'	057° 14.800'	4951	800
M161_201-1	14.02.2020 23:23	CTD	13° 17.996'	056° 59.418'	4948	800
M161_202-1	15.02.2020 02:02	CTD	13° 18.006'	056° 43.811'	4936	800
M161_203-1	15.02.2020 04:50	CTD	13° 08.989'	056° 59.396'	4930	800
M161_204-1	15.02.2020 07:47	CTD	13° 00.048'	057° 14.734'	4744	800
M161_205-1	15.02.2020 10:51	CTD	12° 42.711'	057° 14.713'	4455	828
M161_206-1	15.02.2020 14:03	CTD	12° 25.131'	057° 14.717'	4494	800
M161_207-1	15.02.2020 16:55	CTD	12° 07.509'	057° 14.734'	4470	800
M161_208-1	15.02.2020 19:27	CTD	12° 25.122'	057° 14.734'	4493	800
M161_209-1	15.02.2020 22:36	CTD	12° 42.751'	057° 14.744'	4452	800
M161_210-1	16.02.2020 01:50	CTD	13° 00.046'	057° 14.702'	4742	800
M161_211-1	16.02.2020 04:51	CTD	13° 22.860'	057° 14.719'	4955	799
M161_212-1	16.02.2020 06:54	CTD	13° 22.861'	057° 14.719'	4955	250

M161_213-1	16.02.2020 08:57	CTD	13° 35.643'	057° 14.717'	4827	799
M161_214-1	16.02.2020 11:25	CTD	13° 53.332'	057° 14.720'	4863	800
M161_215-1	16.02.2020 14:21	Glider recovery	14° 11.015'	057° 20.522'	5170	0
M161_216-1	16.02.2020 14:40	Glider recovery	14° 10.984'	057° 20.481'	5168	0
M161_217-1	16.02.2020 15:21	CTD	14° 10.975'	057° 20.610'	5168	1000
M161_218-1	16.02.2020 17:21	CTD	14° 10.916'	057° 25.237'	5174	800
M161_219-1	16.02.2020 19:48	CTD	14° 10.927'	057° 14.761'	5168	800
M161_220-1	16.02.2020 22:27	CTD	14° 10.942'	057° 04.015'	5101	800
M161_221-1	17.02.2020 00:48	CTD	14° 10.922'	056° 54.016'	5128	800
M161_222-1	17.02.2020 03:24	CTD	14° 10.938'	056° 44.063'	5163	800
M161_223-1	17.02.2020 06:22	CTD	14° 19.747'	056° 59.846'	5373	800
M161_224-1	17.02.2020 09:13	CTD	14° 28.580'	057° 14.778'	5508	800
M161_225-1	17.02.2020 12:12	CTD	14° 10.925'	057° 14.725'	5173	800
M161_226-1	17.02.2020 15:37	CTD	13° 53.317'	057° 14.702'	4872	800
M161_227-1	17.02.2020 18:16	CTD	13° 35.643'	057° 14.733'	4827	800
M161_228-1	17.02.2020 20:55	CTD	13° 17.993'	057° 14.736'	4953	800
M161_229-1	17.02.2020 23:46	CTD	13° 00.031'	057° 14.723'	4736	800
M161_230-1	18.02.2020 02:24	CTD	12° 42.751'	057° 14.712'	4459	800
M161_231-1	18.02.2020 05:21	CTD	12° 25.154'	057° 14.747'	4493	800
M161_232-1	18.02.2020 08:09	CTD	12° 07.511'	057° 14.731'	4472	800
M161_233-1	18.02.2020 10:58	CTD	12° 25.139'	057° 14.754'	4493	800
M161_234-1	18.02.2020 14:02	CTD	12° 42.752'	057° 14.711'	4458	800
M161_235-1	18.02.2020 17:15	CTD	13° 00.071'	057° 14.706'	4741	800
M161_236-1	18.02.2020 21:02	CTD	13° 18.011'	057° 14.733'	4952	800
M161_237-1	20.02.2020 15:33	CTD	13° 35.642'	057° 14.703'	4842	800
M161_238-1	20.02.2020 17:00	CTD	13° 35.643'	057° 14.701'	4829	250
M161_239-1	21.02.2020 12:57	CTD	15° 48.690'	055° 16.314'	5503	2000

M161_240-1	21.02.2020 13:53	ARGO float deployment	15° 48.711'	055° 16.184'	5505	0
M161_241-1	21.02.2020 20:24	CTD	16° 32.659'	054° 36.986'	5325	500
M161_242-1	23.02.2020 14:18	CTD	21° 31.580'	050° 04.858'	5383	500
M161_243-1	23.02.2020 17:13	CTD	21° 48.319'	049° 49.763'	4548	500
M161_244-1	23.02.2020 20:06	CTD	22° 04.853'	049° 34.125'	5080	500
M161_245-1	24.02.2020 15:40	CTD	24° 30.443'	047° 17.849'	4253	1000
M161_246-1	25.02.2020 13:30	CTD	27° 06.681'	044° 48.634'	3301	1000
M161_247-1	25.02.2020 17:11	CTD	27° 26.053'	044° 29.989'	2910	500
M161_248-1	25.02.2020 20:08	CTD	27° 43.338'	044° 13.007'	2880	500
M161_249-1	26.02.2020 11:49	CTD	29° 36.715'	042° 22.117'	2760	500
M161_250-1	26.02.2020 15:49	CTD	30° 00.102'	041° 58.921'	3989	2000
M161_251-1	26.02.2020 16:38	ARGO float deployment	30° 00.226'	041° 58.678'	4002	0
M161_252-1	26.02.2020 19:08	CTD	30° 11.727'	041° 37.008'	2493	500
M161_253-1	27.02.2020 10:19	CTD	31° 30.439'	039° 07.224'	3562	600
M161_254-1	27.02.2020 13:38	CTD	31° 40.232'	038° 48.882'	3515	2000
M161_255-1	27.02.2020 14:26	ARGO float deployment	31° 40.230'	038° 48.714'	3516	0
M161_256-1	27.02.2020 18:10	CTD	31° 56.606'	038° 13.446'	2950	500
M161_257-1	28.02.2020 08:09	CTD	33° 05.437'	036° 01.127'	2762	2000
M161_258-1	28.02.2020 08:52	ARGO float deployment	33° 05.590'	036° 01.173'	2763	0
M161_259-1	28.02.2020 15:11	CTD	33° 35.206'	034° 55.261'	3286	500
M161_260-1	28.02.2020 20:52	CTD	34° 00.005'	034° 00.018'	2971	999
M161_261-1	29.02.2020 07:46	CTD	34° 48.300'	032° 13.776'	2762	1000
M161_262-1	29.02.2020 12:16	CTD	35° 07.898'	031° 30.843'	3167	500
M161_263-1	29.02.2020 15:08	CTD	35° 18.497'	031° 06.799'	3225	500
M161_264-1	29.02.2020 19:16	CTD	35° 32.273'	030° 36.845'	3196	1000

M161_265-1	01.03.2020 08:24	CTD	36° 15.468'	028° 59.296'	3363	1000
M161_266-1	01.03.2020 17:27	CTD	36° 58.684'	027° 21.005'	2108	1000

7.2 Station list of radiosonde launches

Time and locations of the MPI-M radiosondes launches during the M161 cruise of the R/V METEOR. In addition, one extra radiosonde (not listed here) was launched by the station of German Weather Service (DWD) onboard the R/V METEOR each day, usually at 16:33 UTC during the EUREC^{4}A campaign and at 22:33 UTC during the transit to the Azores.

	Date	Time (UTC)	Latitude	Longitude
1	18.01.2020	06:45	13.170	-59.404
2	18.01.2020	10:45	13.170	-59.404
3	18.01.2020	14:45	13.338	-59.041
4	18.01.2020	18:45	13.566	-58.538
5	18.01.2020	22:45	13.731	-58.176
6	19.01.2020	02:45	13.834	-57.783
7	19.01.2020	06:45	13.798	-57.381
8	19.01.2020	10:45	13.785	-57.252
9	19.01.2020	14:45	13.573	-57.316
x	19.01.2020	18:45		
10	19.01.2020	22:45	13.577	-56.609
11	20.01.2020	02:45	13.770	-57.175
12	20.01.2020	06:45	13.790	-57.302
13	20.01.2020	10:45	13.783	-57.359
14	20.01.2020	14:45	14.026	-57.245
15	20.01.2020	18:45	14.451	-57.248
16	20.01.2020	22:45	14.030	-57.245
17	21.01.2020	02:45	13.511	-57.245
18	21.01.2020	06:45	13.118	-57.252
19	21.01.2020	10:45	13.253	-57.245
20	21.01.2020	14:45	13.692	-57.373
21	21.01.2020	18:45	14.169	-57.709
22	21.01.2020	22:45	14.187	-57.424
23	22.01.2020	02:45	14.182	-56.975
24	22.01.2020	06:45	14.373	-57.079
25	22.01.2020	10:45	14.182	-57.245
26	22.01.2020	14:45	14.182	-57.245
27	22.01.2020	18:45	14.182	-57.245
28	22.01.2020	22:45	14.182	-57.245
29	23.01.2020	02:45	14.182	-57.245
30	23.01.2020	06:45	14.182	-57.245
31	23.01.2020	10:45	14.182	-57.338

32	23.01.2020	14:45	14.182	-57.338
33	23.01.2020	18:45	14.094	-57.426
34	23.01.2020	22:45	14.272	-57.246
35	24.01.2020	02:45	13.991	-57.242
36	24.01.2020	06:45	13.746	-57.246
37	24.01.2020	10:45	13.913	-57.245
38	24.01.2020	14:45	13.970	-57.180
39	24.01.2020	18:45	13.884	-57.200
40	24.01.2020	22:45	13.675	-57.199
41	25.01.2020	02:45	13.365	-57.245
42	25.01.2020	06:45	12.999	-57.245
43	25.01.2020	10:45	12.658	-57.245
44	25.01.2020	14:45	12.255	-57.245
45	25.01.2020	18:45	12.368	-57.061
46	25.01.2020	22:45	12.419	-57.321
47	26.01.2020	02:45	12.419	-57.630
48	26.01.2020	06:45	12.679	-57.290
49	26.01.2020	10:45	12.419	-57.245
50	26.01.2020	14:45	12.331	-56.818
51	26.01.2020	18:45	12.191	-56.137
52	26.01.2020	22:45	12.263	-56.479
53	27.01.2020	02:45	12.310	-56.908
54	27.01.2020	06:45	12.125	-57.246
55	27.01.2020	10:45	12.419	-57.245
56	27.01.2020	14:45	12.766	-57.245
x	27.01.2020	18:45		
57	27.01.2020	22:45	13.291	-57.233
58	28.01.2020	02:45	13.612	-57.245
59	28.01.2020	06:45	14.029	-57.245
60	28.01.2020	10:45	14.460	-57.247
61	28.01.2020	14:45	14.182	-57.245
62	28.01.2020	18:45	13.793	-57.240
63	28.01.2020	22:45	13.521	-57.246
64	29.01.2020	02:45	13.112	-57.245
65	29.01.2020	06:45	12.881	-57.245
66	29.01.2020	10:45	12.651	-57.245
67	29.01.2020	14:45	12.355	-57.245
68	29.01.2020	18:45	12.361	-57.245
69	29.01.2020	22:45	12.713	-57.246
70	30.01.2020	02:45	13.021	-57.245
71	30.01.2020	06:45	13.457	-57.245
72	30.01.2020	10:45	13.328	-57.400
73	30.01.2020	14:45	13.300	-57.356
74	30.01.2020	18:45	13.300	-56.923
75	30.01.2020	22:45	13.300	-57.049
76	31.01.2020	02:45	13.300	-57.386

77	31.01.2020	06:45	13.300	-56.872
78	31.01.2020	10:45	13.457	-57.006
79	31.01.2020	14:45	13.786	-57.245
80	31.01.2020	18:45	14.175	-57.245
81	31.01.2020	22:45	14.476	-57.246
82	01.02.2020	02:45	14.272	-57.431
83	01.02.2020	06:45	14.092	-57.432
84	01.02.2020	10:45	13.949	-57.231
85	01.02.2020	14:45	13.676	-57.245
86	01.02.2020	18:45	13.301	-57.246
87	01.02.2020	22:45	13.000	-57.250
88	02.02.2020	02:45	12.713	-57.326
89	02.02.2020	06:45	12.713	-56.914
90	02.02.2020	10:45	12.711	-57.246
91	02.02.2020	14:45	12.419	-57.245
92	02.02.2020	18:45	12.276	-57.243
93	02.02.2020	22:45	12.628	-57.245
94	03.02.2020	02:45	12.438	-57.703
95	03.02.2020	06:45	12.029	-58.379
x	03.02.2020	10:45		
96	03.02.2020	14:45	11.780	-59.248
97	03.02.2020	18:45	12.066	-59.104
x	03.02.2020	22:45		
98	04.02.2020	02:45	12.472	-57.942
x	04.02.2020	06:45		
99	04.02.2020	10:45	12.683	-57.334
100	04.02.2020	14:45	12.815	-57.245
101	04.02.2020	18:45	12.986	-57.245
102	04.02.2020	22:45	13.300	-57.246
103	05.02.2020	02:45	13.672	-57.245
104	05.02.2020	06:45	14.071	-57.244
105	05.02.2020	10:45	14.460	-57.250
106	05.02.2020	14:45	14.182	-57.246
107	05.02.2020	18:45	14.090	-57.315
108	05.02.2020	22:45	14.080	-57.250
x	06.02.2020	02:45		
109	06.02.2020	06:45	14.082	-57.246
110	06.02.2020	10:45	14.082	-57.246
111	06.02.2020	14:45	14.082	-57.246
112	06.02.2020	18:45	14.082	-57.246
113	06.02.2020	22:45	13.637	-57.245
114	07.02.2020	02:45	13.301	-57.234
115	07.02.2020	06:45	12.967	-57.246
116	07.02.2020	10:45	12.576	-57.245
117	07.02.2020	14:45	12.436	-57.246
118	07.02.2020	18:45	12.312	-57.231

119	07.02.2020	22:45	12.357	-57.245
120	08.02.2020	02:45	12.419	-57.245
121	08.02.2020	06:45	12.419	-57.245
122	08.02.2020	10:45	12.417	-57.252
123	08.02.2020	14:45	12.374	-57.422
124	08.02.2020	18:45	12.373	-57.291
125	08.02.2020	22:45	12.419	-57.245
126	09.02.2020	02:45	12.419	-57.245
127	09.02.2020	06:45	12.419	-57.245
128	09.02.2020	10:45	12.419	-57.245
129	09.02.2020	14:45	12.419	-57.245
130	09.02.2020	18:45	12.419	-57.245
131	09.02.2020	22:45	12.584	-57.245
132	10.02.2020	02:45	13.001	-57.245
133	10.02.2020	06:45	13.300	-57.245
134	10.02.2020	10:45	13.550	-57.245
135	10.02.2020	14:45	13.894	-57.231
136	10.02.2020	18:45	14.180	-57.250
137	10.02.2020	22:45	14.180	-57.250
138	11.02.2020	02:45	14.182	-57.245
139	11.02.2020	06:45	14.182	-57.245
140	11.02.2020	10:45	14.182	-57.245
141	11.02.2020	14:45	14.182	-57.245
142	11.02.2020	18:45	14.182	-57.245
143	11.02.2020	22:45	13.995	-57.097
144	12.02.2020	02:45	13.677	-56.937
145	12.02.2020	06:45	13.068	-57.081
146	12.02.2020	10:45	12.586	-57.181
147	12.02.2020	14:45	12.419	-57.120
148	12.02.2020	18:45	12.419	-56.761
149	12.02.2020	22:45	12.258	-57.013
150	13.02.2020	02:45	13.677	-56.937
151	13.02.2020	06:45	13.068	-57.081
152	13.02.2020	10:45	12.586	-57.181
153	13.02.2020	14:45	12.419	-57.120
154	13.02.2020	18:45	12.419	-56.761
155	13.02.2020	22:45	12.258	-57.013
156	14.02.2020	02:45	14.351	-57.245
157	14.02.2020	06:45	14.182	-57.246
x	14.02.2020	10:45		
158	14.02.2020	14:45	13.416	-57.245
159	14.02.2020	18:45	13.300	-57.416
160	14.02.2020	22:45	13.300	-57.077
161	15.02.2020	02:45	13.300	-56.730
162	15.02.2020	06:45	13.060	-57.128
163	15.02.2020	10:45	12.712	-57.245

164	15.02.2020	14:45	12.419	-57.245
165	15.02.2020	18:45	12.289	-57.245
166	15.02.2020	22:45	12.713	-57.246
167	16.02.2020	02:45	13.005	-57.236
x	16.02.2020	06:45		
168	16.02.2020	10:45	13.778	-57.245
169	16.02.2020	14:45	14.184	-57.342
170	16.02.2020	18:45	14.182	-57.364
171	16.02.2020	22:45	14.182	-57.067
172	19.02.202	11:00	13.160	-59.400
173	21.02.2020	10:34	15.580	-55.480
174	22.02.2020	10:46	18.100	-53.220
175	23.02.2020	10:32	21.070	-50.510
176	24.02.2020	10:33	23.880	-47.890
177	25.02.2020	10:32	26.780	-45.140
178	26.02.2020	10:52	29.530	-42.450
179	27.02.2020	10:37	31.510	-39.120
180	28.02.2020	10:32	33.200	-35.780
181	29.02.2020	10:32	34.990	-31.820
182	01.03.2020	10:34	36.330	-28.820

8 Data and Sample Storage and Availability

Table 8.1 Overview of data availability (n/a = dates not available yet)

Type	**Data/Samples** **Database**	**Available**	**Free Access**	**Contact**
Raman Lidar	by request	n/a	n/a	bjoern.bruegmann@mpimet.mpg.de ludwig.worbes@mpimet.mpg.de ilya.serikov@mpimet.mpg.de
Ceilometer	ftp://ftp-projects.zmaw.de/aerocom/ships/ceilometer_M	4/1/2020	n/a	stefan.kinne@mpimet.mpg.de
Cloud camera	by request	n/a	n/a	stefan.kinne@mpimet.mpg.de
Microtops	https://aeronet.gsfc.nasa.gov/new_web/cruises_new/Meteor_20_0.html	4/1/2020	4/1/2020	stefan.kinne@mpimet.mpg.de alexander.smirnov-1@nasa.gov
Radar, microwave radiometer, spectrometer	by request	n/a	n/a	heike.kalesse@uni-leipzig.de
Wind lidar	by request	n/a	n/a	louise.nuijens@tudelft.nl
Eddy covariance	by request	n/a	n/a	imke.schirmacher@studium.uni-hamburg.de
Water vapor isotopes (Picarro)	by request archive planned	n/a	n/a	galewsky@unm.edu slos@unm.edu
MAX-DOAS	by request	n/a	n/a	steffen.doerner@mpic.de
In-situ aerosol	by request	n/a	n/a	m.pohlker@mpic.de

PAX and Locomotive	by request	n/a	n/a	makuch@iopan.pl mich@igf.fuw.edu.pl
Radiosondes	by request	n/a	n/a	Claudia.stephan@mpimet.mpg.de yanmichel.morfa-avalos@mpimet.mpg.de
UAV	by request	n/a	n/a	dbaranowski@igf.edu.pl
Cloudkite	by request	n/a	n/a	marcel.schroeder@ds.mpg.de eberhard.bodenschatz@ds.mpg.de
CTD and Rodnei	PANGAEA (planned); by request	n/a	n/a	dbaranowski@igf.edu.pl makuch@iopan.pl
Seagliders	CLIMSERV server; by request	n/a	n/a	c.rollo@uea.ac.uk
ADCP	by request	n/a	n/a	k.heywood@uea.ac.uk
ARGO floats	BSH; by request	n/a	n/a	anja.schneehorst@bsh.de
Autonaut	by request	n/a	n/a	k.heywood@uea.ac.uk
Microbial Oceanography	PANGAEA/Gen bank (where applicable); by request	n/a	n/a	wmohr@mpi-bremen.de

9 Acknowledgements

The scientific party of R/V METEOR cruise M161 would like to thank Captain Rainer Hammacher and his entire crew for the professionalism and support as well as the friendly and enjoyable atmosphere during the cruise. We are grateful to the German coordination office (Leitstelle Deutsche Forschungsschiffe) for their support before, during and after the cruise. This cruise (Fördernummer: GPF18-1_69, EUREC^{4}A^{++}) was funded by the German Research Foundation (Deutsche Forschungsgemeinschaft, DFG) and the German Federal Ministry of Education and Research (Bundesministerium für Bildung und Forschung, BmBF) as well as contributions by the Max Planck Society and other individual institutions and their funded projects as listed in 2.3.

10 References

Beirle, S., Remmers, J. and Wagner, T., 2019. The Mainz profile algorithm (MAPA). Atmospheric Measurement Techniques, 12(3), pp.1785-1806.

Illingworth, A.J., Hogan, R.J., O'Connor, E.J., Bouniol, D., Brooks, M.E., Delanoë, J., Donovan, D.P., Eastment, J.D., Gaussiat, N., Goddard, J.W.F. and Haeffelin, M., 2007. Cloudnet: Continuous evaluation of cloud profiles in seven operational models using ground-based observations. Bulletin of the American Meteorological Society, 88(6), pp.883-898.

Martínez-Pérez, C., Mohr, W., Löscher, C.R., Dekaezemacker, J., Littmann, S., Yilmaz, P., Lehnen, N., Fuchs, B.M., Lavik, G., Schmitz, R.A. and LaRoche, J., 2016. The small unicellular diazotrophic symbiont, UCYN-A, is a key player in the marine nitrogen cycle. Nature Microbiology, 1(11), pp.1-7.

Platt, U. and Stutz, J., 2008. Differential absorption spectroscopy. In Differential Optical Absorption Spectroscopy (pp. 135-174). Springer, Berlin, Heidelberg.

Pöhlker, M.L., Pöhlker, C., Klimach, T., de Angelis, I.H., Barbosa, H.M., Brito, J., Carbone, S., Cheng, Y., Chi, X., Ditas, F. and Ditz, R., 2016. Long-term observations of cloud condensation

nuclei in the Amazon rain forest–Part 1: Aerosol size distribution, hygroscopicity, and new model parametrizations for CCN prediction. Atmospheric Chemistry and Physics, 16(24), pp.15709-15740.

Rose, D., Gunthe, S.S., Mikhailov, E., Frank, G.P., Dusek, U., Andreae, M.O. and Pöschl, U., 2008. Calibration and measurement uncertainties of a continuous-flow cloud condensation nuclei counter (DMT-CCNC): CCN activation of ammonium sulfate and sodium chloride aerosol particles in theory and experiment.

Sargent, J.R., 1976. The structure, metabolism and function of lipids in marine organisms. In: Malins, D.C., Sargent, J.R. (Eds.), Biochemical and Biophysical Perspectives in Marine Biology. Academic Press, London, pp. 149-212.

Smith Jr, K.L., Ruhl, H.A., Kaufmann, R.S. and Kahru, M., 2008. Tracing abyssal food supply back to upper-ocean processes over a 17-year time series in the northeast Pacific. Limnology and Oceanography, 53(6), pp.2655-2667.

Wagner, T., Beirle, S., Brauers, T., Deutschmann, T., Frieß, U., Hak, C., Halla, J.D., Heue, K.P., Junkermann, W., Li, X. and Platt, U., 2011. Inversion of tropospheric profiles of aerosol extinction and HCHO and NO 2 mixing ratios from MAX-DOAS observations in Milano during the summer of 2003 and comparison with independent data sets. Atmospheric Measurement Techniques, 4(12), pp.2685-2715.

Wagner, T., Dix, B.V., Friedeburg, C.V., Frieß, U., Sanghavi, S., Sinreich, R. and Platt, U., 2004. MAX-DOAS O4 measurements: A new technique to derive information on atmospheric aerosols—Principles and information content. Journal of Geophysical Research: Atmospheres, 109(D22).

Wendisch, M., Müller, D., Schell, D. and Heintzenberg, J., 2001. An airborne spectral albedometer with active horizontal stabilization. Journal of Atmospheric and Oceanic Technology, 18(11), pp.1856-1866.

Wex, H., Dieckmann, K., Roberts, G.C., Conrath, T., Izaguirre, M.A., Hartmann, S., Herenz, P., Schaefer, M., Ditas, F., Schmeissner, T. and Henning, S., 2016. Aerosol arriving on the Caribbean island of Barbados: physical properties and origin.

Wiedensohler, A., 1988. An approximation of the bipolar charge distribution for particles in the submicron size range. Journal of Aerosol Science, 19(3), pp.387-389.

11 Abbreviations

Abbreviations are explained within text.

12 Appendices

12.1 Supplementary information to chapter 5

Table 5.1.1.1 Technical characteristics of the Raman Lidar

Pulse repetition rate	10 Hz		
Laser pulse energy	@ 355 nm	@ 532 nm	@ 1064 nm
	125 mJ	125 mJ	200 mJ
Laser beam diameter	80 mm		
Laser beam divergence	70 µrad		
Operating range	@ 355 nm	@ 532 nm	@ 1064 nm
	0 - 15 (29) [1)] km	0 - 15 (29) [1)] km	0 - 15 km
Receiving telescopes:			
telescope ID	**Focal length**	**Diameter**	**Field-of-view**
"Far-range"	2000 mm	500 mm	250 µrad
"Near-range"	450 mm	150 mm	450 µrad
"Close-range"	100 mm	22 mm	2000 µrad
"Depolarization"	500 mm	50 mm	400 µrad

[1)] measurement height limit for counted channels has been extended from 15 to 29 km on June 14, 2017

Table 5.1.1.2 Parameters measured.

Product	**Wavelength of emission stimulating lidar return**
Attenuated backscatter	1064, 532, 355 nm
Particle backscatter	532, 355 nm
Particle extinction	532, 355 nm
Volume linear depolarization ratio	532 nm
Particle linear depolarization ratio	532 nm
Cloud mask	532, 355 nm
Water vapor mixing ratio	355 nm
Air temperature	355 nm
Relative humidity	355 nm

Table 5.1.5.1 Specifications of the two wind-lidars operating during M161.

	Windcube WLS70	**Windcube V2**
Type	Long-Range	Short-range
Range	100-2000 m	40-250 m
Levels	100, 200, 300, … 1900, 2000 m	40, 60, 70, 80, 90, 100, 110, 130, 150, 170, 200, 250 m
Sampling frequency	0.1 Hz	1 Hz
Wavelength	1.54 µm	1,54 µm
Accuracy	0.3 m/s	0.1 m/s
Data availability	17/01-02/03	27/01-14/02 and 21/02-02/03

Table 5.1.13.1 Description of the instruments of the mini-MPCK (from 24 Jan 2020 to 08 Feb 2020) and micro-MPCK (from 20 Feb 2020 to 01 Mar 2020).

Probe	**Platform**	**Measurement variables**	**Sample rate [Hz]**	**Resolution**	**Spatial resolution @ 10 m/s relative wind speed**
CDP-2	Mini-MPCK	D_p, n	2	Depending on droplet size (Lance et al., 2010)	5m x 0.28 mm^3
uSonic3 Class A MP	Mini-MPCK	u, v, w, T	30	u, v, w: 1.5 % @ 5 m/s, T: 0.01K (accuracy)	0.3 m
miniCTA	Mini-MPCK, Micro-MPCK	u’	8000	TBD	0.002 m
UFT	Mini-MPCK	T’	8000	< 0.1 K	0.005 m
in-house hotwire prototype	Micro-MPCK	u’	8000	TBD	0.002 m
PSS8	Mini-MPCK, Micro-MPCK	p, u, T	100	p: 0.03 hPa, u: 0.1 m/s, T: 0.1 K	0.1 m
HMP7	Mini-MPCK	T, RH, D	0.2	RH: >0.8%, T: 0.1 K	50 m

BMP388	Mini-MPCK, Micro-MPCK	p, T	1	p: 0.5 hPa , T: 0.3 K	10 m
AM2315	Mini-MPCK, Micro-MPCK	T, RH	0.5	RH: 2 %, T: 0.1 K	20 m
BNO055	Mini-MPCK, Micro-MPCK	roll, pitch, yaw	100	Not specified in the datasheet from Bosch	
SBG	Mini-MPCK	lat, lon, alt, roll, pitch, yaw	200	lat, lon, alt: 2 m, yaw: 0.5 ˚, roll, pitch: 0.2 ˚	
ZED-F9P	Mini-MPCK, Micro-MPCK	lat, lon, alt	1	lat, lon, alt: < 1.5 m	

CTD system configuration, calibration and data processing

1) One CTD system was prepared. The initial water sampling arrangement was 24-way stainless steel frame system and the initial sensor configuration was as follows:

- Sea-Bird 9plus underwater unit,
- Sea-Bird 3P temperature sensor, Frequency 0 (S/N 5272, primary)
- Sea-Bird 4C conductivity sensor, Frequency 1 (S/N 3732, primary)
- Digiquartz temperature compensated pressure sensor, Frequency 2 (S/N 0979)
- Sea-Bird 3P temperature sensor Frequency 3 (S/N 5600, secondary)
- Sea-Bird 4C conductivity sensor, Frequency 4 (S/N 3734, secondary)
- Sea-Bird 5T submersible pump (primary)
- Sea-Bird 5T submersible pump (secondary)
- Sea-Bird 32 Carousel 24 position pylon
- Sea-Bird 11plus deck unit

2) The auxiliary input initial sensor configuration was as follows:

- Sea-Bird 43 dissolved oxygen sensor (S/N 1812, V0)
- Fluorometer, WETLabs (S/N 2718, V2)
- Turbidity, WETLabs (S/N 2718, V3)
- Benthos PSAA-916T altimeter (S/N 49768, V4)
- PAR Irradiance, Licor (S/N 70279, V6)
- Surface PAR sensor, Licor (S/N 20353, SPAR V)

3) Changes to instrumental set up

For stations 002-005 Sea-Bird 9plus configuration file M161_002.XMLCOM was used. Before station 005 secondary temperature and salinity sensors were replaced with spare parts by WTD. New sensors were Sea-Bird 3P temperature sensor (S/N 5655) and Sea-Bird 4C conductivity sensor (S/N 3717). Since that point onward configuration file M161_006.XMLCOM was used.

For the full depth cast (station 142b) and since station 237 PAR sensor was removed from configuration.

4) water sampling for physical properties

Initial test cast (station 001) revealed bottle firing problem with bottle nr 4 and multiple leaking bottles. All o-rings on Niskin bottles were replaced for station 003. Firing mechanisms was replaced by the WTD and all bottles were firing before station 050. No leaking bottles except two casts due to misplaced o-rings. Three casts were done with collection of water samples across profiles for post-cruise calibration. Casts at stations 029 and 217 with water samples at depths: 1000 m to 100 m every 100 m were done during deployment and recovery of UEA gliders. Cast on station M161_142-2 was done down to depth 4485 m with multiple water samples across the profile. This station was done in close vicinity and in parallel with R/V MARIA S. MERIAN.

5) Data processing

Initial data processing was done using SBE Data Processing software.

Data Conversion – converts the raw frequency and voltage data to engineering units where applicable by applying factory calibrations from the CON file. The converted downcast and upcast data is then saved to the M161_nnn.cnv output file.

Align CTD – takes the .cnv file as input and applies an alignment to the oxygen sensor in time relative to pressure. Typical value of 3 sec was used for all casts.

Cell Thermal Mass – takes align file as input and applies a thermal correction of the conductivity cell to minimize bad salinity readings in steep vertical gradients due to temperature/conductivity discrepancies. Typical values of parameters alpha (0.03) and 1/beta (7) were used for both primary and secondary T/C sensors.

Bin Average – averages raw 24 Hz data to 1 db vertical resolution data.

Slit – splits upcasts and downcasts, which are saved separately to uM161_nnn.cnv and dM161_nnn.cnv, respectively.

Table 5.2.2.1 Glider details and deployment statistics.

	SG579 Humpback	**SG620 Melonhead**	**SG637 Omura**
Owner	**UEA**	**UEA**	**NOC-MARS**
Sensors	Seabird CT sail Photosynthetically Active Radiation (PAR) sensor WETLabs Eco Puck optical sensor	Seabird CT sail	Seabird CT sail
Loggers	-	Rockland Scientific MicroPods - microstructure shear and temperature	Nortek 1 MHz acoustic Doppler dual current profiler
Directly measured variables	Temperature Salinity Pressure Photosynthetically Active Radiation Chlorophyll-a fluorescence Optical backscatter at 700 nm CDOM fluorescence	Temperature Salinity Pressure Turbulent kinetic energy dissipation rate	Temperature Salinity Pressure Vertical shear of horizontal velocity
Inferred variables	Dive-average horizontal current velocity Vertical current velocity	Dive-average horizontal current velocity Vertical current velocity	Dive-average horizontal current velocity Vertical current velocity
Deployment	2020-01-28 14:14 UTC 58° 48.61′ W 13° 20.95′ N	2020-01-23 15:13 UTC 57° 20.52′ W 14° 10.98′ N	2020-01-23 14:35 UTC 57° 20.49′ W 14° 11.01 N
Recovery	2020-02-16 14:42 UTC 57° 20.34′ W 14° 10.97′ N	2020-02-05 16:00 UTC 57° 23.46′ W 14° 07.85′ N	2020-02-16 14:31 UTC 57° 20.44′ W 14° 11.0′ N
Days of data	19	13	24
Dive cycles completed	295	131	155

Table 5.2.3.1 ADCP configurations for the M161 cruise.

	OS75	**OS38**
Operating frequency	75 kHz	38 kHz
Profile mode	Broadband	Narrowband
Bin size	8 m	32 m
Blanking distance	4 m	16 m
Ambiguity velocity	390 cm/s	390 cm/s
Bottom track	Disabled	Disabled
Data output	Velocity, correlation, echo intensity, percent good	Velocity, correlation, echo intensity, percent good
Ping frequency	As fast as possible	As fast as possible
Output coordinate system	Beam data	Beam data
Transducer depth	5 m	5 m
Transducer misalignment	0	45
Salinity	35 ppt	35 ppt
Miscellaneous	Set to calculate speed-of-sound, no depth sensor, external synchro heading sensor, no pitch or roll being used, no salinity sensor, use internal transducer temperature sensor	Set to calculate speed-of-sound, no depth sensor, external synchro heading sensor, no pitch or roll being used, no salinity sensor, use internal transducer temperature sensor

Table 5.2.5.1 ARGO deployment details during M161

	Float S/N	**Lat (N)**	**Lon (W)**	**Day**	**Time**	**CTD**	**Z (m)**	**Bot (m)**
1	AI2600-19DE031	12°11.204’	56°07.009’	1/26/2020	20:17	M161-057	- 2000	- 4498
2	AI2600-19DE034	15°48.711’	55°16.184’	2/21/2020	13:54	M161-239	- 2000	- 5505
3	AI2600-19DE034	30°00.226’	41°58.921’	2/26/2020	16:38	M161-250	- 2000	- 4002
4	AI2600-19DE028	31°40.230’	38°48.714’	2/27/2020	14:26	M161-254	- 2000	- 3515
5	AI2600-19DE038	33°05.437‘	36°01.171’	2/28/2020	08:52	M161-257	- 2000	- 2764

Table 5.2.6.1 Meteorological and oceanographic sensors on the Autonaut, Caravela.

Instrument	**Parameters measured**	**Parameters calculated**	**Sampling rate**	**Position on Caravela**	**Additional information**
Airmar 120WX	Apparent wind speed (m s^{-1}), Apparent wind direction (deg), Air Temperature (˚C)		10 minute average	On mast, approx. 1m above sea surface	
Rotronic HC2A –S3 standard meteo probe, Rotronic MP402H-082000 sensor, Rotronic AC1003 unit	Humidity (%RH), Air Temperature (˚C)		1 second	On mast, approx. 1m above sea surface	
Apogee SP-110-SS Pyranometer		Shortwave solar radiation (W m^{-2})	1 second	On mast, approx. 1m above sea surface	Range: 360 – 1120 nanometres
Apogee SL510 Pyrgeometer		Incoming longwave radiation (W m^{-2})	1 second	On mast, approx. 1m above sea surface	Range: 5 - 30 micrometres
Valeport miniCTD	Pressure (dBar), Water temperature (˚C), Conductivity (mS cm^{-1})		1 second	Fixed through Caravela's hull	
Nortek Signature1000 1 MHz Acoustic Doppler Current Profiler (ADCP)	Relative velocity with 5 beams (m s^{-1})	Velocity shear earth relative (ENU) (m s^{-1})	10 minutes	Mounted under the centre of Caravela, forward of the Seaglider release mechanism.	Range: 30m

12.2 Selected Pictures of Shipboard Operations

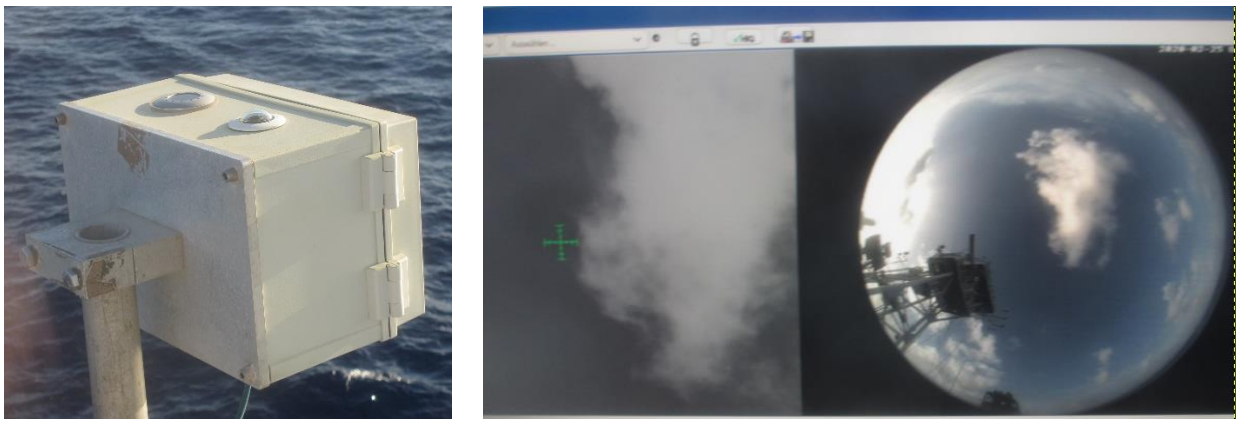

Figure 5.1.2.1 The M161 camera system with its visible frog-eye and thermal imager (left) and images of a cloud scene (which are recorded every 10 seconds) on a monitor (right).

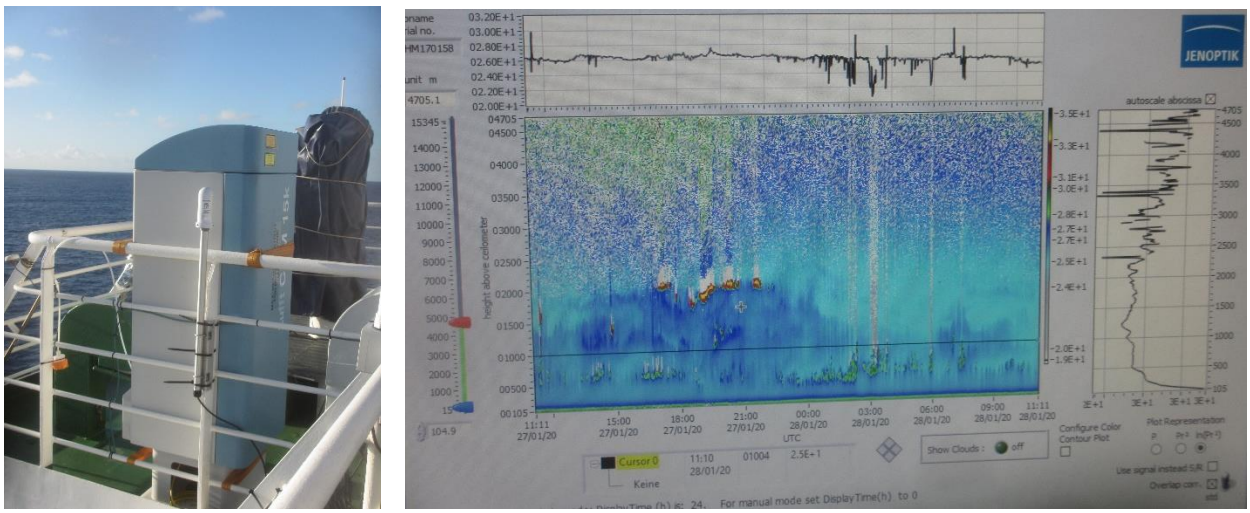

Figure 5.1.2.2 The ceilometer on R/V METEOR (left) and a screenshot with data of the last 24 hrs (right). A selection of daily summaries for selected days during the EUREC^{4}A campaign are presented.

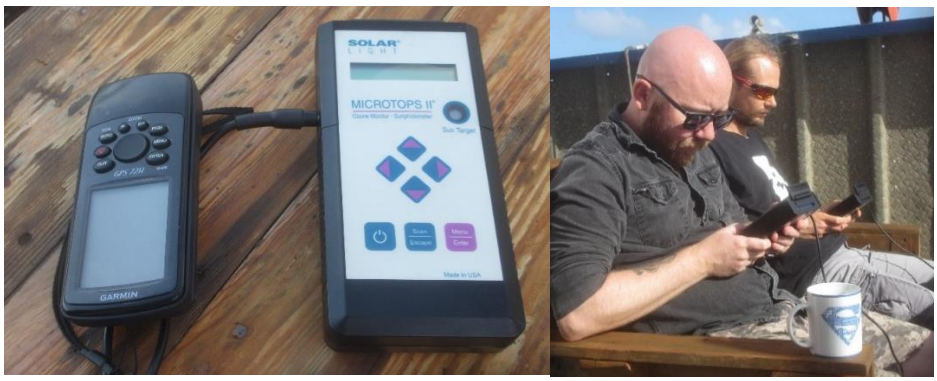

Figure 5.1.3.1 The MICROTOPS sunphotometer (left) and its handheld operation into the sun (right).

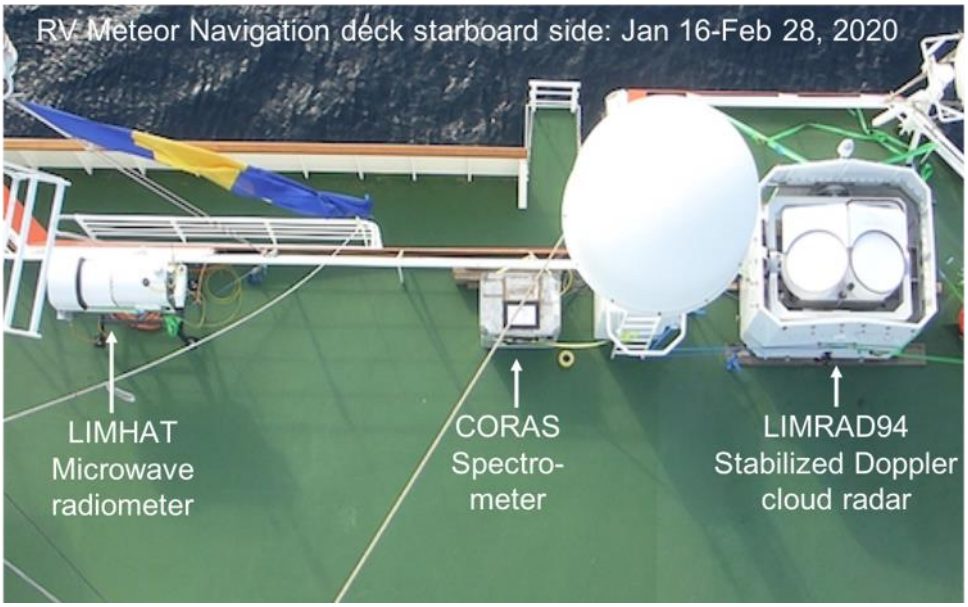

Fig. 5.1.4.1 Installation of instruments of Leipzig Institute of Meteorology (LIM) University of Leipzig during M161.

Figure 5.1.5.1 Position of the two Wind LiDARs on the Meteor. Left image shows the long-range WLS70 on the left and the short-range V2 on the right of the deck, the image orientation is towards portside. Right image shows the location of the deck above the paint storage where the LiDARs are placed.

Figure 5.1.6.1 Flux instrumentation placements during M161 at the front of the vessel (left panel) and at the top of the mast (right panel): Ultra-sonic anemometer METEK uSonic-3 Scientific (1), LI-COR LI-7500 open path (2), Radiation pyrometer KT19 on sea surface (3), LI-COR Datalogger (4), temperature and humidity probe Vaisala HMT337 (5), Barometer Vaisala PTB (6), GPS receiver (7a,7b), USAT Datalogger (8), Power box (9) and GPS-mouse 10).

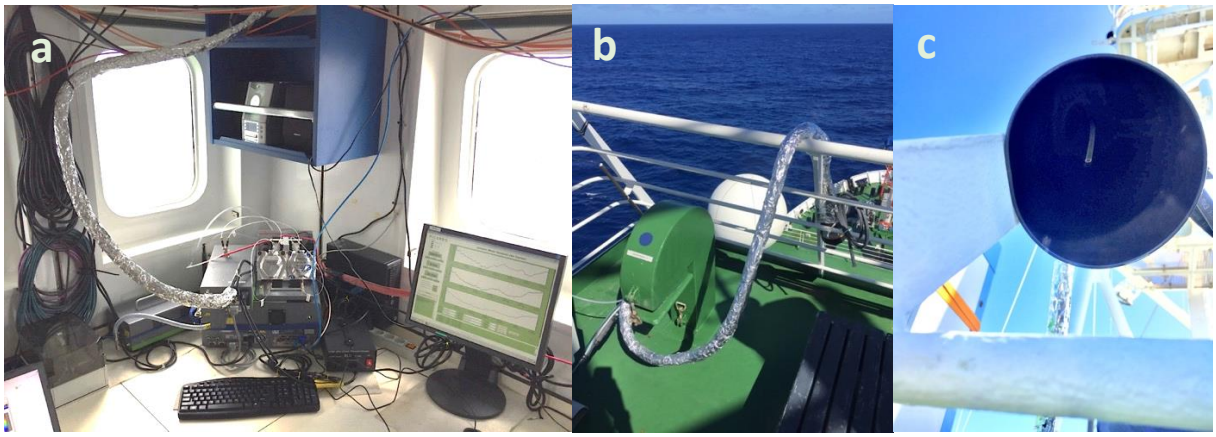

Figure 5.1.7.1 a) Picarro L2130-i analyzer and associated modules as setup in the Air-Chemistry Laboratory on the Navigation Deck (5th superstructure deck), b) inlet line setup on the fore railing of the 6th superstructure deck above the Air-Chemistry Laboratory, c) view up into the black inlet funnel with the clear end of the inlet line.

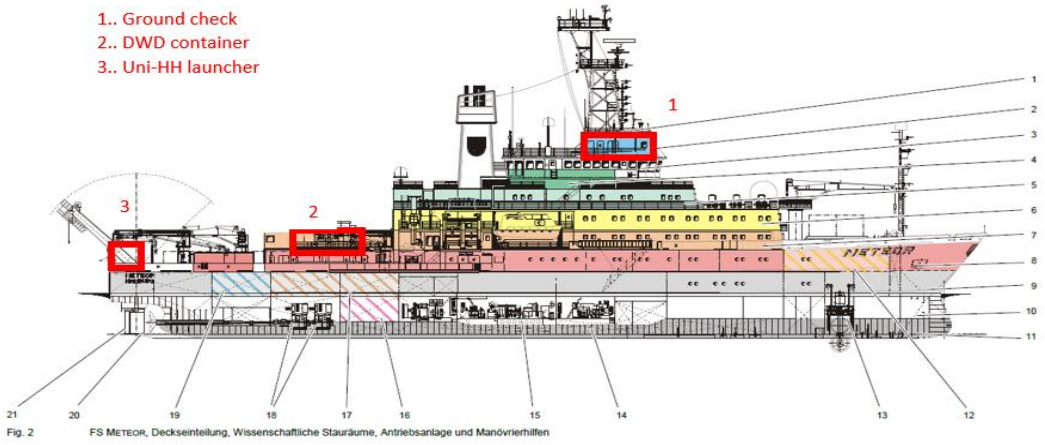

Figure 5.1.11.1 Location of the Air-Chemistry laboratory where the ground check was performed (1), DWD container (2) and Uni-HH launcher (3) on deck.

Figure 5.1.12.1. RBR and HOBO instruments with marked temperature sensors' location on each of the instruments.

Figure 5.1.12.2 Helideck of R/V METEOR prepared for drone take off.

Figure 5.1.12.3 Take off from the palette. iMet instrument on a drone.

Figure 5.1.12.4 iMet on a drone

Figure 5.1.12.5 iMet on a drone

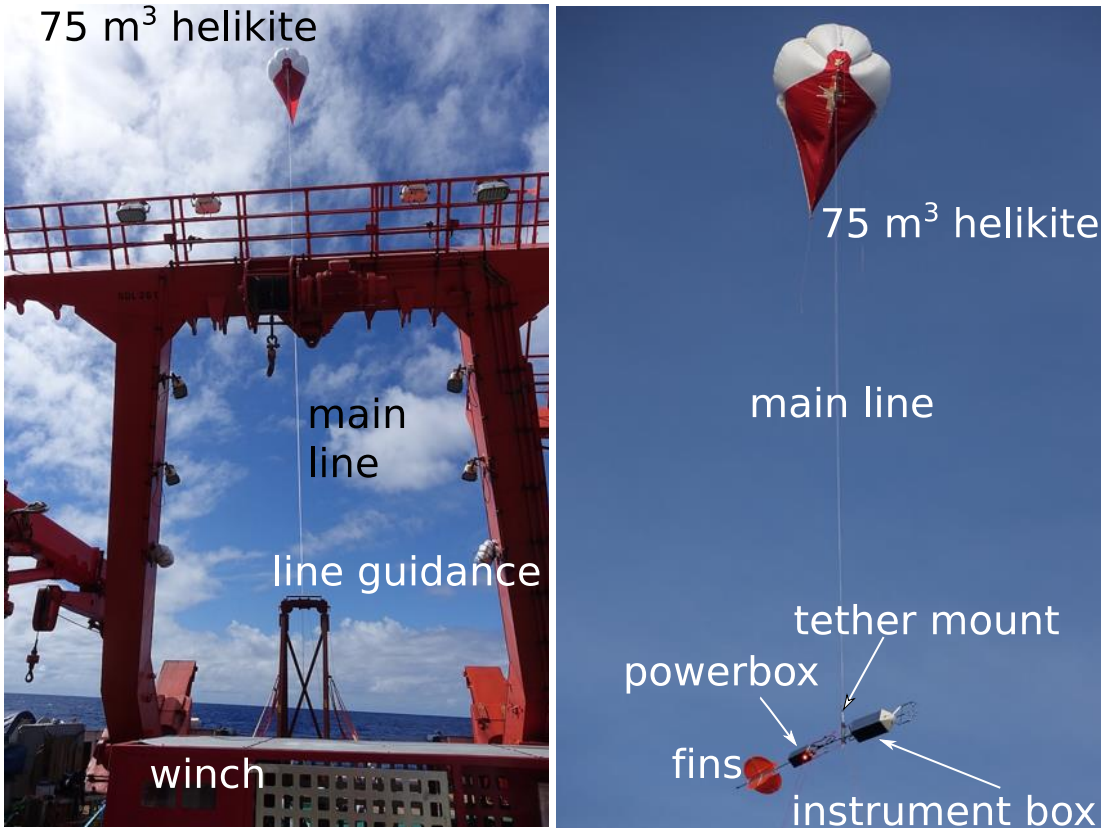

Figure 5.1.13.1 Line guidance on the aft of the working deck of R/V METEOR (left) and setup of the mini-MPCK on the 75 m³ Helikite (right).

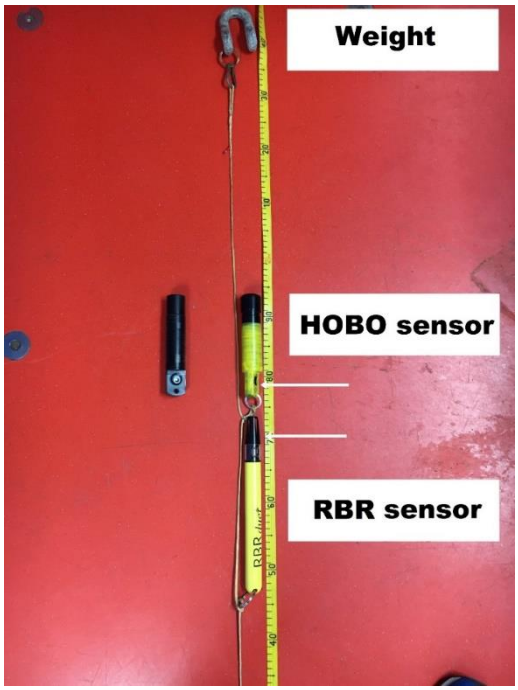

Figure 5.2.1.8 RODNEI setup with two instruments (HOBO data logger and RBR data logger) and weight (approximately 400 g). Both sensors have been fixed at the end of a 30 m long line with a 10 cm gap between them. The line had also markers every 0.5 m to control an immersion of the sensors. One of Hobo instruments used was covered with yellow tape to reduce radiative heating from the sunlight absorption (the unwrapped instrument is located on the left side). Arrows show sensors' locations for Hobo and RBR instruments. The instrumental setup had about 1 m length in total.

Figure 5.2.2.1 Glider deployment from the R/V METEOR's workboat as photographed by a drone.

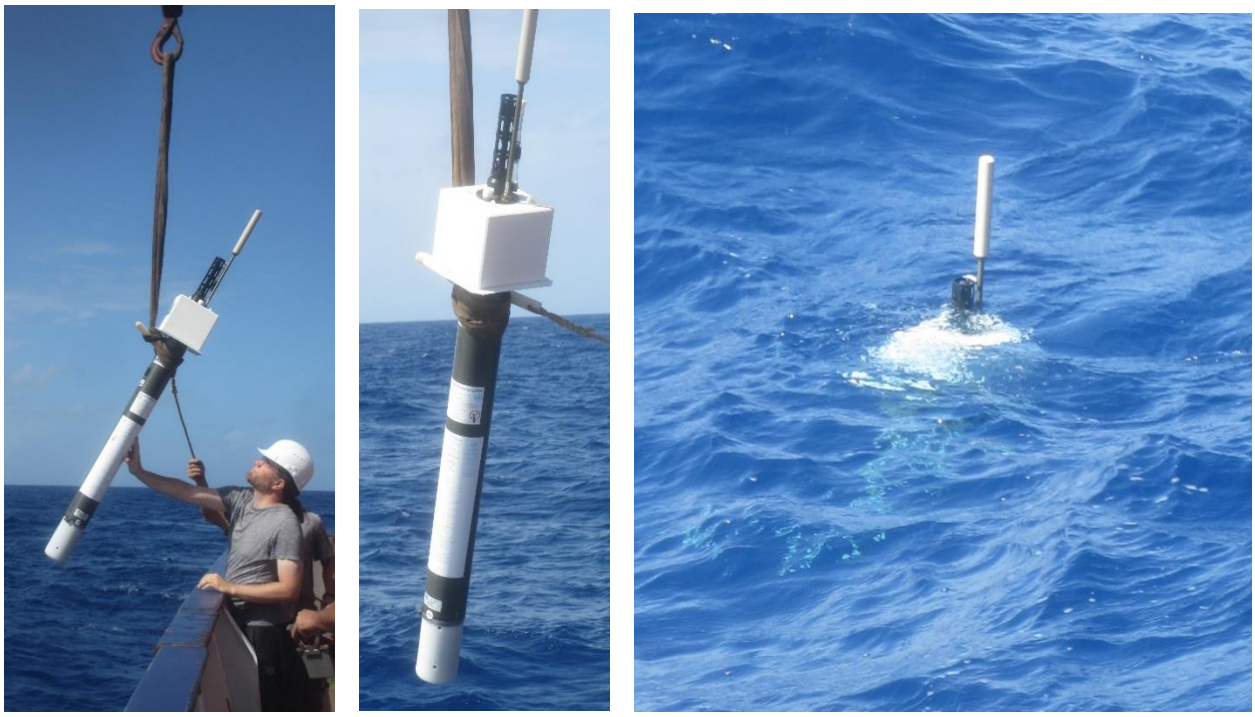

Figure 5.2.5.2 Deployment of the ARGO float on 21 Feb 2020.

Figure 5.2.6.1 The Autonaut Caravela in front of the R/V METEOR (photographed by C. Rollo)